CRACK IDENTIFICATION PROCEDURES IN BEAMS USING EXPERIMENTAL MODAL ANALYSIS

GBADEBO MOSES OWOLABI

INFORMATION TO USERS

This manuscript has been reproduced from the microfilm master. UMI films the text directly from the original or copy submitted. Thus, some thesis and dissertation copies are in typewriter face, while others may be from any type of computer printer.

The quality of this reproduction is dependent upon the quality of the copy submitted. Broken or indistinct print, colored or poor quality illustrations and photographs, print bleedthrough, substandard margins, and improper alignment can adversely affect reproduction.

In the unlikely event that the author did not send UMI a complete manuscript and there are missing pages, these will be noted. Also, if unauthorized copyright material had to be removed, a note will indicate the deletion.

Oversize materials (e.g., maps, drawings, charts) are reproduced by sectioning the original, beginning at the upper left-hand corner and continuing from left to right in equal sections with small overlaps.

Photographs included in the original manuscript have been reproduced xerographically in this copy. Higher quality 6" x 9" black and white photographic prints are available for any photographs or illustrations appearing in this copy for an additional charge. Contact UMI directly to order.

ProQuest Information and Learning
300 North Zeeb Road, Ann Arbor, MI 48106-1346 USA
800-521-0600

CRACK IDENTIFICATION PROCEDURES IN BEAMS USING EXPERIMENTAL MODAL ANALYSIS

by

Gbadebo Moses Owolabi

A thesis submitted to the School of Graduate Studies
in partial fulfilment of the requirements for the
degree of Master of Engineering

Faculty of Engineering and Applied Science
Memorial University of Newfoundland
March 2001

St John's Newfoundland Canada

ABSTRACT

Identification of defects in structures and components is an important aspect in decision making about their repair and retirement. Failure to detect the faults has various consequences, and they vary based on the application, and importance of the structures, and components.

In recent years, significant efforts have been devoted in developing non-destructive techniques for damage identification in structures. The work reported in this thesis was on the experimental investigations of the effects of a crack on beams with fixed and simply supported end conditions, with a view to detecting, quantifying and determining its extent and location. Two sets of aluminum beams were used for this experimental study. Each set consisted of seven beams, the first set had fixed ends, and the second set was simply supported. Cracks were initiated at seven different locations from one end to the other end along the length of the beam for each set, with crack depths ratio ranging from 0.1d to 0.7d (d was the beam depth) in steps of 0.1, at each crack location. Measurements of the acceleration frequency responses at seven different points on each beam model were taken using a dual channel frequency analyzer. The measured responses were curve-fitted using a STAR Structural Analysis Software package running on a PC. The results obtained were tabulated, plotted, and discussed in this thesis.

The damage detection schemes used in this study depended on changes in the first three natural frequencies, the abrupt changes in slopes of the mode shapes near the crack

location and changes in the peak amplitudes of the mode shapes. From the observations made, a method was suggested for locating the extent and position of the crack. The fundamental principle of this technique is the fact that the dynamic response of a structure changes when it is damaged. Measurements of these changes can be used as a diagnostic tool when the relationships between the dynamic properties of a structure change, and the damage is established analytically or experimentally.

The experimental results obtained were compared with theoretical results obtained in an earlier study and found to compare very well.

ACKNOWLEDGEMENTS

I would like to express my sincere gratitude to my supervisor (Dr A.S.J. Swamidas) and my co-supervisor (Dr. R. Seshadri) for their moral support and guidance through out the duration of this research. I am so glad for the positive and unforgettable contributions these professors have made towards my academic pursuit. The financial support given by the Faculty of Engineering and Applied Science, and The Graduate Fellowship awarded by the Graduate School are highly appreciated, without which I would not have had the opportunity of pursuing my Master's at Memorial University. I also want to thank Mr. Austin, and the technical personnel for the technical support given me during the experimentation. The academic contributions made by Dr. M.R. Haddara, Dr. S.M.R. Adluri and Dr. G. Sabin are also highly appreciated.

I would like to thank every member of my family back home in Nigeria, particularly my dear mum (Mrs. Esther Owolabi) and my sister (Mrs. Mary Adeyemi), for their words of encouragement, and prayers. This acknowledgement would be incomplete if I fail to mention the financial assistance given by my friends, and uncles towards my flight to Canada. Special thanks to my bosom friend (Ogunlola Raimi), his cousin (Mr. Ogunlola Ismaili), Uncle Laoye Jayeola and my cousin (Mr. Soji Owolabi). I am forever grateful to their friendship and support. Also, the efforts of Mr. Achmad Zubaydi, Mr. Amman Bolar, Mr. Li Pan and Mr. Usama Ebead in explaining how to use some computational software are highly appreciated. I would also like to thank Mr. Xinfeng Yang for providing the theoretical results.

This thesis is dedicated to the memory of my late loving father, Mr. James Ajiboye Owolabi. Though he is no longer around, the memories of his love and care for my life linger on.

Finally, unto the King eternal, the only wise God, be all the glory, honor, and praise.

CONTENTS

Lists of Tables

List of Figures

CHAPTER 1: INTRODUCTION

1.1 Background

The procedure of crack identification through experimental modal analysis started in the early 40s of the last century with the work aimed at getting the modal parameters of an aircraft so that the problem of flutter could be predicted accurately (Allemang, 1990). However, the methods used then were time consuming and not reliable for most real life practical problems because the instruments used to measure the dynamic force were primitive.

In the early 60s of the 20th century, with the invention of digital computer, and the Fast Fourier Transform (FFT) techniques, the modern approach to experimental modal analysis became viable. The ever-increasing advancement of the modern computer technology has made the availability of the microprocessor-based FFT analyzer possible. Many engineers have an interest in the dynamic behavior of the structures during design or operational stage. The microprocessor-based FFT analyzers play an important role in the acquisition and analysis of vibration data. Experimental modal analysis has grown to a stage whereby it has become interdisciplinary in that it integrates computer developments with developments in electrical engineering, mechanics, vibrations, and control systems.

The modal testing procedures offer a promising methodology for detection of defects or faults in the structures. Defects or faults according to Richardson and Mannan (1991) include: loosening of assembly parts; failure of structural materials; flaws, voids, thin spots caused during manufacturing or handling; and improper assembly of parts during manufacturing.

It is a well established fact in vibration theory that modal parameters (frequency, damping, and mode shapes) of a physical system are functions of its physical properties (mass, stiffness, and damping) of the structure. These modal parameters are the solutions of the homogeneous part of the differential equations of motion of a physical model which is expressed by its mass, damping, stiffness, acceleration, velocity, and displacement. Consequently, any changes brought about in the physical properties of a model by the presence of defects or faults will directly cause some changes in the modal parameters. Vibration, being a very powerful detector of the changes in the physical parameters in a structure, could under some circumstances be used to detect the presence of faults in a physical system. These changes could be accurately measured by using the available modal testing methods.

Having sufficient data from a dynamic test could enable engineers to identify the system parameters, and derive a mathematical model that could describe the dynamic behavior of the test structure in diverse vibration environments. Consequently, such a model may be subjected to further analysis such as to predict the effect of modifications in the structure. By observing the developed mathematical model, and the analytical results, at least a

method could be devised to correlate specific shifts in one or more of the modal parameters with the occurrence and growth of defects.

Several methods have been used in the past to detect faults in structures; however, most of the methods available did not go beyond the detection of the faults. A new approach is presented in this thesis which does not only identifies the presence of a crack, but, also indicates its location and quantifies its extent. Two types of beams are considered in the study viz., simply supported and fixed–fixed beams. The changes that occur in a few of its lowest modal frequencies (specifically the first three) are utilized for identifying the crack. The study is primarily experimental, and the results of this study are presented in the thesis.

1.2 Scope of Research

To reiterate, the research reported in this thesis is primarily experimental. Experiments are performed on fourteen beam specimens; seven of them have simply supported ends, and the rest have fixed-fixed ends. All the models are assumed to be identical, in shape, geometry, physical, and mechanical properties for the given set of boundary conditions. Cracks of varying depths are made (with a blade) at different locations on beams having similar boundary conditions. Since the crack is made with a thin blade, the crack always remains open during the vibration test. Several accelerometers (of similar sensitivities) are used to measure the frequency responses at different points on the model. The

acquired data are analyzed, and inferences are drawn based on the analytical results. The basic steps involved in achieving the objectives of the project are:

a) Experimental set up;

b) Experimental data acquisition;

c) Curve-fitting to estimate the modal amplitudes, frequencies, and damping;

d) Obtaining the mode shape plots, and frequency contours; and

e) Drawing inferences and conclusions.

1.3 Objectives

The primary objectives of this research are:

a) Identification of the presence of a crack;

b) Location of its position; and

c) Estimation of the extent of cracking

in the tested beams using results obtained in experimental modal analysis (mode shapes, natural frequencies, and resonant & anti-resonant responses).

1.4 Organization of the Thesis

The thesis is organized as follows; Chapter One gives a brief introduction, and states the

thesis scope and objectives. It also gives the background of the research study. Chapter Two reviews the various techniques that are available for crack identification. The techniques enumerated and discussed briefly include: visual inspection, liquid penetrant, magnetic particle, radiography, ultrasonic, electrical, and Vibration-based testing (used in these experimental investigations study). It also reviews the relevant literature on the topic and states some of the various damage indicators used in vibration-based testing. In Chapter Three, the theories and fundamental principles of modal analysis are stated and discussed. It states the basic linear differential equation of motion of a linear multiple degrees of freedom system and also explains the concept of modes of vibration of a structure. Several ways of representing the dynamic response of a structure and the transformation techniques available in changing from one form to the other are stated and discussed in Chapter Three. The concept of curve-fitting is also stated and explained in chapter three. Chapter Four gives the detailed descriptions of the experimental set up and discusses the various sources of errors. It states and discusses all the equipment used in the experimental investigations. The various ways by which some of the equipment are calibrated are discussed. Chapter Four also gives the details of the experimental procedures. The results obtained are tabulated, plotted, and discussed in Chapter Five, and a technique for identifying the crack location(s), and depth(s) were also stated. The salient features of chapter Five include: changes in natural frequencies; changes in mode shapes; and frequency response functions. A comparison of the experimental and theoretical results was also presented in Chapter Five. Chapter Six gives the conclusions and recommendations. The references and appendices are also included in the thesis.

CHAPTER 2: LITERATURE REVIEW

2.1 Fault Detection Techniques

A number of non-destructive techniques are available to detect faults and defects in a structure. Their use and reliability have consequently become an important factor in the evaluation of the safety of any structure. Various engineers and scientists have devoted their time and efforts towards developing new, more reliable, efficient, and less tedious detection techniques. Some of the many available non-destructive techniques for damage identification are briefly enumerated and discussed below.

2.1.1 Visual Inspection Method

Visual inspection technique is probably the oldest, and the most widely used technique of all the non-destructive methods. It is a very simple, easy to apply, and less time consuming procedure for inspection. Visual inspection by a qualified engineer can reveal appropriate information about the condition of a structure. It could indicate, for instance, the structural quality, presence or absence of defects, the degree of penetration, and surface porosity. It could also serve as a precursor to other test methods. The underlying basis for this technique is the illumination of the test structure with light mostly in the visible region after which it is examined with the human eyes or by using other optical aids such as mirrors, lenses, periscopes, telescopes, projectors, comparators, boroscopes, and other light sensitive devices such as photocells. The optical aids provide a means of

compensating for the limits of visual acuity of the eyes. For rapid inspection of very small precision components, comparators and enlarging projectors provide means of improving viewing conditions. The interior of hollow tubes and other internal chambers can be easily and directly inspected by using a boroscope. Boroscopes have a large field of vision and sufficient illumination, and the image is less distorted. It is to be noted that some of the equipment used in visual inspection requires that the defect location be accessible. In using optical aids, the effects of the illuminating light must be taken into consideration. Its direction should be in such a way that details can easily be viewed, and glare and dazzle effects are reduced or eliminated. The industrial applications of optical aids depend to a greater extent, on the nature of the surface being inspected; several real life engineering surfaces are non specular and curved.

2.1.2 Liquid Penetrant Method

The technique can be used to detect faults that extend to the surface of the structure. It also portrays surface discontinuities to a very great extent. The method can be applied to metals, ceramics, and other non-porous materials. It is also quick, reliable, and cost effective. It can be used to locate surface cracks (grinding, fatigue and welding). This method reveals the discontinuity to a greater extent than the visual inspection. Some cracks in structures can be deep in the core of the structures, yet, with little opening on the surface, and consequently can pose very serious defects on the structures despite the fact that they have little surface indication. By inspecting these structures visually, such cracks can be very difficult to detect. The fundamental principle of operation is the fact

that when a liquid (which often contains a dye or a fluorescent substance which makes the crack visible) is sprayed on a surface, it seeps into the crack (visible or invisible) by capillary action. After a sufficient time has been allowed for the liquid to seep into the structure, the surface of the structure is wiped clean in order to remove the excess liquid. This is followed by the spraying of a substance known as the developer (which draws the penetrant out of the structure). The surface is then examined under appropriate viewing conditions. The basic steps involved can be summarized as follows:

a) Initial surface cleaning;

b) Application of the penetrant;

c) Removal of the excess penetrant;

d) Application of the developer; and

e) Inspection, and interpretation.

Oil and whiting technique is the oldest, and simplest of this method; its procedures are similar to those enumerated above. The liquid used is penetrating oil, and its developer is calcium carbonate, a thin coating of whiting. Some of the other techniques in liquid penetrant methods are: oil vapor blast test, radioactive penetrant method, filtered particles method, etc. Factors such as sensitivity of the required defect, surface finish of the structure, compatibility of the penetrant with the structure, zone to be inspected (size, shape, and accessibility), and usage to which the component is made are taken into consideration while using the liquid penetrant method. The surface could be photographed or video recorded after inspection for permanent record purpose. Its major

demerit is that it is only applicable to flaws opened to the surface. A thorough surface cleaning is required before this method could be applied.

2.1.3 Magnetic Particle Induction Method

Distortion of flux linkages, in a magnetic material, could be caused by the presence of inhomogenities such as inclusions, cracks, etc, in the structure. The magnetic flux path is distorted because the defects have different magnetic properties than the surrounding materials. This method of crack detection is applicable to ferromagnetic materials. The magnetic line of forces will be distorted when they encounter a defect, if the plane of the defect is at a right angle to that of the field. Both surface and subsurface flaws can be detected. The fundamental principles of this method are very simple. They involve basically two steps; magnetization of the components, and the application of magnetic particles. Fine particles, either dry or in a liquid suspension, are spread on the surface of a magnetized body. The particles are attracted to the distorted field caused by the presence of a defect in the material. The mode of assemblage of the particle reveals the presence of the field as well as the defects. Subsurface defects frequently produce particle patterns that are less sharply defined. The nature of the particle patterns determines the extent of the defect.

There are basically two techniques: the dry and wet methods. In the dry method, the magnetic powder is spread over the surface of the magnetized component. The excess powder is removed by blowing on or tapping of the component. It gives a better result

than the wet method in detecting a subsurface defect. The wet method is mostly applicable for detecting defects in machine casting and forging.

The method is very simple, and it does not depend on the size, shape, and composition of the ferromagnetic material. The method, however, has some limitations. It is only applicable to magnetic materials. Its usage also depends on factors such as: depth. sharpness, direction, and orientation. These determine the possibility of locating a subsurface defect. Also sudden changes in permeability of the material can give unreliable indications. The skill and experience of the user are also very vital. The user should have adequate experience in order to be able to distinguish between defects and false indications. An exact defect size cannot be found by using this method, but only an estimate can be made.

2.1.4 Radiography

Radiography technique involves the use of X-rays or gamma radiation. Its history dates back to the early 20s of the last century. The basic principle has to do with differential absorption between the image of an area containing a defect and the image of a defect free area of the structure in order to reveal the flaw. The X-ray method is assumed to be a fundamental test procedure, and quite a large number of experts in the field of non-destructive testing have obtained their first experience using this method. However, a considerable amount of capital is essential for an X-ray facility and also an adequate supply of power is needed for its operation. A great percentage of radiography methods

use X-ray films, which are very expensive. Consequently from an economic view point, it is better to use X-rays on very specialized components or structures such as a pressure vessel, while some other methods could be used for routine inspections. Cracks with small crack width to depth ratios are not easily identified using X-rays, but, blowholes, and cavities can be easily detected. This is due to the fact that the operation of this method depends on differential absorption. Also, the X-ray tube is a very large apparatus that cannot be easily transported or introduced into a small cavity as can be done for a radioactive source. The effectiveness of X-rays depends on: the intensity, the thickness of specimen, and the characteristics of film. It is very vital to look carefully at the component in order to decide on the direction to examine the component considering the likely orientation of defects and the thickness of component in relation to the divergence of the X-rays.

2.1.5 Ultrasonic Technique

Mechanical vibration oscillations with frequencies ranging from 16 Hz to 20 kHz are said to be audible to the human ear. Striking a structure and measuring its echoes or listening for the characteristic "ring" have been used since ancient times for detecting defects in structures. The note emitted by a damaged surface is quite different from that of an undamaged surface. For example, in steel, the damaged structure has a dull and harsh note compared to the one emitted by the undamaged one.

When the vibrating oscillation is at a frequency greater than 20 kHz, the sound becomes inaudible to the human ear; it is referred to as ultrasonic. The classical principles that are

applied to the audible frequencies are also applied to ultrasonic frequencies, but, some phenomena that occur at ultrasonic frequencies are not usually noted at the audible range. There are several ways of producing ultrasonic waves. However, for the purpose of crack identification, it is usually produced by piezo-electricity. This involves the application of mechanical pressure or tension to certain crystals, thereby, developing electric charges, the sign of which changes when the force changes from tension to compression. For crack identification purposes, the ultrasonic waves are introduced into the components. These travel with a very little attenuation, and with a velocity that depends on the material properties (mainly its elasticity and density). On striking the boundary of the material under examination, ultrasonic waves are reflected back depending on the acoustic property of the specimen. They are almost fully reflected at a material-air interface; this is also true when the defect is a crack that has a very small crack to depth ratio. Consequently, ultrasonic wave beam could be used to detect faults such as cracks, blowholes etc. The ultrasonic wave is frequently introduced into the material by direct contact between the crystal and the component. It may often be necessary to interpose a film of viscous coupling medium such as a liquid between the crystal, and the component being examined, due to the fact that even the thinnest air gap could cause a total reflection thereby leading to misleading information. For further details, see McGonnagle (1961).

2.1.6 **Electrical Technique**

This method has so many different ways of being carried out. It includes: electrical

resistance method, thermoelectric effect, triboelectric effect etc. In electrical resistance method for example, the electrical resistivity of the material in the local defect zone differs from that of the undamaged zone. This is because the electric potential difference produced between two points by the flowing of an electric current in the specimen will change when a defect is present. The soundness and homogeneity of some materials have been tested by using this method. Basically, the method involves attaching electrodes firmly to the end of the specimen, and passing high amperage current through it (Direct Current Potential Difference Method or DCPD). Potential contacts are placed at equal distances along the surface of the specimen. The potential difference between each pair is then measured in succession using a voltmeter. The presence of a defect in the component is revealed by a non-uniformity in the values of the potential difference measured between each pair. This technique has been used greatly in the inspection of rails to determine the location of a rail fissure as well as obtaining an estimate of its size.

2.1.7 Vibration Based Inspection Technique

All of the previously mentioned techniques require that the vicinity of the fault be known beforehand and that that portion of the structure be accessible. Because of these limitations, the need to develop a method for global crack identification particularly for complex structures, brought about the development of methods that examine changes in the global characteristics of the structure. The most common of these methods is the vibration based inspection technique.

According to Rytter (1993), the fundamental idea of a vibration based technique of monitoring and inspection of a structure is to get information about the soundness of a structure from its dynamic response to either artificial or in service loads. The method is relatively new in connection with civil engineering structures, but it has been widely used for inspection of machinery for many years. The response of the structure will often be measured by means of strain gauges, accelerometers, and/or laser vibration probes. A local defect in the structure will to some extent lead to a change in the overall dynamic characteristics of the structure. This method is utilized in carrying out the study highlighted in this thesis.

2.2 Crack Detection and Experimental Modal Analysis

Identification of defects in structures is an important aspect of decision making about their repair or retirement. Failure to detect faults has various consequences, and they vary based on the application, and the importance of the structures, machines, or components. However, they can be considerable from safety or an economical point of view. The importance of crack identification cannot be over emphasized; however, the task is not very easy in many of the situation encountered in real life. This has brought forth a great deal of research on various methods of damage detection based on analytical, and/or experimental techniques. Among the various methods of physical/experimental techniques, experimental modal analysis has emerged as a promising tool for use in damage identification. It is defined as the process of determining the modal parameters (frequencies, damping factors, and modal vectors) of a linear, time invariant system

through an experimental approach. This experimental approach has also assisted in the efforts to understand, and to control the various vibration phenomena encountered in practical situations.

In this technique, the structure is excited either in free or forced vibration, and the modal parameters are extracted based on the response data obtained. The fundamental theory underlying this process of crack identification is the fact that a change in the physical parameters of a structure causes a change in its modal parameters (frequencies, damping factors, and mode shapes).

Experimental vibration analysis was initially carried out for two fundamental reasons:

a) Determining the nature, and extent of vibration response; and

b) Verifying theoretical models and predictions.

The first reason was mainly concerned with a test situation where vibration forces or responses were measured during the operation of a machine or structure, and the second one mainly described a test situation in which the machine or structure is vibrated with a known excitation. This second test condition could be properly monitored than the former one, and consequently produces accurate, and more detailed information. It includes data acquisition, and its subsequent analysis, which is nowadays, referred to as modal testing or experimental modal analysis. Its principles have undergone so many changes from the time when they were described as Resonance Testing, and Mechanical Impedance

Measurements to describe the general area of activity. The methods used then were not reliable, and were time consuming until the invention of digital computers, and better measurement procedures and instruments.

2.3 Review of Previous Work on Crack Detection

A large number of studies have been carried out on conventional, and modern approaches to modal testing or numerical modal analysis, and crack detection. The conventional methods have been well developed, and implemented in widely marketed equipment, whereas the dynamic methods are still under development, and implemented in a limited manner in some equipment. While these equipment detect the presence of very large cracks, the available methodologies are still not precise to detect small or medium sized cracks (Cheng, 1998).

The method of using experimental modal analysis for detecting cracks came into being in the 40s of the last century. Several literature, journals, and conference reports from experts working in the field of damage identification are available nowadays. A comprehensive survey of the available literature and interviews with various experts to determine the current state of this method was presented by Richardson (1980). The paper discussed the methods used for structural integrity monitoring of nuclear power plants, large civil engineering structures, and rotating machinery. He, however, concluded that though monitoring the vibration signals for rotating machinery had become so common, the act of relating the structural damage to measured modal

parameter changes was still in its primitive stages. A more detailed report was given by Doebling et al (1996). The report reviewed the various technical literature available on detection, and location of structural damage via vibration based testing. It categorized the methods according to the measured data and analysis techniques. The techniques categorized include: changes in modal frequencies, changes in modal mode shapes (and their derivatives), and changes in measured flexibility coefficients. Techniques that use system's physical properties, detect nonlinear response, and identify crack through neural networks were included. Their applications to numerous engineering problems, and various mechanical, and civil engineering structures were also mentioned.

With regard to beams, the deformation (which results from a crack in the beam) cannot be accurately described by a beam theory in which it is assumed that the beam's cross section remains plane after deformation. Dynamically loaded beams with cross sectional cracks have been investigated in a number of papers. Chondros and Dimarogonas (1980) investigated the effects of cracks in welded joints. The change in the bending stiffness of a beam due to a crack was measured and used in the mathematical model. They modeled the crack as a local flexibility computed using fracture mechanics procedures and also measured experimentally; and thereafter they developed a spectral method to identify cracks in various structures relating the crack depth to changes in natural frequencies of the first three frequencies of the structure for known crack positions. Inagaki et al (1981) estimated the crack size and the crack position by natural vibrations of cracked rotors. It was noted that there was a strong dependence of vibration behavior of cracked rotors on the crack position and the crack magnitude.

Yuen (1985) presented a systematic study of the relationship between damage location, and size, and changes in eigenvalues, and eigenvectors of a cantilever beam. Ju and Mimovich (1986) were able to model cracks in a cantilever beam using a fracture hinge. They used aluminum beams with a cross sectional area of 9.5 mm by 63.5 mm, and of length 457 mm. Twenty beam models were tested with cracks introduced at five positions along the length by milling slots of two depths, and two widths. The frequencies of the first four modes were taken before, and after the damage. They then used the shifts in the frequencies to determine the location, and the extent of damage on the beams. The modeling of the crack was done by introducing a fracture hinge at its location; the fracture hinge was a torsional spring whose stiffness depended on the crack geometry.

Qian et al (1990) studied the effect of a crack on the dynamic behavior of a beam, and investigated the crack detection methodology. In the paper, an element stiffness matrix of a beam with a crack was first derived from an integration of stress intensity factors, and then a finite element model of a cracked beam was established. The model was then applied to a cantilever beam with an edge crack, and eigenfrequencies were determined for different crack lengths and crack locations. In modeling, the effect of the crack in the deformation of a beam has often been considered similar to that of an elastic hinge. In the plane of the crack, the deformation is discontinuous, and the solution can be obtained from a characteristic equation in which boundary conditions for the internal displacement and force are considered.

Hjelmstad and Shin (1996) were able to develop a damage detection and assessment algorithm based on system identification, using a finite element model and the measured modal response of a structure. The measurements were assumed to be sparse and corrupted with noise. A change in the element constitutive property from a baseline value was taken as an indicative of damage. An adaptive parameter grouping updating scheme was proposed to localize the damage zones in the structure, and a Monte Carlo's method was used with a data perturbation scheme to provide a statistical basis for assessing damage.

Detection of the location and the quantification of damage are possible when a single crack is present in a structure. The identification problem becomes more complex if it is cracked in at least two places. Ruotolo and Mares (1987) concluded that for two cracks, the solution depended on four variables viz., the position and the size of each crack. They went further by using experimental data obtained from a real structure to verify their analysis, viz., the experimental results obtained on a double-cracked beam which correlated the crack location, the crack size, and the corresponding changes in modal parameters. Modal analysis techniques were used to investigate the effect of damage on composite materials. The measured eigenparameters of the undamaged structure were compared with those measured after the structure was exposed to a high velocity impact damage. It was observed that the induced damage caused a noticeable change only at higher modes of vibration.

Silva and Gomes (1990) used experimental modal analysis to measure the natural frequencies of slotted free-free beams. Thirty-two steel beams, of 16 mm by 32 mm cross section, and of length 720 mm, were tested. Slots, ranging in depth from 1/8 to 1/2 the beam thickness, were introduced into the beam with a 0.5 mm wide milling cutter. The four natural frequencies of the beams were measured, and presented before, and after the damage. Stubbs (1990) used a theoretical approach to determine the location of defects in a structure. He used the first difference of the homogeneous equation of motion of an undamaged structure to derive expressions for changes in modal stiffness in terms of modal masses, along with changes in modal damping, natural frequencies, and mode shapes. He went further by generating an expression relating variations in stiffness of structural elements to the variations in the modal stiffness using matrix structural analysis. The formulation, when tested using an Euler-Bernoulli beam, indicated the correct crack position.

Perchard and Swamidas (1994) obtained frequency measurements on narrow cantilever plates (or wide beams). Results obtained experimentally, as well as analytically, showed that the crack could be detected mainly through the observation of reduction in natural frequencies for a number of modes. The experimentation performed verified the analytical results, and provided an insight into changes in damping, residue, and amplitude of the dynamic response. The measurement of strain response also proved to be a good indicator of crack presence with major increases in response magnitudes, far exceeding the corresponding acceleration responses.

Budipriyanto and Swamidas (1994) carried out modal testing on narrow cantilever plates in air and in water; the slender plates or (beams) were submerged partially, and fully in water. Notches were introduced symmetrically on both the top and bottom of the surface. Frequency measurements were taken using both accelerometers and strain gauges. The natural frequencies, damping ratios, and peak resonance magnitudes, for combinations of sensor types, and degrees of convergence were presented by the authors.

Prime and Shevitz (1996) performed experimental modal analysis on a polycarbonate cantilever beam having an opening and closing crack. The beam had a cross sectional area of 51 mm by 121 mm, and was 640 mm in length. A crack of 1/2 the thickness of the beam was simulated by bonding together three pieces of polycarbonate. The model was excited by pulling and releasing. Its non-linear response was then monitored through a variety of techniques.

Chen (1996) investigated different aspects of vibration techniques for crack detection in welded T-joints. He incorporated experimental testing, finite element analysis, system identification and model updating procedures in developing a methodology for detecting and quantifying cracks in plated T-joints. He developed a methodology to find out the location, length, and depth of a crack at different intervals of fatigue crack growth by combining the experimental and finite element results and utilizing a model updating procedure.

In the review presented above, it could be observed that the determination or estimation of the exact location and the extent of the damage is still elusive. Consequently, an attempt has been made in this experimental study to address these issues, and to prepare a technique for their predictions.

2.4 Damage Detection Methods Based on Vibration Testing

A damage indicator is a dynamic quantity which can be used to identify the existence of damage in a structure (Rytter, 1993). Since a change in the dynamic behavior of a structure, as a result of damage, is a good indication of its presence, various single-valued parameters can be used in measuring the extent of such damage in the structure.

2.4.1 Resonance and Anti-Resonance Frequencies

In the resonance frequency method, for determining faults in a structure, natural frequencies were identified by locating the peaks in a frequency response function, and comparing them with the previously known frequencies of the undamaged structure. This method was the most widely used one in the past, and nowadays, and numerous papers have been written on it. It is a very easy method for identifying the presence of damage in a structure. In actual fact, one sensor put on a structure, and connected to a frequency analyzer gives values of several natural frequencies, and these natural frequencies are very sensitive to different types of defects. For example, in a linear undamaged beam

with constant cross section, and material properties, the natural frequencies could be calculated by using the formula:

$$f_i = \frac{\beta_i}{2\pi L^2}\left(\sqrt{\frac{EI}{\mu}}\right) \qquad (2.1)$$

where:

μ = mass per unit length;

βi = a constant depending on the boundary conditions;

L = length of the beam;

I = moment of inertia; and

E = Young modulus of elasticity

A slight change caused by a global defect on the beam may also cause changes in I, μ, and also in f_i. Rytter (1993) concluded that a natural frequency, which does not decrease when others do, is very valuable as a damage indicator because this indicates that damage is placed in a zero point for the curvature of that mode shape. For instance, this happened in one of the experiment he had carried out. In one of the models used, the second natural frequency remained unchanged during the test while the other observed natural frequencies decreased.

Brinckell et al (1995) were able to use a statistical method to detect damage in two concrete beams having different degrees of reinforcement ratio. The authors defined a significant indicator for the j^{th} modal frequency as:

$$(S_f)_j = \frac{f_j^u - f_j^d}{\sqrt{((\sigma_f^u)^2_j - (\sigma_f^d)^2_j)}} \qquad (2.2)$$

where:

$(\sigma_f)_j$ = experimentally estimated deviation of the j^{th} modal frequency;

f_j^u = j^{th} frequency of the undamaged structure; and

f_j^d = j^{th} frequency of the damaged structure

By scaling the observed change in the modal frequency by the estimated standard deviation of the frequencies, measured frequencies with high confidence (low standard deviation) were weighted more heavily in the indicator function. A significant indicator was defined for the measured modal damping ratio. They eventually defined a "Unified significant indicator" by adding the frequency, and damping significant indicators over several measured modes. It proved to be a sensitive indicator of structural damage.

Narkis (1994) estimated the crack location by measuring either bending or axial frequencies. He derived solutions for the crack location (L) as a function of the frequency shifts in two modes. For a simply supported beam in longitudinal bending, the function was given by:

$$L = \frac{1}{\pi} a \cos(1 - R_{jj}) \qquad (2.3)$$

and

$$R_{ij} = \frac{\Delta f_i / f_i}{\Delta f_j / f_j} \tag{2.4}$$

where:

a = crack depth;

Δf_i = frequency change for mode i; and

Δf_j = frequency change for mode j

For a simply supported beam in axial vibration, the function was given as:

$$L = a \sin\left(\frac{\pm\sqrt{R_{ij}} - 1}{2}\right) \tag{2.5}$$

It is to be noted that there are cases in which we have low sensitivity of frequency shifts to damage. Consequently, there is a need for precise measurements where there is no large degree of damage. It appears that a controlled environment will be more favorable in using this method of frequency shifts to detect crack. In addition to this limitation, since modal frequency is a global characteristic of the structure, it is not so certain whether or not its shifts are sufficient to get other information apart from detecting the presence of a crack. At higher modes, which are associated mainly with local responses, this limitation could be overcome. However, exciting, and extracting higher modes might

be difficult and as well prove to be hard to identify the crack. Various experts agree on the fact that there are often limited number of frequencies available with the needed significant shifts needed to locate the damage.

Resonance frequencies are global properties of the structure, and hence do not change in magnitude from one end of the structure to another. Anti-resonance frequencies, however, change from one location to another. This property was exploited by Afolabi (1987) to determine the approximate location of certain kinds of defects.

2.4.2 Mode Shapes

Mode shape vectors are used for graphical display of deformation behavior of the structure. The underlying principle in using mode shapes for identifying defects in structure is that when there is a local damage, it will cause a change in the derivatives of the mode shapes at the location of the damage. It is to be noted that while it is possible to estimate the natural frequencies of a structure by taking measurements at a point on it, to get a mode shape, measurements have to be taken at several points on the structure. The higher the number of measuring points, the greater the degree of accuracy of the mode shape estimated. Tsai and Wang (1996) used the change in fundamental mode shapes between the cracked and uncracked shafts to identify a crack location. The crack was modeled as a joint of a local spring. Several authors have used a bilinear device to simulate the crack in beams, and plates by using mode shapes, and curvature to locate a crack.

A criterion that measures mode shape changes in the whole structure is termed as Modal Assurance Criterion (MAC); this MAC is relatively insensitive to a damage in a beam (made using a saw). Fox (1992) established the fact that "Nodal line MAC", which is a MAC based on measured points close to a nodal point for a particular mode was a more sensitive indicator of changes in mode shapes (than the global MAC referred to earlier) caused by damage to the structure. However, he concluded that graphical comparison of relative change in mode shapes is the best way to detect damage position when only resonance frequencies, and mode shapes were examined. The modal assurance criterion (MAC) has been used by several authors as a damage indicator. Its value between two eigenvectors is defined by:

$$MAC(\phi_i, \phi_j) = \frac{\left|\phi_i^T \phi_j\right|^2}{\phi_i^T \phi_i \phi_j^T \phi_j} \tag{2.6}$$

where:

ϕ_i, ϕ_j = mode shape vectors for modes i and j respectively.

It shows the correlation between two sets of estimates for the same mode shape. A full correlation is indicated by a MAC value of 1.

2.4.3 Mode Shape Curvature

Several derivatives of mode shapes could be used as damage indicators. A typical parameter, and most common among them, is the mode shape curvature (which is the second derivative of deformation at a point). Changes in mode shape curvature are good

indicators of damage for beam structures. A beam's curvature is related to its strain by:

$$\varepsilon = \frac{y}{R} = y\kappa = y\frac{\partial^2 w}{\partial x^2} \tag{2.7}$$

where:

ε = strain at the point of reference;

R = radius of curvature;

y = distance of the reference point from the neutral axis; and

κ = curvature

Measurements of strain could be made by using a strain gauge, and any change in strains as a result of damage in the structure will have a direct effect on its curvature. The changes in strains due to the introduction of a crack in a tubular T-joint was evaluated by Nwosu, et al (1995). They discovered that such changes are much greater than any frequency shifts, and are measurable even at a relatively large distance from the crack.

2.4.4 Transmissibility

The word "transmissibility" has various meanings, and interpretations. However, in vibration, the basic definition is that it is a ratio of response (displacement, velocity, acceleration, and force) amplitude of a system to the excitation (force or motion) amplitude. With regard to damage identification, a change in the structure's stiffness caused by a defect will bring about a change in the amplitude of the system's response to

excitation. Several authors have presented a damage identification procedure in which they utilized the transmissibility between acceleration and excitation as a damage indicator. Transmissibility in this regard is defined as:

$$T = \left| \frac{\ddot{X}}{F_m} \right| \tag{2.8}$$

where:

$\ddot{X}$ = amplitude of the acceleration at the response point

F_m = amplitude of the load.

The relative change in transmissibility between the damaged and the undamaged structure is defined as:

$$R_T = \frac{T_d - T_u}{T_u} = \frac{T_d}{T_u} - 1 \tag{2.9}$$

where:

T_d = transmissibility of the damaged structure

T_u = transmissibility of the undamaged structure

For further information on this approach, see Rytter (1993)

2.4.5 Damping

Damping is an energy dissipation process. Modeling of damping is often a complex task. The most popular model for damping is the linear viscous model in which the damping force is directly proportional to the velocity. Defect in a structure will cause a change in its damping capacity. Rytter (1993) was able to conclude from an experiment conducted on a cantilever beam that the modal damping ratios of the beam are extremely sensitive to even small cracks. He stated further that the changes in damping are highly dependent on several factors such as load history and material treatment. He then concluded that an analytical relation between crack length, and damping has never been given. For some real life structures (such as an offshore platform), a lot of time varying and non-structural sources may contribute to the damping and thus influence the response. These include: water, air, soil etc; consequently, these effects need to be separated out to in order to determine the actual influence of a crack on structural damping.

2.4.6 Matrix Update Methods

This method involves the modification of the structural model matrices (mass, stiffness, and damping matrices) to reproduce as closely as possible the obtained static or dynamic response from the data. The updated matrices are solved by formulating a constrained optimization problem with the structural equations of motion as its basis. In order to detect damage in the structure, a comparison is made between the updated matrices to the original correlated matrices.

Kim and Bartkowicz (1993) were able to investigate damage detection techniques with respect to various matrix update methods, model reduction methods, mode shape expansion methods, considering the number of damaged elements, number of sensors (located on the structure), number of modes, and the noise level. They developed a hybrid model reduction and eigenvector expansion approach to match the order of the undamaged analytical model, and mode shapes for numerical simulation; then they used the procedure to estimate, and locate the damage in a structure.

2.4.7 Nonlinear Methods

Nonlinear vibrations of beams are represented by nonlinear equations. A typical example is the transverse vibration of a beam with an opening and closing crack. Krawczuk and Ostachowicz (1992) modeled a Bernoulli-Euler beam with a crack as two sections on either side of the crack connected together by a torsional spring. The length of the crack was assumed to be varying sinusoidally as a function of time during the closing half of the vibration cycle. This was done in order to address its nonlinearity present during vibration. The authors solved equation of motions numerically using the above formulation. Detailed review of the methods using nonlinearity could be found in Doebling et al (1996)

There are several other damage indicators which will not be discussed in this thesis. These include:

a) Phase plane plot;

b) Probability density function;

c) Random decrement signature;

d) Method based on measured flexibility; and

e) Neural Network Methods.

Additional details on the above could be found in Rytter (1993) and Doebling et al (1996).

2.5 Assumptions Inherent in Modal Analysis

When a specimen is subjected to experimental modal analysis, three fundamental assumptions are usually made. They are: the system should be linear, time–invariant, and observable.

2.5.1 Linearity

The structure is assumed to be linear. This implies that it obeys the principle of superposition. That is, the response of the system to any combinations of forces applied simultaneously is the sum of the individual responses to each of the forces acting alone. It is to be noted that for most practical problems, the assumption of linearity is not always valid vigorously. These could be due to environmental problems, geometry of the structure, inappropriate boundary conditions etc.

2.5.2 Time-Invariance

It is generally assumed that the structure is time-invariant. This implies that the parameters of the structure do not change with time. It is to be noted that a structure which is time-variant will have components that have mass, stiffness, and damping that depend on factors that are not likely measured or included in its physical model. In such cases, the modal parameters measured will be time dependent. For a time variant structure, measurements made at different periods during the experimentation would have different modal parameters. Consequently, the parameters measured will not be consistent.

2.5.3 Observation

In this regard, an adequate behavioral model of the structure could be generated based on information contained in the input-output measurements. According to Allemang (1990), structures and machines which have loose components, or more generally, which have degrees of freedom of motion that are not measured, are not completely observable. For example, in describing the motion of a partially filled tank of liquid when sloshing of fluid occurs, sometimes, enough measurement can be made so that the system is observable under the form chosen for the model, and sometimes, no realistic amount of measurements will suffice until the model is changed.

2.6 Applications of Modal Analysis

The various applications of experimental and analytical modal analysis are too numerous to be written and discussed fully in this thesis. Some of the important practical applications include:

a) Modal updating and verification: This involves the use of experimental modal parameters to update numerical models used to predict the dynamic behavior of structure.

b) Trouble shooting: It simply implies the use of modal analysis for diagnostic purposes. It is the most common application of modal analysis that helps in gaining insights to the problems in structural dynamics.

c) Design Optimization: After proper diagnosis has been done on a structure, the structure can be modified in places to improve its dynamic behavior.

d) Response predictions: Modal analysis can be used to identify the modal parameters of a structure. From the results obtained, the dynamic response of such a structure to any combinations of inputs can be predicted.

e) Condition monitoring: This involves monitoring the modal parameters of structures in order to detect failures during operation.

2.7 Summary

Some of the various techniques available for crack identifications have been stated, and

discussed in the chapter. Relevant literature and research studies carried out were also discussed. In the experimental study reported in this thesis, the damage identification technique used is vibration-based. The schemes used depend on changes in the first three natural frequencies, abrupt change in the slopes, and magnitudes of the mode shapes near the crack location. Chapter Three discusses the fundamental principles and theories used in the experimental and numerical analysis of the problem.

CHAPTER 3: FUNDAMENTAL CONCEPTS AND THEORIES

3.1 Vibration Concepts

Modal Analysis is a vibration-based concept. Consequently, a review of some fundamental concepts of vibration is essential for better understanding of modal analysis. Vibration could simply be defined as a periodic or oscillatory response of a mechanical system. Fundamentally, there are two types of mechanical vibrations. When a structure vibrates as a result of imposed initial conditions, or disturbances, (which would be an energy (kinetic or potential) input into the structure), then the vibration is termed a free vibration. This kind of vibration is dominated by the fundamental frequency (lowest natural frequency of the structure), even though higher frequencies are also present to a smaller extent. It vanishes with time since there are no external excitations acting on the system to sustain the motion continuously. The other type of vibration, called forced vibration, usually occurs under the influence of external forces. If the excitation is caused by a periodic source, the vibration comprises of a steady state response, and a transient response. The transient response is completely damped out after some time, and only the steady state response is present in the structure.

When a system is excited by an external force, a situation can be reached in which the natural frequency of the system is the same as the frequency of the external force. When

this occurs, the system will vibrate with a very large magnitude. This condition is known as resonance; the frequency at which this occurs is known as the natural frequency.

In dynamics and vibration, the number of independent coordinates necessary to specify the configuration or position of a system at any time is referred to as the number of degrees of freedom of the system. Generally speaking, a continuous mechanical system has infinite degrees of freedom. However, in selecting appropriate mathematical modeling, the degree of freedom could be reduced to a discrete number and in some cases to a single degree of freedom.

There are situations in which vibration is advantageous, and in some instances, it is harmful. Its applications are in almost every field of engineering. Vibration engineering is a broad-based field, which includes: vibration monitoring, testing, experimentation, which are important to maintenance and repair of engineering systems.

3.2 Equation of Motion

The basic linear differential equation of motion of a multi-degree of freedom (MDOF) structure is given by:

$$[M]\{\ddot{x}\}+[C]\{\dot{x}\}+[K]\{x\}=\{F(t)\} \tag{3.1}$$

where:

$[M]$ = mass matrix;

$[C]$ = damping matrix;

$[K]$ = stiffness matrix;

$\{x(t)\}$ = displacement vector;

$\{\dot{x}(t)\}$ = velocity vector; and

$\{\ddot{x}(t)\}$ = acceleration vector.

The above equation balances the structure internal forces, which are a combination of mass (inertial), damping (dissipative), and stiffness (elastic restoring) terms (referred to as the spatial model) with the externally applied forces. When an external force is applied to a structure, it begins to vibrate, and the resulting energy is trapped within its boundaries. If the applied force is removed, the structure will continue its vibration but eventually the motion will be damped out by the dissipative properties (damping), and the structure will stop vibrating.

Defects in a structure cause a change in its stiffness, and could also affect its mass distribution, and damping properties. Consequently, there would also be a change in the dynamic response of the structure. In addition to the equation above, the linear dynamics could also be represented by other equivalent expressions such as frequency response function, modal parameters or impulse response function. Consequently, if the acquired frequency response function, modal parameter or the impulse response of the structure is changed, these changes would be due to a change in its mass, damping, and stiffness

properties. The transformation between the various representations of the dynamic equilibrium of a structure is shown in Fig. 3.1. In Eqn. (3.1), vector $\{x(t)\}$ represents the motion at a particular point in a particular direction. Motion at a particular point may be represented by up to six degrees of freedom of motion (three translational and three rotational). Only a finite number of degree of freedoms are used to represent the dynamics of a structure in a typical modal testing. Most often, they are translational simply because rotational degrees of freedom are not easily measured.

3.3 Modes of Vibration

Modal analysis results in the characterization of the dynamic properties of an elastic structure in terms of its modes of vibration. A mode of vibration is a global property of the structure. When energy is trapped at the boundaries of a structure during its vibration, it travels back, and forth within the structure, thereby, causing the structure to deform with various clearly defined wave-like motions called " the mode shapes". They occur at distinct frequencies of vibration referred to as natural frequencies. The amplitudes of the mode shapes decrease as they become damped when all the externally applied forces are removed. A mode of vibration is defined by its natural frequency, damping factor, and mode shape (modal residue). These are otherwise known as modal properties or modal model.

Basically, the modal parameters of a structure could be determined in two ways, viz., experimentally, and analytically. The analytical procedure involves the formulation of the

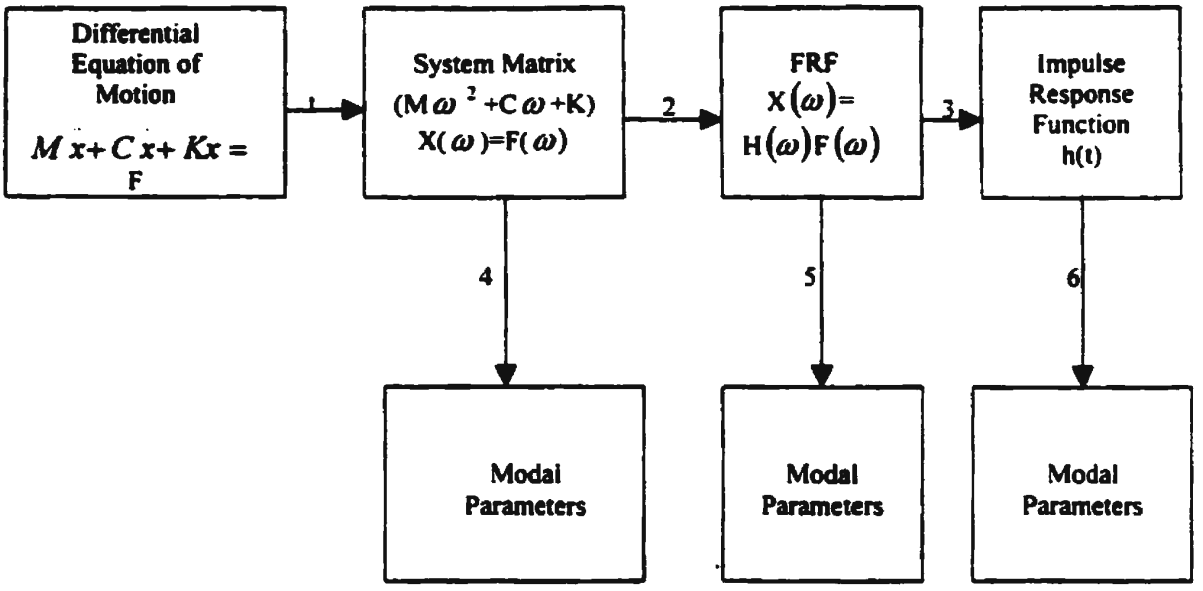

Figure 3.1: Various representations of the dynamic equilibrium equation a structure

(1 and 3 = Fourier Transform; 2 = inversion; 4 = eigensolutions;

5 = curve-fitting; 6 = curve-fitting)

equations of motion of the structure. This is otherwise known as mathematical modeling of the structure. It is commonly achieved by the Finite Element Method (FEM). The modal parameters are the solutions obtained when the homogeneous equations of motion are solved. They are also referred to as eigensolutions (eigenvalues, and eigenvectors). The eigenvalues give the modal frequency, and the damping factor, whereas, the eigenvectors give the mode shape. In the experimental approach, a frequency domain model of the structure is used in conjunction with the frequency response function (FRF) obtained during the experimental modal analysis. Figs. 3.2 and 3.3 illustrate the different stages, and routes involved in both the theoretical, and the experimental approach to characterize structural motions, respectively. Both the theoretical and the experimental

approaches involve three stages as indicated in the figures above, and described as follows:

i) Modeling of the structural dynamics, in terms of the physical properties;

ii) Description of the structural behavior as a set of frequencies, damping factors and vibration modes; and

iii) Dynamic response of the structure to a given excitation force, otherwise known as the response models.

The third stage depends on the structural properties and the magnitude of the excitation force. There are several ways by which the structure could be excited, and consequently these yield numerous types of vibration responses. However, in this study, a sinusoidal force was applied to a particular point on the structure, and the frequency of excitation varied continuously within the selected range (sine sweep function). Consequently, the response model used is a set of frequency response functions (FRF) defined over the applicable range of frequency.

3.4 Transformation Techniques

The various means of representing dynamic response of a structure and the transformation techniques available in changing from one form to the other are stated in this section.

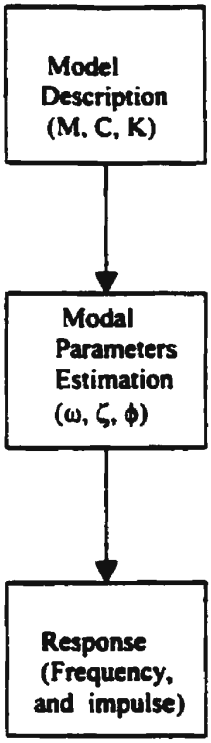

Figure 3.2: Theoretical Approach to Modal Analysis

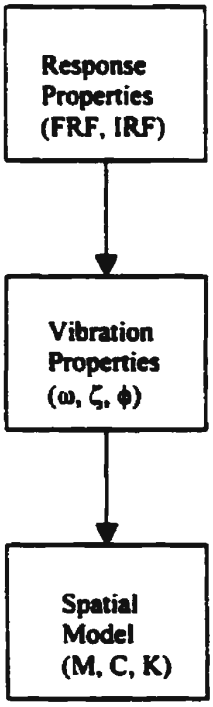

Fig. 3.3: Experimental Approach to Modal Analysis

3.4.1 Basic Definitions

There are two basic means by which vibration analysis could be carried out:

i) Time domain; and

ii) Frequency domain.

The basic difference between the two is in the independent variable of the vibrating signal. In the time domain, time is the independent variable, whereas, in the frequency domain, the independent variable is frequency. In the first case, the system can be modeled by a set of differential equations with respect to time, whereas in the frequency domain, the system is modeled by transfer functions, which are algebraic. The two methods are linked up by the Fourier transform techniques. However, theoretically, it is more convenient to use the Laplace transform in which the independent variable is the Laplace variable (s). The Fourier transform can be obtained from the Laplace transform by replacing the s by $j\omega$. Factors that govern the choice of a domain over the other include: nature of the excitation input, type of available analytical model, parameters to be determined, etc.

3.4.2 Transfer Function

A general link between the analytical solution to the dynamics of a system, and the experimental modal analysis results is the transfer function. An equivalent frequency

domain form of Eqn. (3.1) is described in this section. This form could be written in terms of the system modal parameters. It is to be noted that the different variations of this model can be used to curve-fit the frequency response function, measured in the experimental modal analysis, to obtain the modal parameters.

In transforming a time domain differential equation of motion to a frequency domain algebraic equation in s, the Laplace transform (which is a mathematical technique) is used. Application of this tool to Eqn. (3.1) yields:

$$s^2[M]\{X(s)\} - s[M]\{X(0)\} - [M]\{X(0)\} + s[C]\{X(s)\} - [C]\{X(0)\} + [K]\{X(s)\} = \{F(s)\} \tag{3.2}$$

Homogeneous equation of the above equation would be formed when there are no external forces applied, and the initial conditions are set to zero. In this case, Eqn. (3.2) reduces to:

$$\left(s^2[M] + s[C] + [K]\right)\{X(s)\} = \{0\} \tag{3.3}$$

i.e.,

$$[B(s)]\{X(s)\} = \{0\} \tag{3.4}$$

where:

$$[B(s)] = s^2[M] + s[C] + K \tag{3.5}$$

Eqn. (3.3) is an eigenvalue problem and its solution yields the eigenvalues, which are complex numbers, otherwise known as poles. For Eqn. (3.4) to hold, $[B(s)]$ or $\{X(s)\}$ must be set to zero. Setting $\{X(s)\}$ to zero, however, will give a solution that is not useful. Therefore for a non-trivial solution $[B(s)]$ must be set to zero. The eigenvalues give the modal frequencies, and modal damping values that make the determinant of $[B(s)]$ to be zero. For a particular eigenvalue, there is a unique eigenvector, otherwise known as the system mode shape or modal vector. This can be obtained by solving Eqn. (3.3) for a given value of eigenvalue, which are solutions to the determinant of $[B(s)]$.

$$P_i = \sigma_i + j\omega_i \tag{3.6}$$

where:

P_i = eigenvalue of the i^{th} mode;

σ_i = modal damping of the i^{th} mode;

ω_i = modal frequency of the i^{th} mode;

i = 1,2...m; and

m = number of modes

Note that the eigenvalues occur in complex conjugate pairs. A typical complex pair is illustrated in Figure 3.4. The influence of modal damping on a structure determines its classification.

When external forces are applied to a structure, and the initial conditions are set to zero, Eqn. 3.2 becomes:

$$[B(s)]\{X(s)\} = \{F(s)\} \tag{3.7}$$

Multiplying both sides of Eqn. (3.7) by the inverse of $[B(s)]$ yields:

$$\{X(s)\} = [H(s)]\{F(s)\} \tag{3.8}$$

where:

$$[H(s)] = [B(s)]^{-1} \tag{3.9}$$

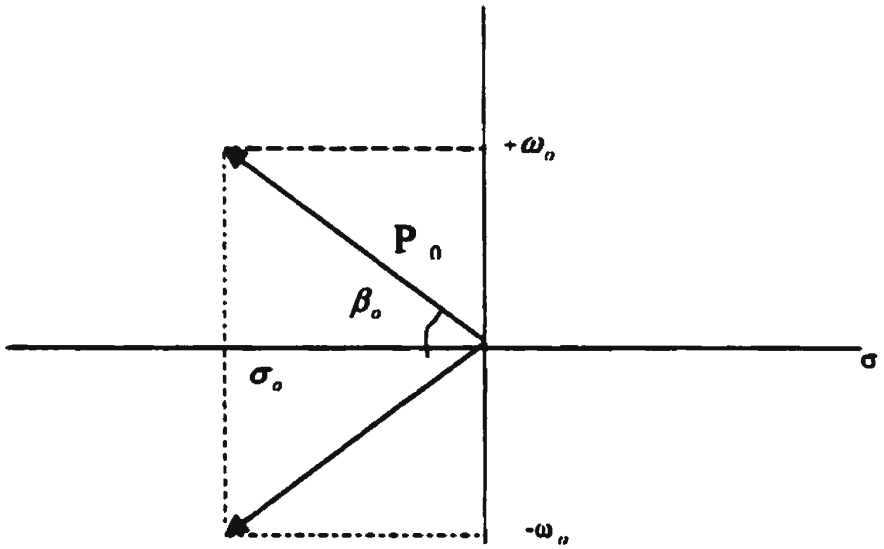

Fig 3.4: Typical complex eigenvalue pair

$[H(s)]$ is known as the transfer function matrix. Each element of the transfer function matrix is a transfer function. It describes the entire dynamic properties of the structure

between a given input DOF, and its given response DOF. In a more general form, Eqn. (3.9) can be written as:

$$\begin{Bmatrix} X_1(s) \\ X_2(s) \\ . \\ . \\ . \\ X_n(s) \end{Bmatrix} = \begin{bmatrix} H_{11}(s) & H_{12}(s) & . & . & . & H_{1n}(s) \\ H_{21}(s) & . & & . & & . \\ . & . & & . & & . \\ . & . & & . & & . \\ . & . & & . & & . \\ H_{n1}(s) & . & & . & & H_{nn}(s) \end{bmatrix} \begin{Bmatrix} F_1(s) \\ F_2(s) \\ . \\ . \\ . \\ F_n(s) \end{Bmatrix} \tag{3.10}$$

From the above equation, it could be inferred that the Laplace transform of structural response at a particular degree of freedom (DOF) is the summation of terms which are products of the transfer function between a particular input (DOF), and its response DOF, and the applied force Laplace transform of applied force, for example:

$$X_1(s) = H_{11}(s)F_1(s) + H_{12}F_2(s) + \ldots\ldots\ldots H_{1n}(1)F_n(s) \tag{3.11}$$

It is to be noted that each transfer function contains the Laplace variable, and can be written as a ratio of two polynomial functions of the s variable. The function $[B(s)]$ is a matrix of order 2n, where n is the degree of freedom of the structure. Since $[H(s)]$ is the inverse of $[B(s)]$, it follows that the elements of $[H(s)]$ will be polynomials with the determinant of $[B(s)]$ in the denominator of the transfer function. In an n-DOF structure, the determinant of $[B(s)]$ is a polynomial of order 2n. This is called the characteristic polynomial, and it has 2n roots or n-pairs of complex conjugate roots called the poles,

which are the above-mentioned complex eigenvalues. Each eigenvalue represents the roots of the determinant of $[B(s)]$, and the transfer function matrix $[H(s)]$ can be written in partial fraction form as indicated below:

$$[H(s)] = \sum_{i=1}^{n} \left(\frac{R_i}{s - p_i} + \frac{R_i^*}{s - p_i^*} \right) \tag{3.12}$$

where:

R_i = Matrix of residues for the i^{th} mode.

Eqn. (3.12) has 2n terms, which are written as n-pairs of conjugate poles. The partial fraction above contains the pole value in the denominator, and a constant in the numerator. The numerator is known as the residue. For a single pole, say p_i, only the numerators of the (nth order) partial fraction equation are different. Consequently, the residues in the transfer function matrix for each pole can be assembled into a residue matrix as follows:

$$[R_i] = \begin{bmatrix} R_{11}(i) & R_{12}(i) & \cdots & R_{1n}(i) \\ \vdots & \vdots & \cdots & \vdots \\ R_{n1}(i) & \cdots & \cdots & R_{nn}(i) \end{bmatrix}. \tag{3.13}$$

Eqn. (3.12) can be simplified in such a way that the residue matrix could be written in terms of the modal vectors/mode shapes. Consequently, the transfer function matrix is reduced to a form known as the parametric form, which contains only the modal

parameters. In the parametric form, each mode of vibration is defined by a pair of complex poles (frequency and damping value), and a pair of complex conjugate mode shapes. At this point, no attempt has been made at diagonalising the equations of motion. Hence, the mode shapes are still complex valued. This is not necessary in order to get the parametric form from the transfer function matrix. The parametric form is given as

$$[H(s)] = \sum_{i=1}^{n} \left(\frac{\{\phi_i\}\{\phi_i\}^T}{s - p_i} + \frac{\{\phi_i^*\}\{\phi_i^*\}^T}{s - p_i^*} \right) \tag{3.14}$$

Changing the transfer matrix to the parametric form, as indicated above, greatly reduces the number of measurement data needed to estimate the modal parameters of a structure. Hence, the modal parameters of the structure can be obtained from any row or column of the transfer function matrix with the exception of the situation in which these rows, and columns, correspond to components of the modal vector which are zero, otherwise known as nodal points. The parametric form of the residue allows defining the entire (n x n) matrix, once the n-dimensional modal vector is known. For example, using the transfer function alone without a prior knowledge of its parametric form, it would require 2500 measurements in building a 50-DOF model. However, if the parametric form of the transfer function matrix is used, only 50 measurements are required. The parametric form of the transfer function for a two-DOF case is given below:

$$\begin{aligned}[H(s)] = &\frac{1}{s - p_1}\left[\begin{Bmatrix}\phi_{11}\\ \varphi_{12}\end{Bmatrix}\begin{Bmatrix}\phi_{11} & \phi_{12}\end{Bmatrix}\right] + \frac{1}{s - p_1^*}\left[\begin{Bmatrix}\phi_{11}^*\\ \phi_{12}^*\end{Bmatrix}\begin{Bmatrix}\phi_{11}^* & \phi_{12}^*\end{Bmatrix}\right] + \\ &\frac{1}{s - p_2}\left[\begin{Bmatrix}\phi_{12}\\ \phi_{22}\end{Bmatrix}\begin{Bmatrix}\phi_{12} & \phi_{22}\end{Bmatrix}\right] + \frac{1}{s - p_2^*}\left[\begin{Bmatrix}\phi_{12}^*\\ \phi_{22}^*\end{Bmatrix}\begin{Bmatrix}\phi_{12}^* & \phi_{22}^*\end{Bmatrix}\right]\end{aligned} \tag{3.15}$$

The first pair represents the first mode, and the second pair stands for the second mode.

3.4.3 Frequency Response Function

In most practical modal testing, the transfer function is measured only along the imaginary (i.e. frequency) axis, and not in the entire s-plane. The values obtained are known as frequency response functions. Theoretically, the Fourier Transform results can be obtained from the Laplace transform by setting $s = j\omega$. This section formally introduces the frequency response function, and illustrates how the technique is useful in the response analysis of a vibrating structure. The frequency response function is the most commonly used approach in estimating the modal parameters of a structure.

By definition, a frequency response function is a complex ratio of output response to input excitation as a function of frequency for a single input–single output situation. There are various methods of estimating the frequency response function depending on where the noise enters the measurement. Table 3.1 indicates the characteristic of the three methods commonly used. There are several forms in which FRF could be represented, and plotted. Table 3.2 shows the details of FRF parameters.

Graphically, the frequency response function could be represented by:

i) A plot of modulus (magnitude, or log magnitude) of the FRF, and phase versus the frequency. This is known as the Bode plot.

ii) A plot of the real part of the FRF and imaginary part versus frequency. This is a two-part representation, and is known as Co-quad plot.

iii) A plot of the real part versus the imaginary part. This is referred to as the Nyquist plot.

3.4.3.1 Frequency Response Function Matrix

The easiest way to obtain the matrix of a frequency response function is to take measurement of the FRFs one at a time. Consider a two-modal measurement case given below, and replacing s in Eqn. (3.11) by s = jω, we would have:

$$\begin{Bmatrix} X_1(\omega) \\ X_2(\omega) \end{Bmatrix} = \begin{bmatrix} H_{11}(\omega) & H_{12}(\omega) \\ H_{21}(\omega) & H_{22}(\omega) \end{bmatrix} \begin{Bmatrix} F_1(\omega) \\ F_2(\omega) \end{Bmatrix} \tag{3.16}$$

From Eqn. (3.16) we have:

$$X_1(\omega) = H_{11}(\omega)F_1(\omega) + H_{12}(\omega)F_2(\omega) \tag{3.17}$$

$$X_2(\omega) = H_{21}(\omega)F_1(\omega) + H_{22}(\omega)F_2(\omega) \tag{3.18}$$

If we set $F_2(\omega)$ to zero, then eqns. (3.17) and (3.18) reduce to:

$$X_1(\omega) = H_{11}(\omega)F_1(\omega) \tag{3.19}$$

$$X_2(\omega) = H_{21}(\omega)F_1(\omega) \tag{3.20}$$

Eqns. (3.19) and (3.20) could be written as:

$$H_{11}(\omega) = \frac{X_1(\omega)}{F_1(\omega)} \tag{3.21}$$

$$H_{21}(\omega) = \frac{X_2(\omega)}{F_1(\omega)} \tag{3.22}$$

It could be inferred from the above equations that for measuring a column of the frequency response function matrix, there is no need to vary the location of the applied force. The first element in the first row is found by exciting the structure at point 1 and measuring the response at that same point. Also the first element in the second row is found by exciting the structure at point 1 and taking the response at point 2. In this research, a single input, multiple output (response) system was employed. The responses, however, were taken one at a time.

3.5 Global Modal Parameter Concept

This concept implies that there is only one solution for each modal parameter, and the modal parameter estimation procedure must enforce this constraint. Every frequency or impulse function measurement contains the information presented in the characteristic equation (i.e., modal frequencies and damping). Treating each measurement in the Treating each measurement in the parameter estimation procedure to be independent one

another does not guarantee that a single set of modal frequencies, and damping will be obtained.

Table 3.1: Frequency Response Estimation Methods

Frequency Response Function		
Technique	Noise Location	
	Force input	Response
H_1	No noise	Noise
H_2	Noise	No noise
H_v	Noise	Noise

Table3.2: Representations of FRF

Response Parameters(R)	Representation(R/F)	Inverse(F/R)
Displacement	Receptance, Admittance, Dynamic compliance, Dynamic flexibility	Dynamic stiffness
Velocity	Mobility	Mechanical impedance
Acceleration	Accelerance, Inertance	Apparent mass

F = Force excitation input

Likewise, if more than one reference is measured in a data set, redundant estimates of the modal vectors can be estimated except all the references are utilized by the solution procedure. Hence, most of the recent modal parameters estimation algorithms estimate the modal frequencies, and damping in a global sense, but, very few estimate the modal vectors in a global sense.

3.6 Curve-fitting

In curve-fitting, the modal parameters of the responses are estimated. There are various ways of achieving this objective, and some of the methods available are discussed in this section.

3.6.1 Introduction

After the data have been obtained, an analysis of the data is expected to be carried out. There are various stages involved in analyzing experimental modal data. A crucial stage involves curve-fitting of the frequency response functions obtained. Curve-fitting is basically the process of matching an analytical model of the frequency response function to the measured data in order to extract the modal parameters. There are various methods involved in achieving this goal. Some of them are discussed in this section. The task involved in carrying out the curve-fitting could be categorized into two: the first is automatic, the measured frequency data are input, and modal parameters are extracted

without any further involvement of the user; and the second procedure, the user is expected to participate in various decisions throughout the curve fitting process.

It should be noted that the various methods involved could operate either in the frequency domain or in time domain. However, most of the recent curve-fitting techniques are done on the response characteristics in frequency domain. The time domain procedures operate on the basis that the inverse Fourier transform of the frequency response function (FRF) is also another characteristic function of the structure. This is referred to as the impulse response function. However, only the frequency domain, which was actually used in the subsequent experimental analysis, will be discussed in this section.

3.6.2 Single-degree-of–freedom (SDOF) Methods

These are the simplest approaches in curve-fitting, and most of the other methods available today are based on the SDOF models developed for FRF. They are easily applied on most test data, and can provide adequately accurate results in a large majority of test cases.

3.6.2.1 Peak Amplitude Method

Modal parameters extraction for structures, where modes are well separated, could be adequately made using this peak amplitude method. The various steps involved in this method are (see Fig. 3.5):

i) Locate individual resonance peaks on the FRF plot, and take the frequency of maximum response as the natural frequency of that mode (ω_i).

ii) The maximum value of the frequency response ($|\beta|$) is noted. and the frequency band width of the function for a response level of $1/\sqrt{2}$ times the peak value ($|\beta|$) is determined ($\Delta\omega$). The two points identified as ω_a *and* ω_b are the half–power points.

iii) Estimation of the modal damping can be done by using the formulae:

$$\eta_i = \frac{\omega_a^2 - \omega_b^2}{2\omega_i^2} \cong \frac{\Delta\omega}{\omega_i} \tag{3.23}$$

$$\xi_i = 2\eta_i \tag{3.24}$$

iv) The residue of the particular mode is obtained by using the formula:

$$R_i = 2|\beta|\omega_i^2\xi \tag{3.25}$$

Though this method is simple, and can give quick results, it has some limitations. From the equation above, since the modal damping, and residue depend on the value of (β), the reliability of their estimates depends on the accuracy of (β). Furthermore, most situations do not follow the single-mode assumption. The method is, however, useful in the preliminary estimation of the modal parameters

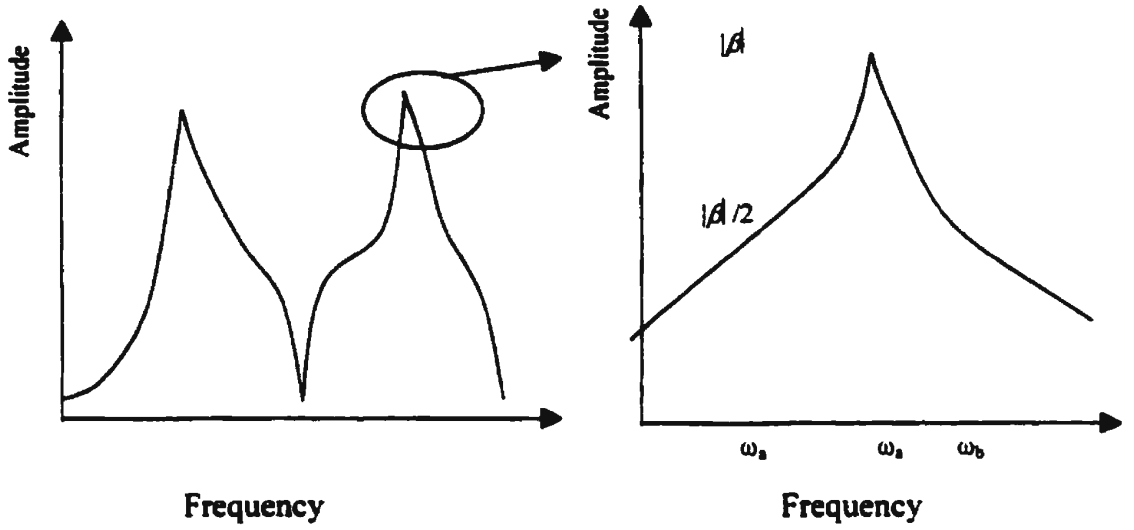

Fig 3.5: Peak Amplitude Method

3.6.2.2 Circle-fit Method

This method involves curve-fitting of the frequency response function in the region of resonance. The fundamental principle on which this method depends on is the fact that a Nyquist representation of the frequency response properties produces a circle-like curve. Hence, an exact circle can be produced by selecting appropriate parameter for the type of damping model. This method is based on the assumption that the structure is dominated by a single mode for a small range of frequency in the vicinity of the natural frequency of a particular mode (see Fig.3.6).

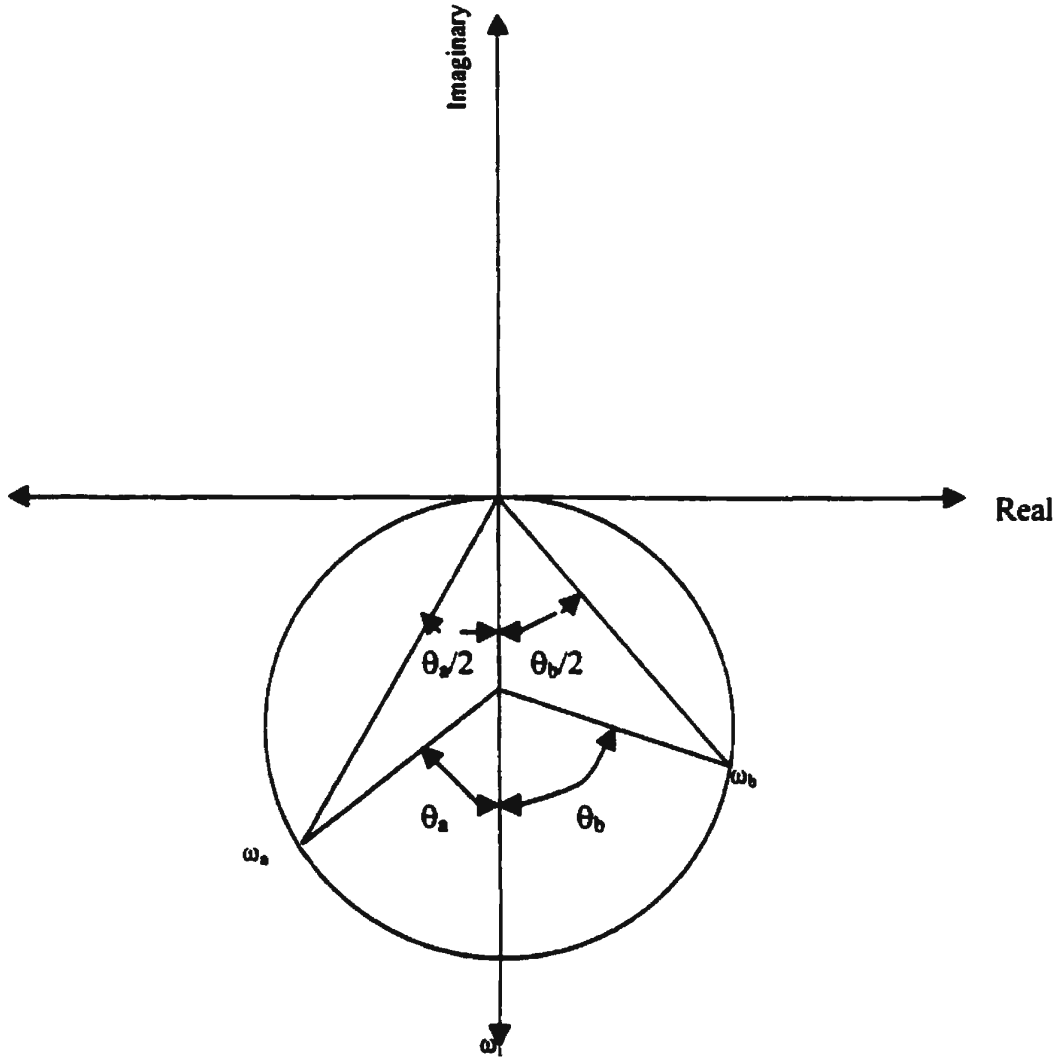

Fig. 3.6 A Typical Modal Circle

From Fig. 3.6, the following deductions could be made:

i) The natural frequency of the system could be estimated by locating the point of maximum sweep rate. At this point, $\omega = \omega_r$, the natural frequency of the structure.

ii) The modal damping is estimated by using two points on the circle with frequencies of ω_a (below the natural frequency) and ω_b (above the natural frequency) as follows:

$$\xi_r = \frac{\omega_b^2 - \omega_a^2}{2\omega_r\left\{\omega_a \tan\left(\frac{\theta_a}{2}\right) + \omega_b \tan\left(\frac{\theta_b}{2}\right)\right\}} \tag{3.26}$$

In case where $\theta_a = \theta_b = 90^0$ (i.e. the half power points), the expression above yields:

$$\xi_r = \frac{\omega_b - \omega_a}{2\omega_r} \tag{3.27}$$

3.6.3 MDOF Curve-fitting Procedures

The previous section discussed the SDOF curve-fitting methods. However, there are quite a number of situations in which the SDOF methods are not appropriate or sufficient. In such cases, the MDOF methods are utilized. A typical example is a situation in which the FRF is heavily coupled. For this case, the modal parameters are estimated simultaneously using the MDOF method. Several methods are available in MDOF curve fitting which could be carried out either in the time domain or frequency domain. However, an attempt will be made in this section to discuss only one of the three frequency domain methods. The frequency domain methods are:

i) Extension of the SDOF method;

ii) General curve-fit approach; and

iii) Method suited for lightly damped structures.

3.6.3.1 SDOF Extension Method

In the circle fit method, it is assumed that the effects of all other modes near the vicinity of a natural frequency could be denoted by a constant. In the SDOF extension method, however, this restriction is removed. This is achieved, for example, by having good estimates for the coefficients which make up the second terms, assuming that the SDOF estimation has been completed. A set of data point could be taken around the resonance at ω_i, and then for each frequency of known FRF value, the magnitude of the second term could be computed, and subtracted from the known value. This system is an iterative process.

3.6.4 Curve-fitting Using the STAR Structural Analysis Package

This section discusses the various curve-fitting methods available in the software used in this research investigation called the STAR Structural Analysis Package (Star reference Manual, 1990). Both the SDOF, and the MDOF curve fitting methods are available in this package. It uses frequency response functions to identify the modal parameters of a structure. Some of the basic steps involved are:

i) Determining the number of modes in the FRF;

ii) Setting up auto-fitting band;

iii) Auto fitting all measurements; and

iv) Displaying mode shapes, and examining results.

A mode of vibration is represented by a peak in the frequency response plot. This is referred to as the resonance peak. However, the accuracy of this assumption is affected by the noise content in the FRF, and by any other errors made in making experimental measurements.

In identify a peak, the following points must be noted:

i) Use imaginary part of the measurement to identify peak in receptance or inertance measurements;

ii) For mobility measurements, the real part is used;

iii) The magnitude could be used, and is independent of the quantity measured;

iv) Visual inspection of the FRFs could be used to identify the majority of modes present in the plots; and

v) No peak is observed for response taken at a nodal point.

The absence of modal peaks in a large number of measurements indicates the presence of a local mode (i.e., a mode with zero mode shape for many degrees of freedom of the structure). The "Identify Modes" command of the " Analysis Menus" in a STAR software package is used to identify the modes of interest in the present FRF measurement data.

3.6.4.1 Curve-fit Methods

Several curve-fitting methods are available in the STAR package. The one chosen depends basically on the degree of damping in the measurement and the modal parameters to be estimated. For light modal damping, the SDOF curve fitting is sufficient, whereas, for a MDOF system, curve-fitting methods are used for a closely (heavily) damped FRF. Using a consistent method throughout the experimental modal analysis is however advisable.

The various methods available in STAR package include:

i) Coincident;

ii) Quadrature;

iii) Peak;

iv) Polynomial; and

v) Global F & D

Both the Coincident, and Quadrature methods can be used to estimate the residue, and modal frequency from the FRF data, but, do not estimate modal damping. The difference in these methods is basically on the type of plot used. In the coincident procedure, the real part of the FRF is used while the imaginary part is used in Quadrature. The Peak method uses the complex value of the FRF as in the previous two methods. It estimates the residue, and the modal frequency, but, does not estimate the modal damping.

Polynomial curve fitting is applicable to both the SDOF modes, and the MDOF modes. It was actually used in this research. It fits a polynomial function in a rational fraction form in a least square error sense. Hence, it is otherwise known as Rational Fraction Least Square (RFLS) method. The modal frequency, modal damping, complex magnitude (magnitude, and phase) are estimated when using this method for a single mode. Likewise, the modal parameters are estimated for a range of modes when using this method for a multi-degree of freedom system.

3.7 Summary

The chapter describes the various theories and fundamental principles relevant to modal analysis (experimental, and analytical). Obviously, there are numerous other topics in Modal Analysis Theory that could not be presented in this chapter. Some of the references listed in the thesis could be consulted for additional information. A very comprehensive theory of Modal Analysis is presented in Ewins (1995). Chapter Four gives a detailed description of the experimental study.

CHAPTER 4: INSTRUMENTATION AND EXPERIMENTAL PROCEDURE

4.1 Instrumentation

Monitoring the dynamics of a structure experimentally involves the use of several instruments. Some of the instruments used in this experimental study are: a function generator, power amplifiers. an exciter, a load cell, accelerometers, a filter, a scanner, a personal computer, a dual channel analyzer, and an oscilloscope. Proper functioning and calibration of the instruments are very essential to obtaining reliable results.

4.1.1 Accelerometer

Modal testing requires the measurement of forces as well as responses. There are various methods for doing this. The methods include: laser, optical fibres, magnetic sensors, and piezoelectric transducers. In the present study, piezoelectric transducers were used to measure the acceleration of the tested beams at various locations.

Piezoelectric transducers are mainly used in accelerometers and force gauges. For this experiment, about seven accelerometers were attached to the model. Piezoelectric accelerometers are commonly used because of their smallness in size, high stiffness, and high range of sensitivity. It is to be noted that they are charged generators that require a

special amplifier called charge amplifier. The amplifier converts the generated charge into an output voltage which could be easily measured, and recorded.

Each accelerometer can be modeled as a single degree of freedom mechanical system. The accelerometer responds to both sinusoidal and transient forces. There are two basic types of acceleration sensing elements viz., a strain gauge and a piezoelectric crystal. The second type was used in the present experiment. It is very light, and has a high sensitivity. The fundamental principle of operation of a piezoelectric accelerometer is that an element of piezoelectric material generates a charge across its faces when subjected to a mechanical stress.

Accelerometers are of varying sensitivities. The commonly available ones have sensitivities that vary between 1 to 10,000 pC/g. It is to be noted that a high sensitivity is required for accelerometers. However, the higher the sensitivity, the greater is its mass. This could interfere with the dynamic response of the structure, and consequently reduce the transducer's resonant frequency. As a result of these considerations, coupled with some environmental factors, a compromise is always made in the choice of accelerometers with regard to its size and sensitivity. Hence, small mass accelerometers with relatively higher charge sensitivity are usually preferred.

Before accelerometers are used to measure the response, they must be calibrated. Normally, there are two basic methods that could be used to calibrate accelerometers, viz.;

i) Absolute calibration; and

ii) Comparison calibration

In absolute calibration, the sensitivity of the accelerometer is determined by measurements based on fundamental and derived units for the physical quantities involved. Nowadays, this is conveniently done by the use of a laser interferometer. Comparison calibration implies the measurement of a transducer relative to a standard reference transducer with known sensitivity. This is practically less involved than absolute calibration, and requiring cheaper and simpler instrumentation.

It is to be noted that standard transducers are classified into three major groups, based on the mode of calibration:

1) Primary standard transducer - These are calibrated by absolute method;
2) Transfer standard transducer- Calibrated by either absolute or comparison method; and
3) Working reference standard transducers: They are used for calibration of accelerometers in common use.

An alternate method which is far simpler than any of the above-mentioned methods was used. This involves the use of a hand-held calibrator (PCB) and an oscilloscope. The block diagram of this method is shown in Fig. 4.1. The features and the sensitivities

(calibration factors) of the eight accelerometers used for this experiment are shown in Table 4.1.

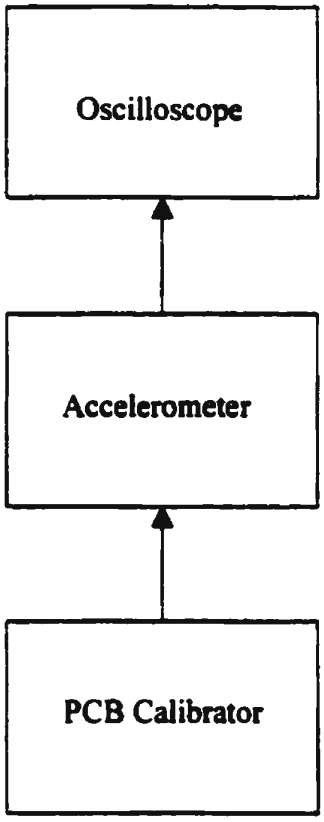

Figure 4.1: Flow Chart for Accelerometers Calibration

Table 4.1: Characteristics of Accelerometers

Frequency Range (Hz)	1-1000
Excitation (DVC)	15
Temperature Range (°F)	0-130
Mass (gm)	2
Connectors (Pins)	3

Table 4.2: Sensitivities of Calibrated Accelerometers

Accelerometer	Series Number (S/NO)	Sensitivity (mV/g)
1	20093	160
2	20502	180
3	20502	180
4	20502	200
5	20403	200
6	19906	160
7	19907	200
8	20505	170

4.1.2 Function Generator

Numerous types of excitation are available that can be used to generate forces that act on the model and also allow it to respond dynamically:

a) Sine sweep;

b) Random excitation;

c) Transient;

d) Periodic; and

e) Sinusoidal.

In this experiment, sine sweep was used. The sine sweep is a sinusoidal command signal that will generate sinusoidal signals of various frequencies within the specified frequency sweep range. The amplitude of excitation needs to be controlled since it can become very large to have a natural frequency (or frequencies) located within the specified sweep range. However, the frequency and its amplitude are chosen in such a way as to avoid large resonant responses that could lead to a nonlinear response function.

The generator used was a HP 3314A function generator featuring sine, square, and triangular functions from 0.001 Hz to 19.99 MHz. Though the function generator has sophisticated operating modes, it was very easy to use it in the experimental testing. The 3314A can operate from AC power sources with voltage deviations within +5% to −10% of the selected value. The line voltage selector on the rear panel setting should be made compatible with the RMS voltage of the AC power source.

The main keys used during the generation of the linear sine sweep function, and their various actions are stated briefly below:

a) PRESET: This sets the 3314A to its basic operating state. It is very useful as the common starting point for all operations. It is to be noted that FREE RUN is the active mode after the instrument is preset.

b) SWEEP: The 3314A output frequency sweeps linearly in increasing manner from the starting frequency to the stop frequency, in the time interval set by SW/TR INTVL

c) START FREQ and STOP FREQ: These two keys set the frequency sweep limits.

d) SW/TR INTVL: This sets the sweep time interval for repeating the sweep signal

e) MAN SWEEP: When this is ON, the output frequency is limited to frequencies between the start, and stop frequencies.

The following points must also be noted when using this type of generator for sine sweep:

1) STOP FREQ must be greater than or equal to the START FREQ.

2) STOP FREQ/START FREQ ratio varies from 1 to 100.

3) Sweep interval can vary from 7.20 ms to 1999 s.

For more comprehensive information, see the Hewlett Packard System Operating Manual (1987)

4.1.3 Exciter

Modal testing requires an exciter in conjunction with the function generator to generate forces that move the structure to respond dynamically. There are various types of exciters available with different capabilities, and modes of operations. Three basic types of exciters are readily available for use:

a) Hydraulic exciters;

b) Inertial exciters; and

c) Electromagnetic exciters.

An electromagnetic exciter was used during the present experiment. It provided a large enough force output to give easily measurable and controllable responses. In this type of exciters, the provided input electrical signal is converted to an alternating magnetic field in which is placed coils attached to the moving part of the device. The moving head is connected to the structure through a rod and a load cell. The frequency and amplitude of the signal can be controlled independently of each other. The impedance of the exciter varies with the amplitude of motion of the moving coil. Consequently, it is practically impossible to measure the excitation force by measuring only the voltage applied to the exciter nor is it proper to measure the excitation force by taking measurement of the current passing through the exciter. This slight differential between the force generated by the exciter and the actual force applied to the model must be taken note of since it has a direct effect on the frequencies near the resonance. The actual input into the tested system was measured by the use of a load cell in contact with the tested system.

The exact type of electromagnetic exciter used for the experiment was a compact, permanent magnet electro-dynamic exciter of the type 4809 with a force rating of 44.5 N (10 lbf) for vibrating small specimens (beams in this experimental case) at frequencies ranging from 10 Hz to 20 kHz. Its moving coil had a nominal impedance of 20% with a current rating of 5 A RMS. Its usefulness apart from vibrating small specimens includes: calibration of accelerometers, educational demonstrations, and mechanical impedance

measurements. It is a small versatile equipment with an impressive performance. The exciter was driven by an amplified force generated by the function generator. The amplification was done by a power amplifier connected to the function generator, and the exciter. The amplifier used was a Bruel and Kjaer power amplifier Type 2706, rated at 75 VA.

4.1.4 Load Cell

A load cell was used for measuring, and transmitting the force signal to the beam model. The load cell used was a Kistler model 912 quartz type. It is a compact, sensitive, and fast response transducer for measuring dynamic, and short time dynamic forces. It could be used to measure both compressive and tensile forces. The load cell is a piezoelectric transducer with a sensing element of stacked quartz wafers assembled under an initial static compressive pre-load greater than five hundred pounds. The sensitivity is measured in pico-Coulombs per pound of force (pC/lbf). It has a screw hole at one end and a screw at the other end. A threaded rod from the exciter was connected to the screw while the other end of the load cell was screwed directly to the beam at a point close to the center. The excitation force was applied perpendicular to the beam surface. The applied force is converted by the quartz–wafer sensing elements into a proportionate electrical charge signal which was measured. Every effort was made to ensure that the load cell was placed between two parallel surfaces of the beam, and the exciter head. Care was taken to see that no overloading occurred throughout the duration of the experiment.

Before the load cell was used, it was calibrated. The calibration of the load cell was done based on the nominal sensitivity of 9.10 pC/lbf provided by the manufacturer. The weight of the load cell was 16.82 gm. A 5 gm mass was placed on it. Consequently, the force acting on the load cell was calculated using the basic formula:

$$F = (1/2\, mass\, of\, load\, cell + applied\, mass) * 9.81 * 0.2284 \qquad (4.1)$$

where : 1 N = 0.2248 lbf

Substituting the previous information into the above equation yields:

F= 0.0300 lbf

The actual sensitivity of the load cell can then be determined by using the formula:

$$S = V/F * \text{Nominal sensitivity} \qquad (4.2)$$

where:

V= output voltage from the oscilloscope.

The calibration set-up used is shown schematically in Fig. 4.2.

When the 5 gm weight was placed on it, and connected to the oscilloscope, and the PCB calibrator, the measured voltage was 30.5 mV. Therefore, the actual sensitivity of the load cell found on substituting V, and F into Eqn. (4.2) is:

S = 9.25 pC/lbf

Using 9.25 pC/lbf, a weight of 5 N was added to verify the accuracy of the calibration. Additional information could be found in the Sundstrand Instruction manual (1972)

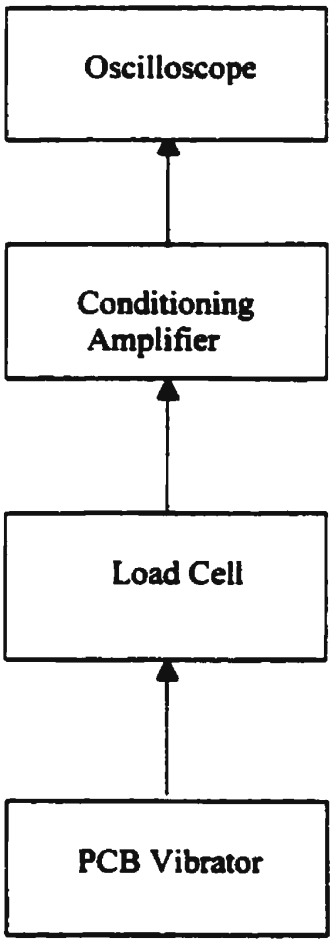

Fig. 4.2: Calibration Procedure for the Load Cell

4.1.5 Amplifiers

The magnitude of an electrical signal could be represented by variables such as voltage, current, charge, and power. This signal magnitude must be properly adjusted for good performance of the components, and the overall system. For example, forces input to an exciter must have adequate power to drive it. This could be achieved by signal amplification, which has to do with proper regulation of the signal level in order to perform a specific function. Signal amplifications are carried out by amplifiers.

Two amplifiers were used during the experiment. One was a small-sized Bruel and Kjaer power amplifier, Type 2076, connected between the function generator, and exciter. The other was a charge amplifier connected to the load cell. The charge amplifier was a Dual–Mode Amplifier Model 504E. It converted the electrical signal input and produced an analog voltage output. The front panel transducer sensitivity was set at the transducer sensitivity of the calibrated load cell (9.25 pC/lbf in this case). The charge amplifier has a very high input impedance and a very low output impedance. This eliminates virtually every loading error. The charge amplifier also has a large time constant and this decreases the charge leakage speed.

4.1.6 Scanner

When we connect several channel inputs (coming from different accelerometers placed on the beam), one signal could be measured at a time if there is an equipment which can connect inputs from several channels. Such an equipment is known as a scanner. In this study, the seven acceleration responses from the transducers were transferred at the same time to an eight-channel scanner. The signals were acquired one at a time in a sequential manner (one to seven, in this case) by the frequency analyzer from the scanner through a filter.

4.1.7 Filter

The degree of accuracy of modal test results could be greatly affected if undesired signals

such as external disturbances, and internally generated noise, which are spurious signals, are not eliminated or reduced. A filter was used to reduce the effects of unwanted signals. It allowed the passage of the desirable frequencies, and rejected the unwanted components. Four types of filters are generally available for use, viz.,

a) Low pass filters;

b) High pass filters;

c) Band pass filters; and

d) Band reject filter.

Detailed discussions of the above could be found in De Silva (1999) and McConnell (1995). It is to be noted however that a low pass filtering method was used during the present experiment. This allowed all the signals below a certain frequency, known as the cut-off frequency, and cut off frequency components above it.

4.1.8 Frequency Analyzer

The signal analyzer usually employs digital techniques to extract useful information contained in the signals (force and response). It implements digital signal analysis that uses the Fast Fourier Transform (FFT) techniques to produce the frequency spectrum of the time signals. To generate the frequency response function of the dynamic response of the model, at least two data signals (force and response, in this case) are needed. Consequently a Bruel and Kjaer Dual Channel Signal Analyzer (Type 2034) was used.

Its basic operational principles, and keys are too numerous to be discussed in this thesis. For a more comprehensive review of its features, see the Bruel and Kjaer Instrumentation Manuals, volumes 1 to 3 (1987).

The dual channel analyzer used performed four basic operations in order to produce the frequency response, coherence function etc., viz.,

a) Anti-aliasing filtering (analog);

b) Conversion of signals from analog to digital (i.e., signal sampling);

c) Cutting of the data, and multiplying by a window function; and

d) Fast Fourier analysis of the data to produce the frequency response function, coherence function etc.

4.1.9 Oscilloscope

The basic function of an oscilloscope is to observe one or two signals separately or at the same time in order to obtain adequate information on its amplitude, frequency, and/or phase. It is a signal modifier as well as a monitoring and displaying device. The oscilloscope was used in this experiment purposely to monitor the vibration signals (force and response) of the beam model obtained from the force, and response transducers.

4.2 Experimental Model Description

Two sets of aluminum beams were used for this experimental investigation. Each set consisted of seven beam models, the first set had fixed ends, and the second set was simply supported. Each beam model was made of aluminum bar of a cross-sectional area 25.4 mm by 25.4 mm with a length of 650 mm. The mass of each model was 812.3 gm. It had the following material properties, viz.,

Young's modulus E = 70 GPa

Density $\rho = 2.696$ gm/cm^3

Poisson ratio $\nu = 0.35$

The dynamic behavior of each model was investigated in this study. The experimental procedure was carried out carefully to guarantee a high degree of accuracy, and was carried out for several combinations of crack locations and depths. Though there were slight discrepancies in the dimensions of the models, they were assumed to be the same for the sake of uniformity in measurements, particularly the uncracked model.

4.3 Experimental Set Up and Procedures

The beam model was clamped at each end, between two thick square steel plates, supported over a short and stiff steel H-section column. This was achieved by using two rectangular steel plates (3/4" thick) with four holes each for bolting the beam model on

the stiff supporting column. The exciter was suspended using a slotted square flat plate. The plate was fixed to the top beam (of the steel frame) by four threaded rods. This made possible the adjustment of the position of the exciter at any time a model was to be fixed.

The first three natural frequencies of the uncracked beam were measured; in addition, the accelerations of the locations of the seven accelerometers were also measured. Then, the cracks were generated, and made to the desired depth using a thin saw cut (around 0.4 mm thick). For each set, seven beam models were tested with cracks at different locations, from one of the clamped or simply supported end, as shown in Table 4.3. The crack depth varied from 0.1d to 0.7d (d is the depth of the beam = 25.4 mm) with an increment of 0.1d at each crack position, as shown in Table 4.4.

By exciting the model at a point, and measuring the acceleration responses of the beam at different points on the beam model, it was possible to get all the frequency response functions between these positions which would lead to the extraction of the modal parameters. To this end, each model was excited by a fast sine sweep signal produced by the frequency generator, which was then amplified, and used to drive the exciter, which eventually transmitted the force to the beam model through the load cell. This served as the input to the system. It is to be noted that the model was excited at a point which was a few millimeters away from the center of the model. This was done to avoid exciting the beam at a nodal point (of a mode), since the beam would not respond in that mode at that point.

The dynamic responses of the beam model were measured by seven accelerometers placed at different points on the model as indicated in Fig. 4.3. Note that it was practically impossible to have ideal boundary conditions. In fact, deep slots had to be made on the second set of beams as shown in Fig. 4.4, in order to get the simply supported end conditions. The pictorial views of the fixed and the simply supported beams are shown in Figs. 4.5 and 4.6, respectively. The response measurements were acquired one at a time using the dual channel signal analyzer described in the previous section of the thesis. Before the responses were taken by the analyzer, they were passed through a filter to reduce the noise contents, as mentioned earlier. Similarly, the oscilloscope was used some times to monitor the excitation and response signals to prevent overloads, and also to ensure that good sine sweep signals were obtained.

Measuring the frequency response appropriately over a large frequency band was not possible in this experiment, since the energy required for the beam to vibrate varied drastically depending on the frequency band. Consequently, the test region was zoomed into frequency bands. Dynamic testing was carried out in each band. Tables 4.5 and 4.6 show the different frequency bands used for each set of experiments. Note that three response readings for three frequency readings in a frequency band were cross-checked with same frequencies in the subsequent band to ensure accuracy in matching the different bands.

The measured frequency response acquired using the signal analyzer were given a 100 ensample averaging before transferring them through GPIB to the PC on which a

Structural Testing, Analysis, and Reporting (STAR) software package was installed for data analysis. The schematic diagram of the experimental set up is shown in Fig. 4.7. Figs. 4.8 to 4.10 show the pictorial views of the experimental set up.

A total of 3 modes were identified in the four frequency ranges (for fixed ends beams), and the three frequency ranges (for simply supported ends beams), respectively. It was observed that some unwanted resonant peaks were introduced by the vibration of the floor plate and supports. These were identified using an eighth accelerometer placed on floor/support and monitoring the responses to see whether the frequency response was due to the floor/support vibration or due to actual structural (in this case, the tested beam) vibration.

Table 4.3: Crack Locations

Beam specimen	Crack positions from one end (fixed-fixed beam) (mm)	Crack positions from one end (simply supported) (mm)
1	41	41
2	122	122
3	203	203
4	284	284
5	325	324
6	447	446
7	609	608

Table 4.4: Crack Depths

No. Of depths	Depths of cuts (mm)
1	2.54
2	5.08
3	7.62
4	10.16
5	12.70
6	15.24
7	17.78

Table 4.5: Frequency Bands for Beams with Fixed Ends

No.	Frequency bands (fixed-fixed models) (Hz)
1	100-300
2	292-492
3	488-888
4	880-1680

Table 4.6: Frequency Bands for Beams with Simply Supported Ends

NO	Frequency Bands (simply supported) (Hz)
1	52-252
2	248-648
3	640-1440

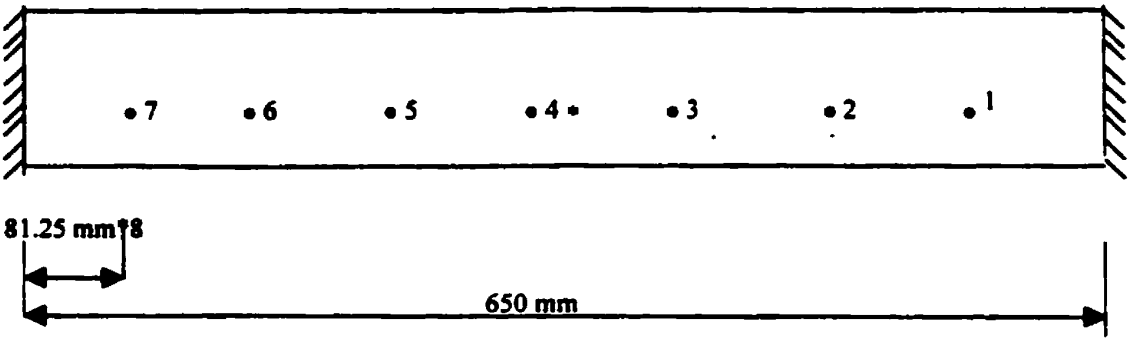

- Point of excitation
- Accelerometer point

Fig 4.3: Locations of Accelerometers.

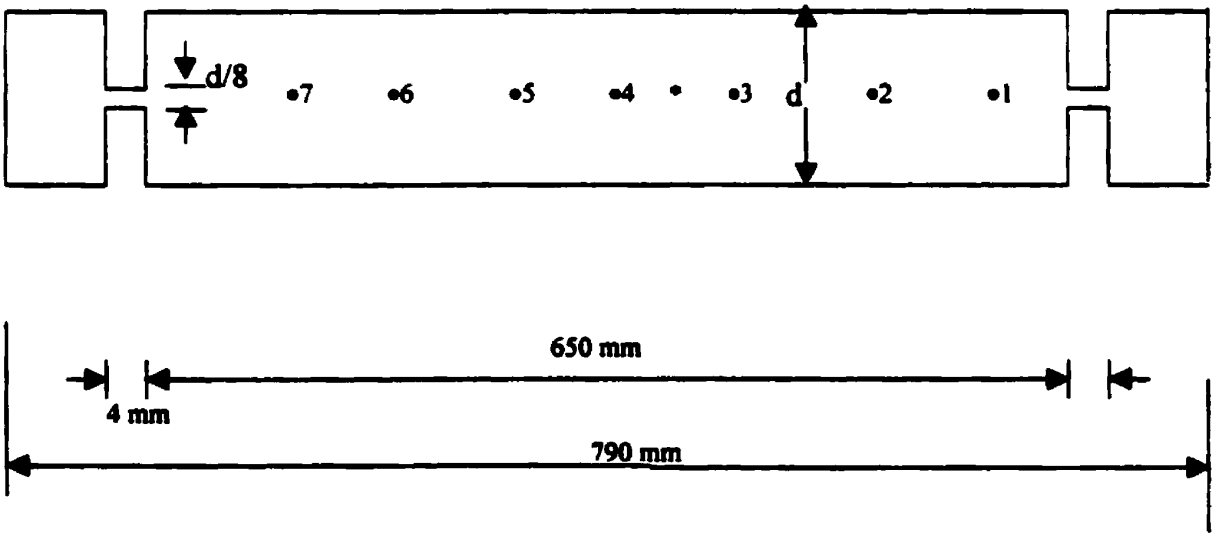

- Point of excitation
- Accelerometer point

Fig 4.4: Simply Supported Beam Model

Fig.4.5: Pictorial View of a Fixed Beam with a Crack at L/16

Fig.4.6: Pictorial View of the Simply Supported Beam with a Crack at L/16

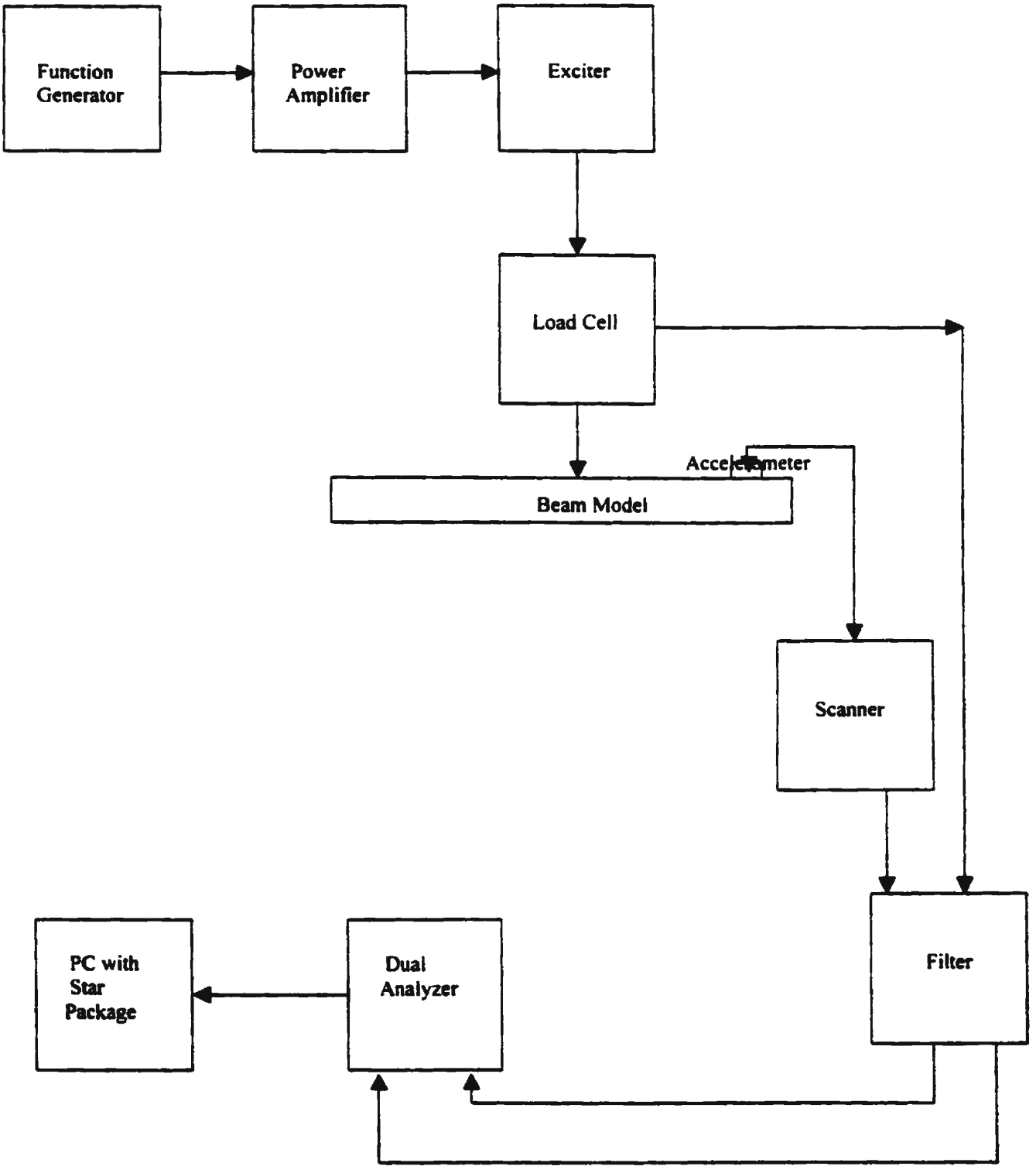

Fig 4.7: Block Diagram of the Experimental Set Up

Fig.4.8: Side View of the Experimental Set Up Showing the Electronic Equipment

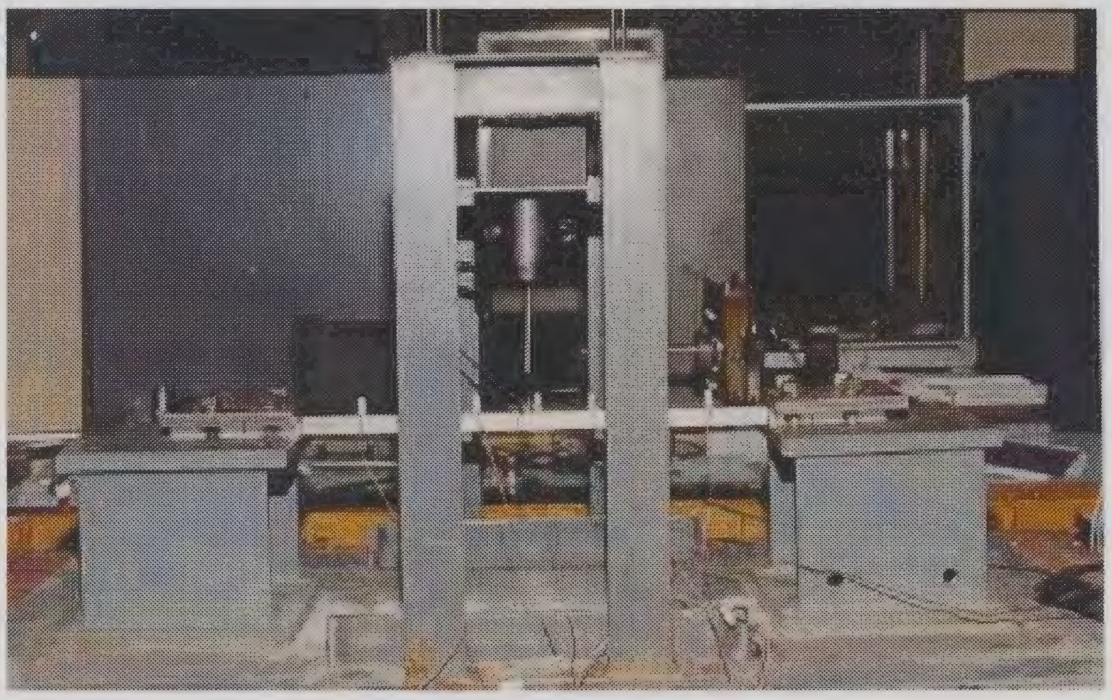

Fig.4.9: Side View of the Experimental Set Up Showing the Frame

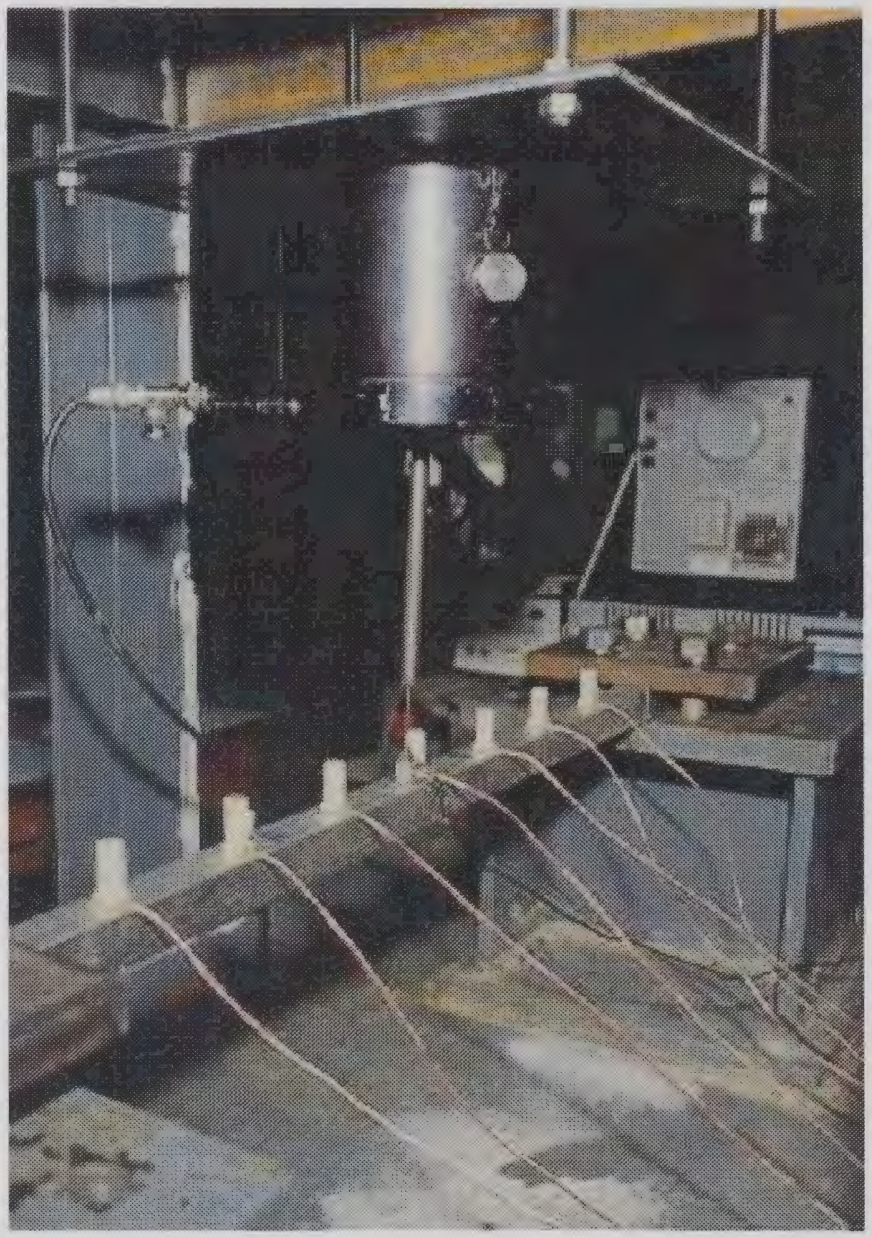

Fig. 4.10: Side View of the Experimental Set Up Showing a Connected Beam Model

4.4 Experimental Errors

There are several factors that affect the quality of the frequency response functions

Measured. These factors introduce errors into the measurements. Performing an experiment that is free of errors is almost unattainable in real life problems. However, some of the sources of errors are known, or traceable, and hence could be avoided, reduced or eliminated. Most errors are due to mistakes in measurements. A proper measuring method could prevent the introduction of errors such as overloading of input, extraneous signal pick-up, etc. Also, efforts should be made not to violate some assumptions on which the experimental study is based, as this also could be viewed as a mistake. For example, if a system is assumed to be linear, an introduction of nonlinearity can introduce energy shift from a frequency to several frequencies in such a way that it may be difficult to recognize. This causes a distortion in the modal parameters estimation.

4.4.1 Sources of Errors

In this experimental study, some errors were observed during experimentation, and some during the analysis. These errors could have resulted from any of the following:

i) Aliasing and leakage errors could be introduced by the signal analyzer during the digitization of the analog signals.

ii) Improper attachment of the accelerometers to the beam. The accelerometers must maintain proper contact with the surface of the structure, as misalignment will result in a poor contact region with corresponding loss of stiffness and a high response range. There are various ways by which this could be achieved.

Wax was used to attach the accelerometers during experimentation.

iii) Improper attachment of the exciter can affect the force transmitted. In this experimental study, the exciter was fixed on a plate with four threaded rods bolted to the frame. Loose bolts could affect the positioning of the exciter consequently affect the force transmitted.

iv) It was practically impossible to achieve ideal fixed ends, and simply supported ends. Hence, the boundary conditions used were approximate ones.

iii) Slight geometric discrepancies, in the aluminum beams used, were also observed. Though they appeared to be very small, they could have resulted in the differences of dynamic behavior of the uncracked beams, observed in results obtained for similar boundary conditions.

iv) The supports and the floor vibrations introduced unexpected response peaks. These were detected by observing the phase changes for all the peaks present in each frequency response taken. System vibrations produced a phase change of 180°, whereas those introduced by vibrations from other parts of the set-up did not give 180° phase change. When such peak was observed, the source was checked by the eighth accelerometer. Most of such undesirable peaks present were introduced by the floor and the support vibrations.

v) Improper calibrations of the load cell and the accelerometers would introduce errors into the measurement. These would greatly affect the experimental results, and the modal parameters estimated during the analysis.

Though errors are inevitable, they could, however, be reduced. Doing this, would minimize their effects on the experimental data obtained. A careful reviewing of the previous or related projects carried out by experienced personnel could be of great help.

4.4.2 Reduction of Errors

Five additional methods of reducing error in the frequency response are:

i) Using frequency response function estimation algorithms (H_v compared to H_1) will reduce the effects of leakage error in estimating frequency response function.

ii) Using signal averaging reduces errors due to bias and variance.

iii) Nonlinearity in the measurements can be easily verified using selective excitation. This also reduces bias error introduced by the system.

iv) Zooming the frequency band also increases the frequency resolution, which reduces the leakage, and bias errors as a result of the increased length of time sample.

v) The use of weighting functions (otherwise known as windows) primarily compensates for the bias error.

4.5 Additional Precautions

Apart from taking care of the points mentioned in the preceding section, which could serve as precautions, the following additional precautions should also be noted:

i) Reduction of the effects of noise by using a larger number of signals averaging.

ii) Prevention of overloading by proper monitoring of the input and output signals. using the oscilloscope must be done often.

iii) Assurance of proper control of the system input by exciting the system at the frequency range for which measurements are expected.

4.6 Summary

Detailed descriptions of the various instruments used have been given in this chapter. The need for proper functioning and adequate calibrations of the instruments cannot be over-emphasized. The results obtained were tabulated, plotted, and discussed in Chapter Five. A technique for identifying the location and the depth of an unknown crack is also presented in Chapter Five.

CHAPTER 5: RESULTS AND DISCUSSIONS

5.1 Results

Successful development of a monitoring procedure using parameters of dynamic responses as defect indicators relies mainly on its ability to monitor the natural frequencies and modes of the structure. The effects of a crack, present at different locations, on the first three natural frequencies, and corresponding vibrating modes of beams (with fixed and simply supported end conditions) have been determined in this research investigation. The theoretical analyses were previously carried out by Yang et al (2000).

Before the experiments were carried out, the first three natural frequencies of the beams (with fixed and simply supported ends) were calculated analytically. From the results obtained, it was decided that using a frequency range between 52 Hz and 2000 Hz for experimental measurements would be sufficient to include the first three natural frequencies and mode shapes.

The frequency response functions obtained were curve-fitted using the STAR Structural Analysis software package. The experimental data from the curve-fitted results were tabulated and plotted (in a three dimensional plot) in the form of frequency ratio (ω_c/ω) (ratio of the natural frequency of the cracked beam to that of the uncracked beam) versus

the crack depth ratio (a/h) [the ratio of the depth of a crack (a) to the thickness of the beam (h)] for various crack location ratios (c/l) (ratio of the location of the crack to the length of the beam). The results that could not be obtained due to experimental errors were regarded as non available (NA). Tables 5.1 to 5.6 show the variation of the frequency ratio as a function of the crack depth and crack location for beams with fixed and simply supported ends. It is to be noted here that during curve fitting, the values for the computed third natural frequency were approximate values due to the inability of the STAR software package to give figures with the number of digits greater than four. Hence, it was approximated to the nearest whole number.

5.2 Natural Frequencies

The first three natural frequencies obtained for different combinations of crack depth and crack location are given in Appendix A. Figs. 5.1 to 5.6 show the plots of the first three frequency ratios as a function of crack depths for some of the crack positions considered for each set of boundary conditions (seven locations for each set of boundary conditions). The complete set of plots of the variations of natural frequency ratio, as a function of crack depth (for all of the cases considered) are given in Appendix B. Figs. 5.7 and 5.8 illustrate the variations of the first two natural frequencies as a function of crack location for a fixed-end beam and for a simply supported beam when the crack depth ratio is 0.2, respectively. Note that due to insufficient data, the variation of the third natural frequency as a function of crack location could not be plotted accurately.

Table 5.1: Fundamental Natural Frequency Ratio (ω_c/ω) as a Function of Crack Location and Crack Depth for a Fixed Beam

a/h	c/l = 1/16	c/l = 3/16	c/l = 5/16	c/l = 7/16	c/l = 8/16	c/l = 11/16	c/l = 14/16
0	1	1	1	1	1	1	1
0.1	NA	1	1	0.9977	0.9985	1	0.9995
0.2	NA	1	0.9975	0.9900	0.9923	0.9989	0.9980
0.3	NA	1	0.9923	0.9767	0.9746	0.9952	0.9864
0.4	NA	1	0.9825	0.9666	0.9608	0.9815	0.9735
0.5	NA	1	0.9712	0.9222	0.9159	0.9773	0.9602
0.6	NA	1	0.9576	0.8744	0.8726	0.9686	0.9349
0.7	NA	1	0.9523	0.7986	0.8443	0.9318	0.9068

Table 5.2: Second Natural Frequency Ratio (ω_c/ω) as a Function of Crack Location and Crack Depth for a Fixed Beam

a/h	c/l = 1/16	c/l = 3/16	c/l = 5/16	c/l = 7/16	c/l = 8/16	c/l = 11/16	c/l = 14/16
0	1	1	1	1	1	1	1
0.1	0.9994	0.9982	0.9986	0.9989	1	0.9986	0.9988
0.2	0.9972	0.9938	0.9902	0.9972	1	0.9945	0.9910
0.3	0.9932	0.9875	0.9800	0.9955	1	0.9805	0.9849
0.4	0.9898	0.9864	0.9661	0.9911	1	0.9686	0.9815
0.5	0.9877	0.9596	0.9312	0.9832	1	0.9511	0.9779
0.6	0.9859	0.9498	0.9042	0.9774	1	0.9177	0.9719
0.7	0.9839	0.9284	0.8634	0.9729	1	0.9040	0.9683

Table 5.3: Third Natural Frequency Ratio (ω_c/ω) as a Function of Crack Location and Crack Depth for a Fixed Beam

a/h	c/l = 1/16	c/l = 3/16	c/l = 5/16	c/l = 7/16	c/l = 8/16	c/l = 11/16	c/l = 14/16
0	1	1	1	1	1	1	1
0.1	1	1	1	0.9932	0.9932	0.9932	1
0.2	1	0.9932	1	0.9864	0.9864	0.9932	1
0.3	1	0.9863	1	0.9796	0.9728	0.9864	1
0.4	1	0.9658	1	0.9728	0.9524	0.9864	1
0.5	0.9932	0.9521	0.9932	0.9524	0.9388	0.9864	0.9864
0.6	0.9932	0.9315	0.9932	0.9388	0.8980	0.9796	0.9864
0.7	0.9932	0.9041	0.9932	0.898	0.8844	0.9796	0.9864

Table 5.4: Fundamental Natural Frequency Ratio (ω_c/ω) as a Function of Crack Location and Crack Depth for a Simply Supported Beam

a/h	c/l = 1/16	c/l = 3/16	c/l = 5/16	c/l = 7/16	c/l = 8/16	c/l = 11/16	c/l = 14/16
0	1	1	1	1	1	1	1
0.1	1	0.9980	0.9923	0.9960	0.9940	0.9980	0.9994
0.2	1	0.9956	0.9892	0.9849	0.9770	0.9968	0.9990
0.3	1	0.9881	0.9758	0.9686	0.9530	0.9797	0.9978
0.4	0.9995	0.9781	0.9507	0.9418	0.9234	0.9617	0.9971
0.5	0.9974	0.9664	NA	0.8961	0.8724	0.9225	0.9945
0.6	0.9930	0.9371	0.8680	0.8318	0.8119	0.8546	0.9893
0.7	0.9848	0.8756	0.7896	0.7065	0.7085	0.7713	0.9829

Table 5.5: Second Natural Frequency Ratio (ω_c/ω) as a Function of Crack Location and Crack Depth for a Simply Supported Beam

a/h	c/l = 1/16	c/l = 3/16	c/l = 5/16	c/l = 7/16	c/l = 8/16	c/l = 11/16	c/l = 14/16
0	1	1	1	1	1	1	1
0.1	1	0.9962	0.9967	0.9994	0.9999	0.9979	0.9994
0.2	0.9991	0.9889	0.9903	0.9976	0.9998	0.9889	0.9975
0.3	0.9963	0.9712	0.9767	0.9952	0.9995	0.9774	0.9936
0.4	0.9817	0.9481	0.9524	0.9918	0.9995	0.9613	0.9905
0.5	0.9848	0.9232	NA	0.9861	0.9995	0.9337	0.9824
0.6	0.9714	0.8818	0.8902	0.9811	0.9990	0.8988	0.9696
0.7	0.9544	0.8175	0.8424	0.9704	0.9986	0.8693	0.9578

Table 5.6: Third Natural Frequency Ratio (ω_c/ω) as a Function of Crack Location and Crack Depth for a Simply Supported Beam

a/h	c/l = 1/16	c/l = 3/16	c/l = 5/16	c/l = 7/16	c/l = 8/16	c/l = 11/16	c/l = 14/16
0	1	1	1	1	1	1	1
0.1	1	1	1	1	1	1	1
0.2	0.9915	1	1	0.9915	0.9915	1	1
0.3	0.9915	1	1	0.9829	0.9744	0.9915	1
0.4	0.9829	0.9741	1	0.9744	0.9573	0.9915	0.9914
0.5	0.9658	0.9569	NA	0.9402	0.9402	0.9915	0.9828
0.6	0.9573	0.9483	1	0.8547	0.9145	0.9915	0.9483
0.7	0.9402	0.9310	1	0.8245	0.8014	0.9915	0.9310

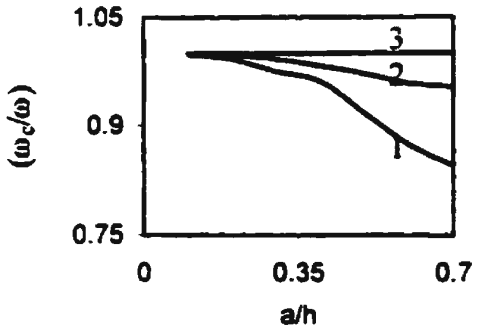

Fig.5.1: Fundamental Natural Frequency in Terms of Crack Depth for a Fixed–fixed Beam for Various Crack Position Ratio c/l (1→8/16; 2→5/16; 3→3/16)

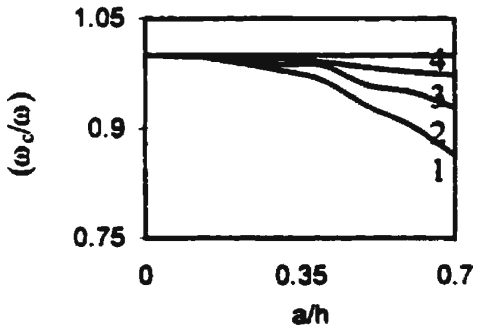

Fig.5.2: Second Natural Frequency in Terms of Crack Depth for a Fixed–fixed Beam for Various Crack Position Ratio c/l (1→5/16; 2→3/16; 3→7/16, 4→8/16)

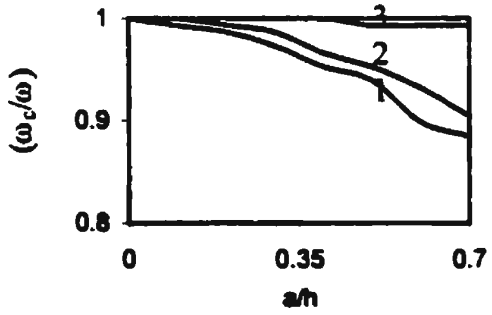

Fig.5.3: Third Natural Frequency in Terms of Crack Depth for a Fixed–fixed Beam for Various Crack Position Ratio c/l (1→8/16; 2→3/16; 3→5/16)

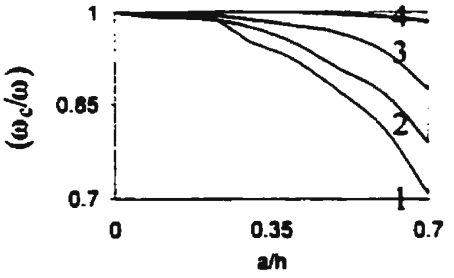

Fig.5.4: Fundamental Natural Frequency in Terms of Crack Depth for a Simply Supported Beam for Various Crack Position Ratio c/l (1→8/16; 2→5/16; 3→3/16; 4→1/16)

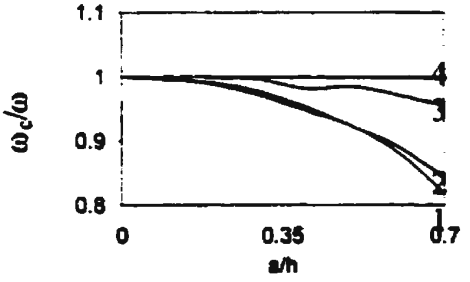

Fig.5.5: Second Natural Frequency in Terms of Crack Depth for a Simply Supported Beam for Various Crack Position Ratio c/l (1→3/16; 2→5/16; 3→1/16; 4→8/16)

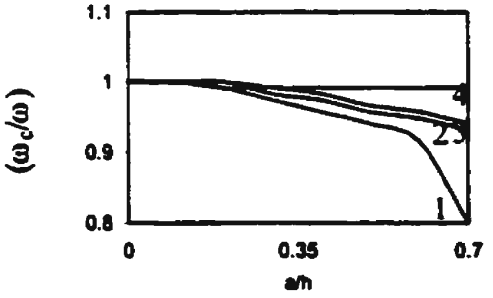

Fig.5.6: Third Natural Frequency in Terms of Crack Depth for a Simply Supported Beam for Various Crack Position Ratio c/l (1→8/16; 2→3/16; 3→1/16; 4→11/16)

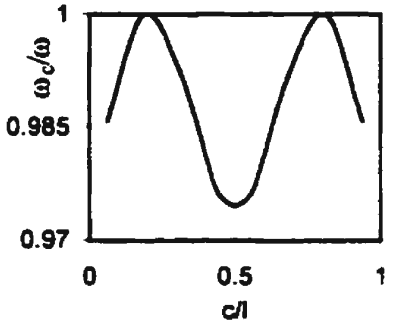

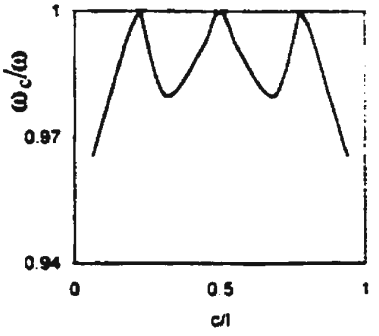

(a) First frequency (b) Second frequency

Fig 5.7: Variation of the First Two Natural Frequencies as a Function of Crack Location for a Fixed-end Beam (Crack Depth Ratio a/h = 0.2)

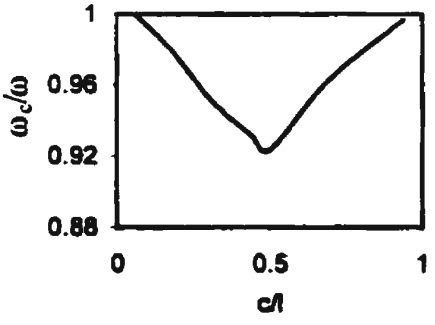

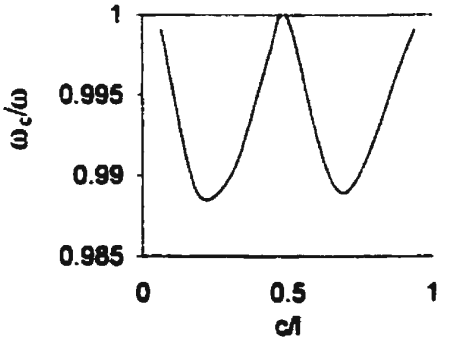

(a) First frequency (b) Second frequency

Fig 5.8: Variations of the First Two Natural Frequencies as a Function of Crack Location for a Simply Supported Beam (Crack Depth Ratio a/h = 0.2)

From the experimental results and plots. the following observations were made for all the cases considered:

i) For all the cases considered, the fundamental natural frequency was least affected when the crack was located at a position where the ratio of crack location to length the beam (c/l) was 1/16, and mostly affected when the crack was located at the center (c/l = 8/16) for a beam with simply supported ends. In case of a beam with fixed ends, the fundamental natural frequency was least affected (mostly) when c/l was 3/16, and mostly affected at the center (actually the largest effect will be felt at the fixed ends, but, no measurements could be made at that location). The results for c/l = 1/16 in a fixed beam were not available due to experimental errors. Hence, it could be inferred (from the measured data) that the fundamental frequency decreases significantly as the crack location moves towards the center of the crack with the highest decrease occurring for a centrally located crack, with the exception of a crack located at the supports, which could not be considered in this study.

ii) The second natural frequency was almost unaffected for a crack located at the center of a fixed beam or a simply supported beam; the reason for this zero influence was that the nodal point for the second mode was located at the center for both types of beams.

iii) The third natural frequencies of both the fixed and the simply supported beams changed rapidly for a crack located at the center.

iv) Due to shifts in the nodal positions (as a consequence of cracking) of the second, and the third modes, the changes in the higher natural frequencies depended on how close the crack location was to the mode shape nodes. Consequently, it could be observed from the Tables 5.2, 5.3, 5.5 and 5.6 that the trend of changes in the second, and the third frequencies are not monotonic, as we have in the first natural frequency. For the second mode, this is due to the fact that the center was the nodal point for the second bending mode.

v) From the results obtained, it is observed, for example, that when the crack depth ratio is 0.6, the third natural frequency was comparatively much less affected than the first and second frequencies for a crack located at 203mm (c/l = 5/16) from one end of the simply supported beam; but, it is highly affected for other crack locations (see Table 5.6). This could be explained by the fact that decrease in frequencies is greatest for a crack located where the bending moment is greatest. It appears therefore that the change in frequencies is not only a function of crack depth and crack location, but also of the mode number.

vi) For a few of the cases considered, the frequency remained unchanged until a certain value of crack depth ratio was attained, after which, the frequency decreased rapidly. For example, in the simply supported beam, at a crack location of 3/16 of the length of the beam, the third natural frequency was almost unchanged until a crack depth ratio of 3/10 was achieved; for greater values of crack depth ratios, the frequencies decreased rapidly (see Table 5.6).

As stated earlier, the decrease in the fundamental natural frequency was greatest when the

crack occurred at the middle point. This could be explained by the fact that the bending moment was the largest at the middle point (where the amplitude of the first mode shape is greatest) for the first mode, thereby, resulting in a greater loss of bending stiffness due to crack. However, the second, and third modes were less affected at this location. The frequencies decreased by about 12.7% & 6.0% (for the simply supported beam), and 8.4% & 6.1% (for the fixed beam) for the first and third modes, respectively, as the crack grew to half of the beam depth (for crack at the center). In Yang et al (cited earlier in the thesis), the theoretical fundamental and the third natural frequencies were shown to decrease respectively, by 11.6% & 8.2%, for a center-cracked simply supported beam. These values are very close to the present experimental values.

Based on the experimental data, and plots, and the observations above, numerous inferences could be made such as follows:

a) For most of the cases considered, the slopes of frequency ratio versus crack depth curves were very small for small crack depth ratios. This implies that small cracks have little effects on the sensitivities of natural frequencies. Hence, using only results based on frequency changes alone for identifying cracks in most practical problems may be misleading as it is very unlikely to have large cracks. It is therefore advisable to use both frequencies and mode shapes changes.
b) For a particular mode, the decrease in frequency and change in mode shape become noticeable as the crack grew bigger.

c) For a given crack depth ratio, the location of the crack greatly affects the dynamic response of the cracked beam.

d) Investigating the mode of vibration at some crack location may indicate a pure bending mode for small crack depth ratios, but, as the crack grows in size, the bending mode may contain a significant influence of longitudinal vibration mode also (occurrence of coupling).

From the above observations, it could be stated that knowing the crack position could result in accurate prediction of its extent in a crack identification problem by using only one mode. Otherwise, it becomes very difficult, as this could be misleading. As an example, the use of data obtained for the third mode of the simply supported beam located at 203 mm (c/l = 5/16) will lead to a conclusion that the beam is undamaged because there is no frequency change for all the crack depths considered. Consequently viewing different modes separately is likely to indicate different crack depths, and crack positions. In general, the higher the number of modes used, the greater the degree of accuracy, and dependability of results.

5.3 Changes in Mode Shapes

The mode shapes obtained for some of the cases considered for both the simply supported and fixed beams are shown in Figs. 5.9 to 5.11. For most of the cases considered, as the crack grows, the mode shapes undergo a highly noticeable change close to the crack location area. The shape becomes almost discontinuous at the crack location. This could

be likened to a beam with a hinge at the crack location. In some cases, as the crack grows deeper, (when the crack depth is equal to or greater than 0.5), there are shifts in the position of the nodes for the second, and third modes. It appears as if changes in the natural frequency and mode shape depended on how close the crack was to nodes of mode shapes for higher modes. Thus, based on the observed changes in the natural frequencies, and mode shapes, the crack position, and crack depth can be estimated.

For a crack located at the center of a fixed-fixed beam, the second mode is almost unaffected for most of the crack ratios considered as shown in Fig. 5.10. The third mode deformations are affected to a greater extent than the first mode. It is also noted that the changes in the deflection shape for first and third modes as a result of a centrally-located crack become significant when the crack ratio is greater than 0.3 (see Fig. 5.10). For high values of crack ratios, the mode shape undergoes severe changes close to the crack location.

5.4 Crack Identification Technique

As stated earlier, both the crack location and the crack depth influence the changes in the natural frequencies of a cracked beam. Consequently a particular frequency could correspond to different crack locations and crack depths. This can be observed from the three-dimensional plots of the first three natural frequencies of beams with fixed and simply supported ends shown in Figs. 5.12 and 5.13, respectively. On this basis, a contour line which has the same normalized frequency change resulting from combining

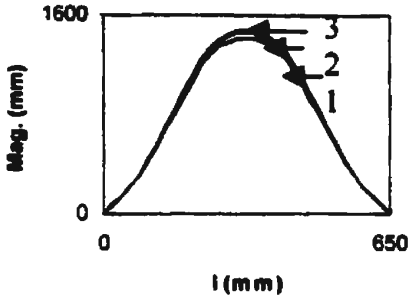

(a) First mode

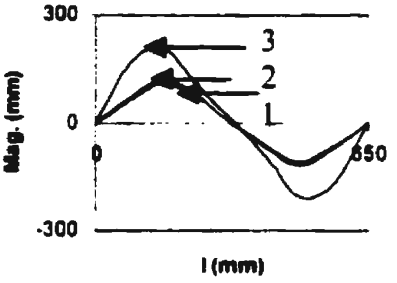

(b) Second mode

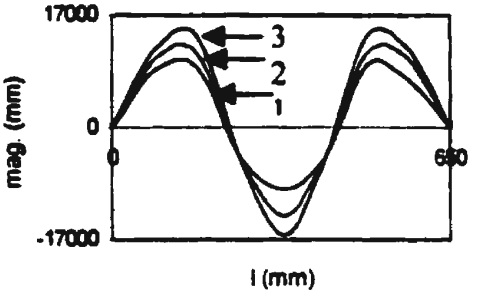

(c) Third mode

Fig. 5.9: Mode Shapes of a Fixed Beam with Crack Location c/l = 3/16 for Different Crack Depths (1: a/h = 0, Uncraked; 2: a/h = 0.3; 3: a/h = 0.5)

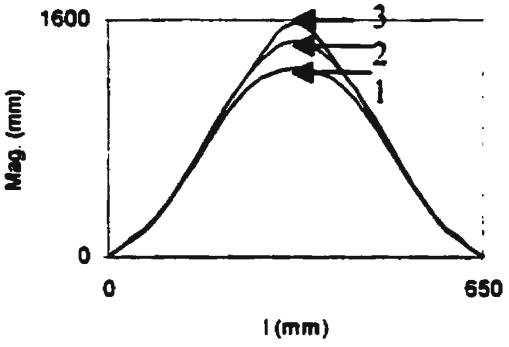

(a) First mode

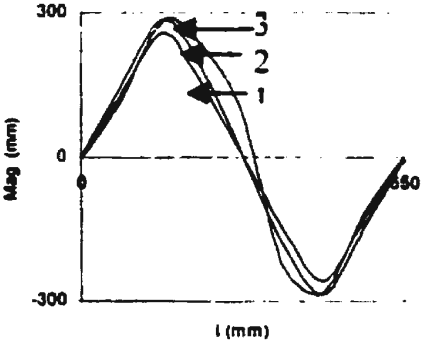

(b) Second mode

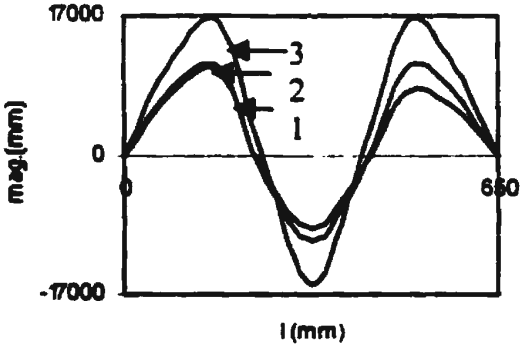

(C) Third mode

Fig. 5.10: Mode Shapes of a Fixed Beam with Crack Location c/l = 8/16 for Different Crack Depths (1: a/h = 0, Uncraked; 2: a/h = 0.3; 3: a/h = 0.5)

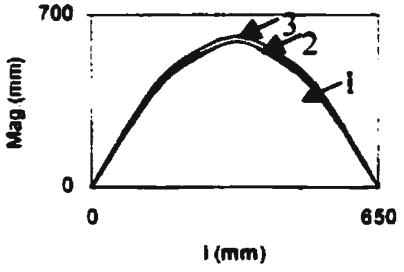

(a) First mode

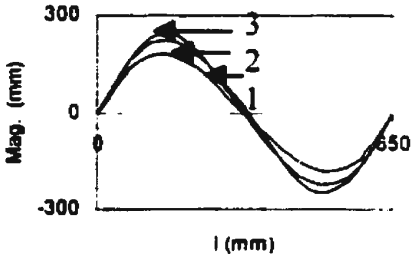

(b) Second mode

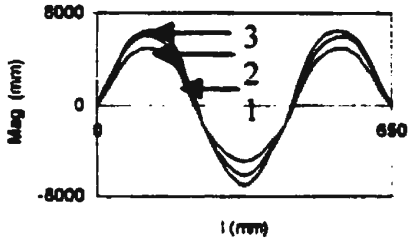

(c) Third mode

Fig.5.11: Mode Shapes of a Simply Supported Beam with Crack Location c/l = 1/16 for Different Crack Depths (1: a/h = 0, Uncraked; 2: a/h = 0.3; 3: a/h = 0.5)

different crack depths and crack locations could be plotted in a curve with crack location and crack depth as its axes. For illustrative purposes, the contour lines for the first and the second modes of simply supported and fixed end beams are shown in Figs. 5.14 and 5.15. respectively. The normalized frequencies shown in the figures are 0.9900 (a decrease of 1% in frequency) for the first mode and 0.9800 (a decrease of 2 % in frequency) for the second mode (these values were obtained by linear interpolation from adjacent values). Any point on the above contour line is a possible crack location and crack depth.

To identify the presence of one or more cracks in the beam, a very vital step is to measure a sufficient number of natural frequencies of the beam, and then use the technique explained in this section to estimate the crack location(s), and depth(s). The number of cracks on the beam determines the required number of frequencies and mode shapes to be measured or computed. Measuring the first three natural frequencies will be sufficient to determine the crack location and the crack depth for a beam with a single crack.

For a beam with a single crack with unknown parameters, the following steps are essential to predict the location, and the depth:

i) Measurements of the first three natural frequencies;

i) Normalization of the measured frequencies;

ii) Plotting of contour lines from different modes on the same axes; and

iii) Location of the point(s) of intersection of the different contour lines. The point(s) of intersection indicate(s) the location(s), and depth(s).

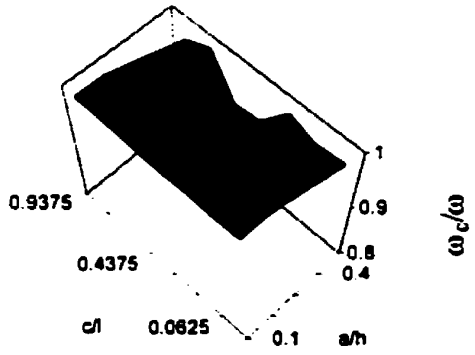

(a) First Frequency

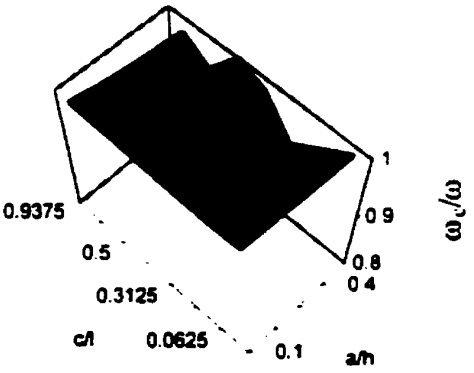

(b) Second frequency

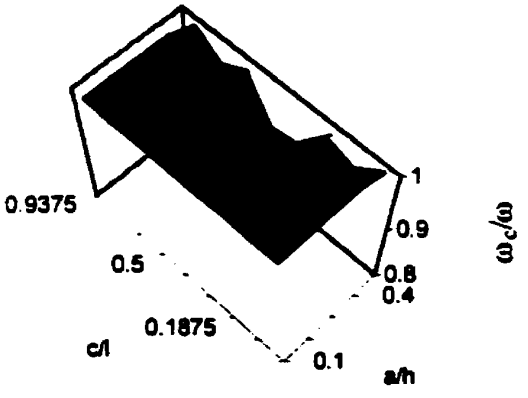

(c) Third frequency

Fig. 5.12: Three-dimensional Plots of Frequency Ratio versus Crack Location, and Crack Depth for a Fixed-end Beam

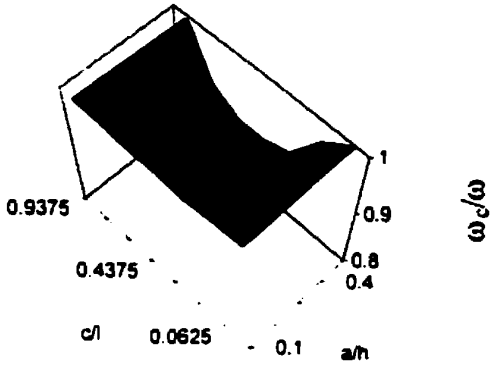

(a) First frequency

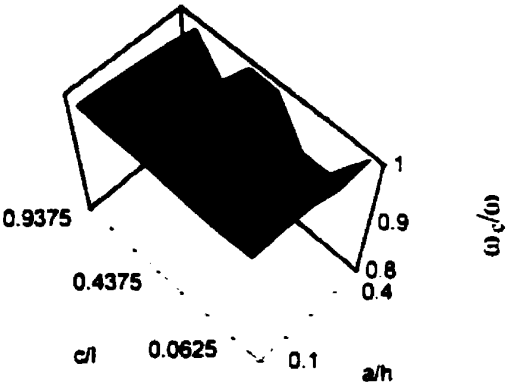

(b) Second frequency

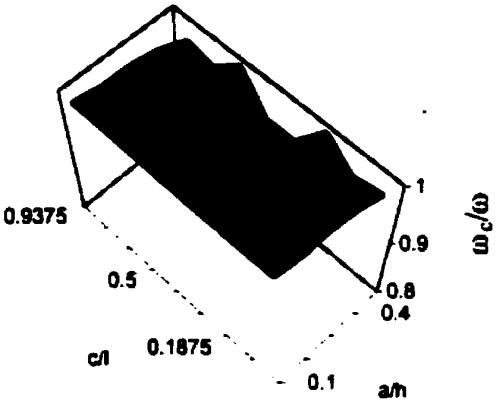

(c) Third frequency

Fig. 5.13: Three-dimensional Plots of Frequency Ratio versus Crack Location, and Crack Depth for a Simply Supported Beam

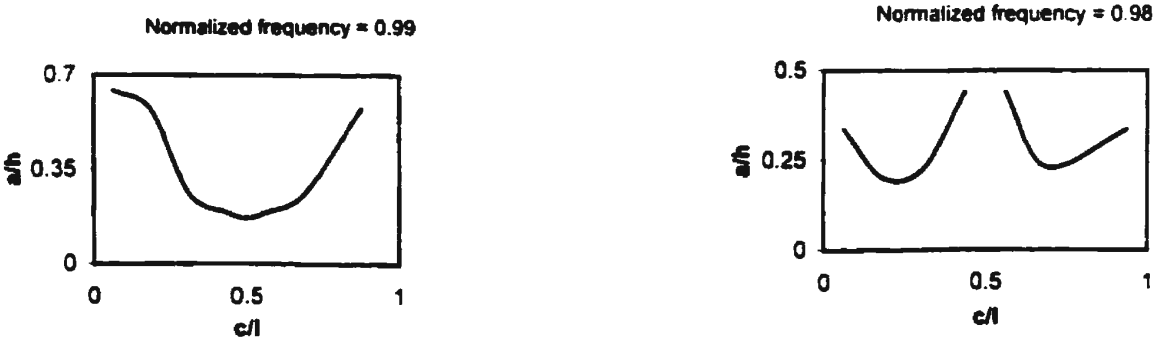

(a) First frequency (b) Second frequency

Fig 5.14: Frequency Contours Plots for a Simply Supported Beam

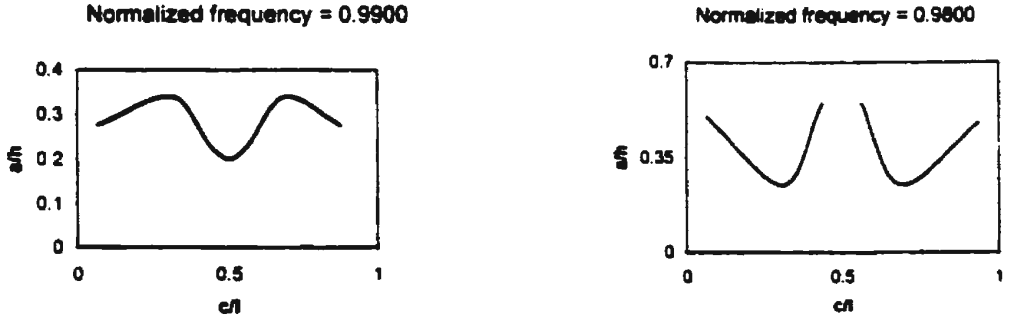

(a) First frequency (b) Second frequency

Fig. 5.15: Frequency Contour Plots for a Fixed–end Beam

The steps outlined above can be used to obtain similar curves once the changes in the natural frequencies of the beam are known either through experimentation or computation.

Using measurements based only on the first two natural frequencies may not be sufficient to estimate a unique crack location, and crack depth for a beam with one crack, because, more than one intersection point may be obtained. Consequently, the third natural frequency is also essential to obtain a unique value that indicates the exact crack location and crack depth.

From Tables 5.1 to 5.3, for a crack depth ratio of 0.1 located at a distance of 7/16 the length of the beam, the normalized frequencies are 0.9977 (i.e. a decrease of 0.23 % in frequency) for the first mode, 0.9989 for the second mode and 0.9932 for the third mode. The contour lines with the values of 0.9977, 0.9989 and 0.9932 were retrieved (by linear interpolation) from the first three modes and plotted on the same axes as shown in Fig 5.16. From the figure it could be observed that there are four intersection points in the contour lines of the first and the second mode. Consequently the contour of the third mode is used to identify the crack location (c/l = 7/16) and the crack depth ratio (a/h = 0.3), uniquely. The three contour lines gave just one common point of intersection, which indicates the crack location and the crack depth. As mentioned earlier, the contour lines obtained are not perfectly symmetrical due to the limited number of measuring points considered during the experimentation. Similar procedures were applied to a simply supported beam (with a crack depth of a/h = 0.3 and located at c/l = 3/16) in which the

normalized frequencies were 0.9881, 0.9712 and 0.9828 for the first three modes, respectively. The contour lines obtained, which indicates the crack location (c/l = 3/16) and the crack depth (a/h = 0.3), are shown in Fig 5.17.

This technique appears to be good in identifying cracks in beams, because, a crack will definitely belong to a contour line for each mode, and measuring the lowest three natural frequencies in a beam is not a difficult task as long as measuring errors are reduced to a minimum or eliminated. In a situation whereby the crack location coincides with a vibration node, the contour line tends to disappear, and no intersections can be obtained. In such a case, higher modes may have to be obtained to predict the location, and the depth of the crack.

5.5 **Frequency Response Functions**

Various methods are available to estimate the modal parameters of fixed–fixed and simply supported beams. However for these experimental investigations, Frequency Response Functions (FRF) were used. Frequency Response Functions (FRF) offer a number of advantages such as easy measurement, broad band excitation methods, reduction of measurement errors by averaging methods, reduction of non linearity effects of the structure by random excitation and averaging, easy measurements of acceleration response which can be converted to displacement and velocity responses etc.

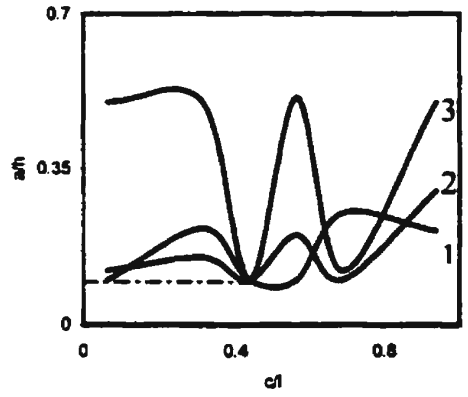

...Identified crack (c/l = 7/16; a/h = 0.1)

Fig. 5.16: Crack Identification Technique by using Frequency Contours of the First Three Modes of a Fixed Beam [1: Mode 1 Normalized Frequency (0.9977); 2 : Mode 2, Normalized Frequency (0.9989); 3: Mode 3, Normalized Frequency (0.9932)]

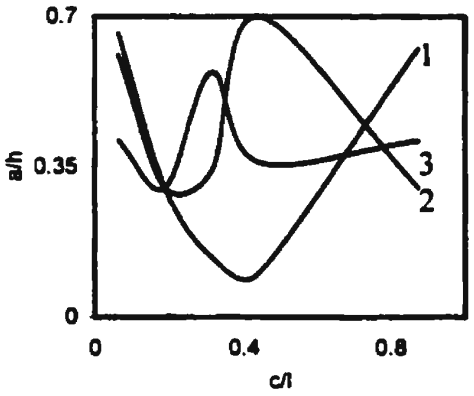

.... Identified crack (c/l = 3/16; a/h = 0.3)

Fig. 5.17: Crack Identification Technique using Frequency Contours of First Three Modes in a Simply Supported Beam [1: Mode 1 Normalized Frequency (0.9981); 2: Mode 2 Normalized Frequency (0.9712); 3: Mode 3 Normalized Frequency (0.9828)]

As stated earlier, several frequency response functions were obtained in these experimental investigations for a combination of different crack depths and crack locations. The measured frequency response functions were curve-fitted to obtain the modal parameters (frequency and mode shapes) which were used in this chapter for crack detection. Due to the fact that the natural frequencies are global properties of the beams, their shifts could be observed by using the FRF measurements taken from virtually any point on the beams. The frequency response functions obtained (at least twenty-one for each of the fourteen models) were too numerous to be shown fully in this thesis. However some of the measured frequency response functions are presented in this section to illustrate the shifts that occurred in the amplitudes and frequencies for the first three modes.

Figs. 5.18 to 5.20 show typical frequency response functions measured for the first three modes of vibration for different crack depth ratios, for a crack located at the center of a fixed beam. From the figures, it could be observed that the fundamental frequency ratios show a vivid downward trend (in its shifting) as the crack depth ratio increases. The amplitude of the FRF also shows a decreasing trend, as the crack grows in size. Comparing Fig. 5.18 to Figs. 5.19 and 5.20, it could be inferred that the frequency shift for the first mode was greater than for any of the remaining higher modes for a centrally located crack. This inference has been noted earlier in this chapter. Fig. 5.19 shows that the shift in the frequency response function of the second mode was random and not very significant. No trend was evident for the second mode; this was due to the fact that the nodal point for the second mode occurred at the crack location point, viz., the center of

the beam and as such no change could be properly detected. This has also been noted in the earlier part of this chapter. The shift in mode three could be observed in Fig. 5.20. It shows a slightly lower trend in the frequency shift than the first mode. The loss in the stiffness at this location (center of the beam) has resulted in the frequency change observed. The amplitude changes observed for the third mode do not show trends similar to mode two for increasing crack depth. The peak noted at a frequency of 1031 Hz in Fig. 5.20 was one of the resonance peak introduced into the measurements by floor vibration. This was detected by using the eighth accelerometer (as mentioned earlier in the thesis).

The shift in the frequencies is also a function of the crack location and the mode number. This is illustrated by observing the shifts in the first three frequencies at other locations in the simply supported and fixed beams. Fig. 5.21 to 5.26 show the frequency response functions for the first three modes of vibration in a simply supported beam for cracks located at crack length ratios (c/l) of 3/16 and 5/16. While there were significant shifts in the second and the third modes (as the crack depth ratio increases) for a crack located at c/l equals 3/16, there was no significant shift in the first mode at this location of the crack. Similarly, for a crack located at c/l equals 5/16, there were significant shifts in the first, and second modes, but, no significant shift in the third mode (since this point is very close to one of the nodes of the third mode).

5.6 Measurement Errors

As stated in chapter four, the acquired frequency response functions were subject to some

errors. This was noted particularly while taking the measurement of the natural frequencies of the uncracked beams. Though, every effort was made (by applying equal torque) to ensure similar boundary conditions for each set of aluminum beams used, slight discrepancies were still observed for the natural frequencies of the uncracked beam for different locations. This might also be caused by the slight dimensional differences in the cross sections of some of the beams used. For example, from Table A1 in Appendix A, the fundamental frequencies for the uncracked fixed-fixed beam, when the crack locations were 1/16 and 5/16 of the length of the beam, were 263.91 and 263.57. respectively. The percentage error (about 0.12% in this case) was very small. In order to minimize the effects of the errors, the analysis was done by using the normalized frequencies (discussed in this chapter).

5.7 Comparison of the Experimental and Theoretical Results

As stated earlier in this chapter, the theoretical analyses were carried out by Yang et al (2000). In this paper, an energy-based numerical model was developed to investigate the influence of cracks on the structural dynamic characteristics during the vibration of a beam. Upon the determination of strain energy in the cracked beam, the equivalent bending stiffness over the beam length was computed. The cracked beam was then taken as a continuous system with varying moment of inertia, and equations of transverse vibration were obtained for a rectangular beam containing one or two cracks ratio was calculated.

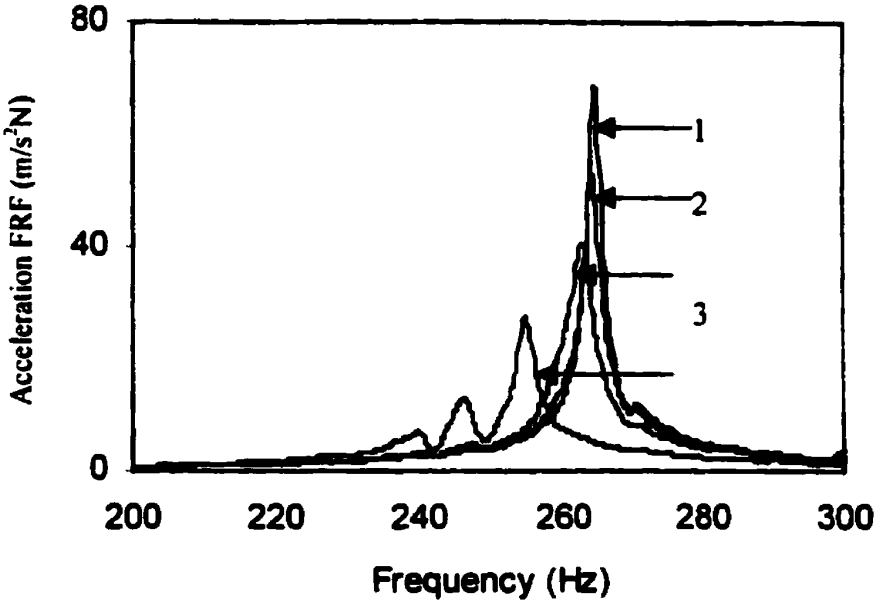

Fig. 5.18: Fundamental Natural Frequency Shifts and FRF Amplitude Reduction for a Crack Located at the Center of a Fixed Beam for Various Crack Depth Ratios a/h (1:Uncracked; 2: a/h = 0.1; 3, a/h = 0.2; 4: a/h = 0.4)

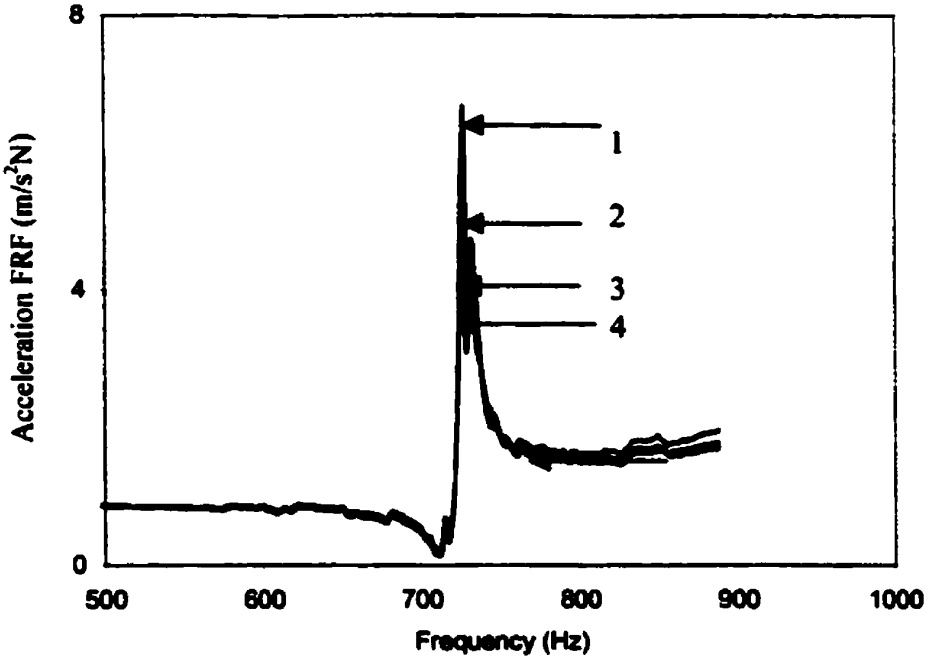

Fig. 5.19: Second Natural Frequency Shifts and FRF Amplitude Reduction for a Crack Located at the Center of a Fixed Beam for Various Crack Depth Ratios a/h (1:Uncracked; 2: a/h = 0.1; 3, a/h = 0.2; 4: a/h = 0.4)

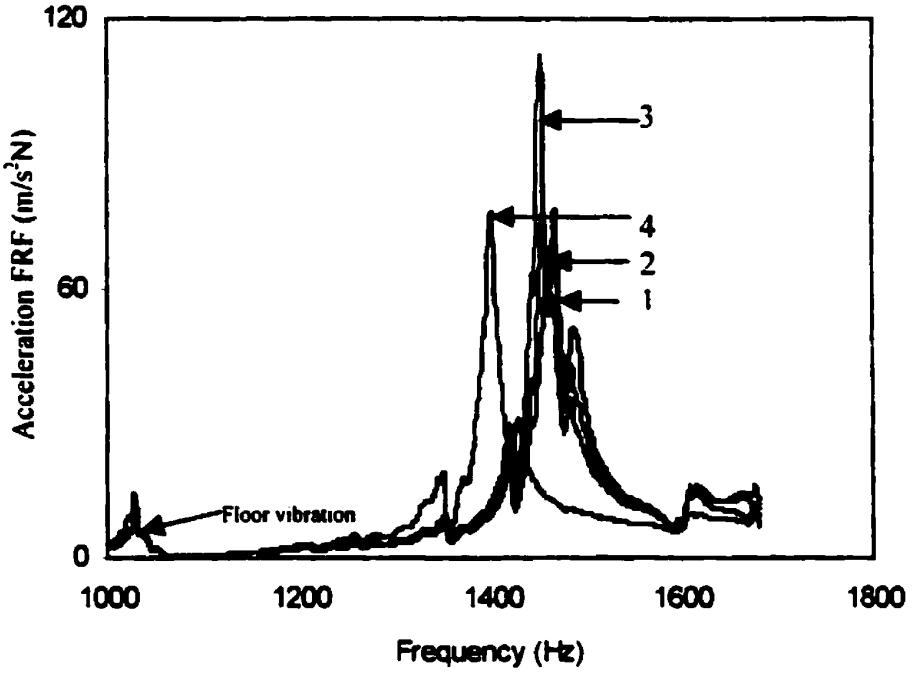

Fig. 5.20: Third Natural Frequency Shifts and FRF Amplitude Reduction for a Crack Located at the Center of a Fixed Beam for Various Crack Depth Ratios a/h (1:Uncracked; 2: a/h = 0.1; 3. a/h = 0.2; 4: a/h = 0.4)

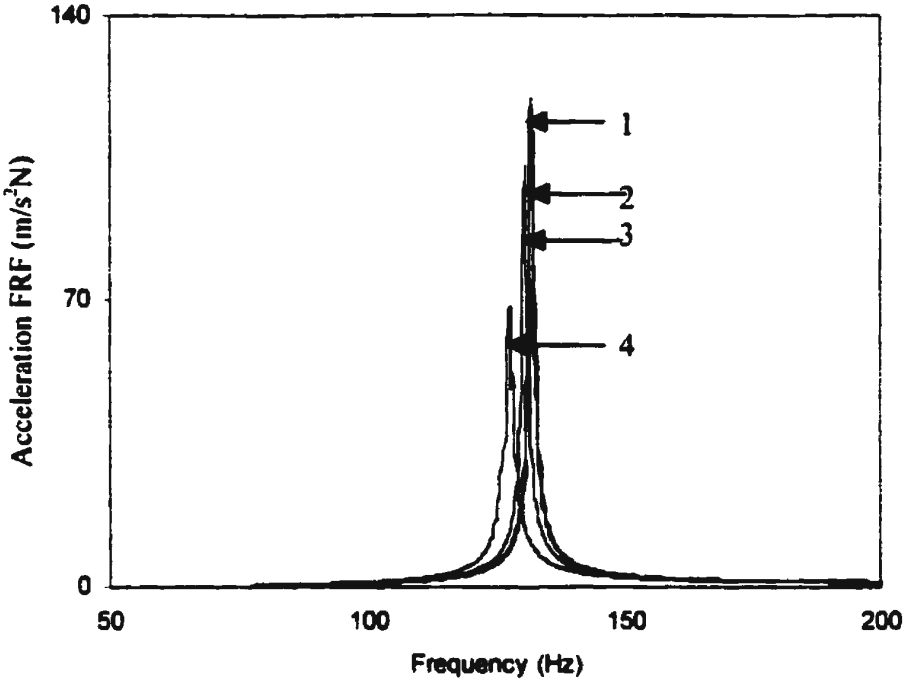

Fig. 5.21: Fundamental Natural Frequency Shifts and FRF Amplitude Reduction for a Crack Located at a Crack Length Ratio c/l of 3/16 of a Simply Supported Beam for Various Crack Depth Ratios a/h (1:Uncracked; 2: a/h = 0.1; 3, a/h = 0.2; 4: a/h = 0.4)

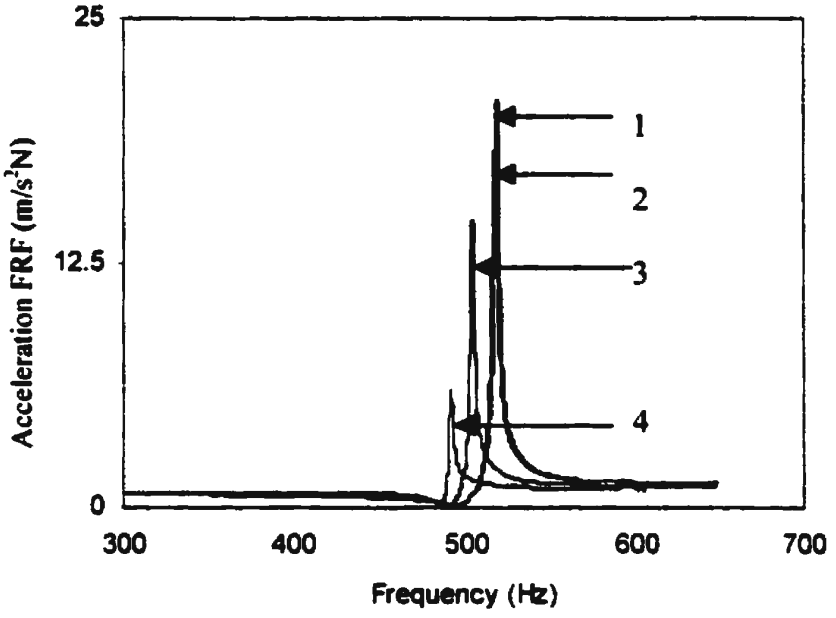

Fig. 5.22: Second Natural Frequency Shifts and FRF Amplitude Reduction for a Crack Located at a Crack Length Ratio c/l of 3/16 of a Simply Supported Beam for Various Crack Depth Ratios a/h (1:Uncracked; 2: a/h = 0.1; 3, a/h = 0.2; 4: a/h = 0.4)

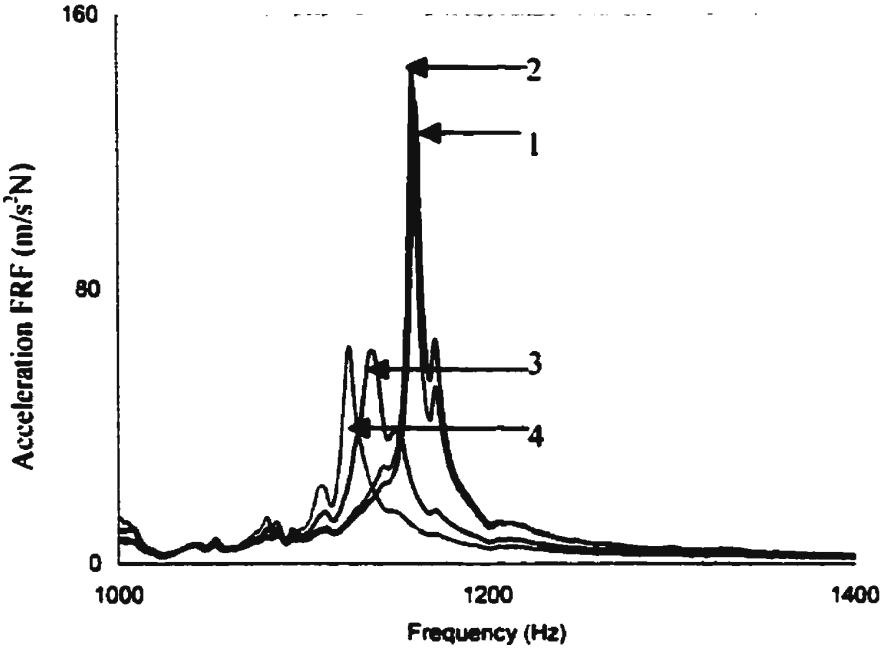

Fig. 5.23: Third Natural Frequency Shifts and FRF Amplitude Reduction for a Crack Located at a Crack Length Ratio c/l of 3/16 of a Simply Supported Beam for Various Crack Depth Ratios a/h (1:Uncracked; 2: a/h = 0.1; 3, a/h = 0.2; 4: a/h = 0.4)

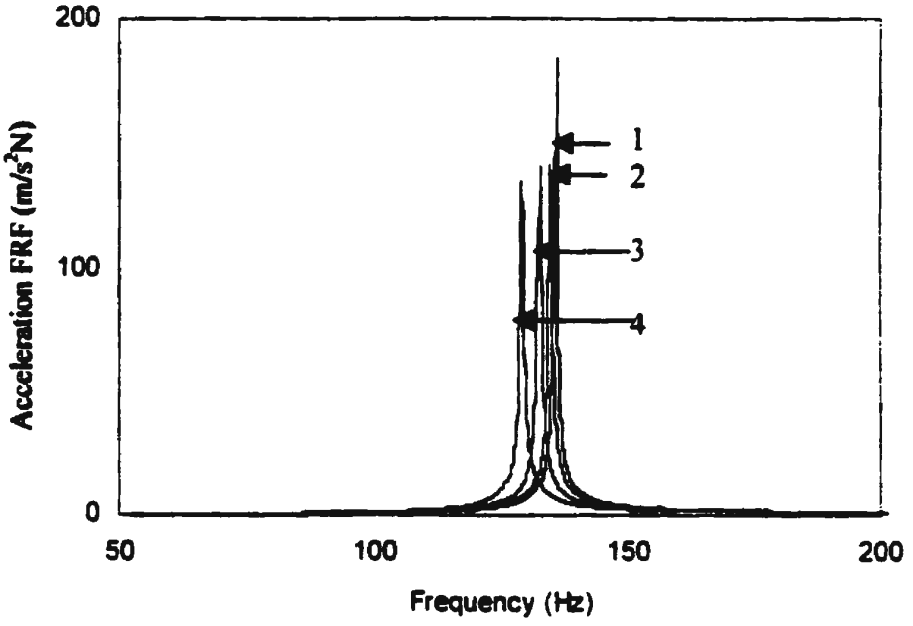

Fig. 5.24: Fundamental Natural Frequency Shifts and FRF Amplitude Reduction for a Crack Located at a Crack Length Ratio c/l of 5/16 of a Simply Supported Beam for Various Crack Depth Ratios a/h (1:Uncracked; 2: a/h = 0.1; 3, a/h = 0.2; 4: a/h = 0.4)

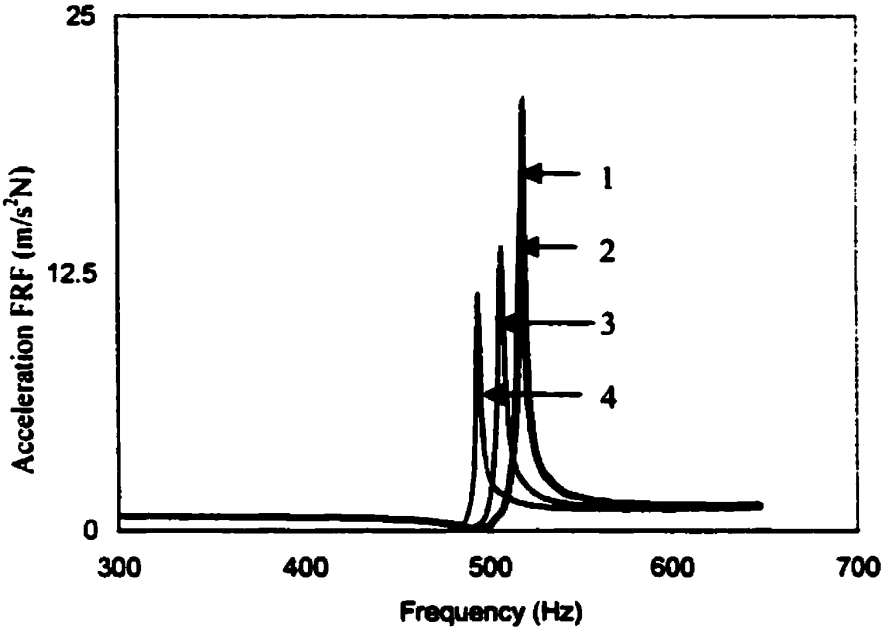

Fig. 5.25: Second Natural Frequency Shifts and FRF Amplitude Reduction for a Crack Located at a Crack Length Ratio c/l of 5/16 of a Simply Supported Beam for Various Crack Depth Ratios a/h (1:Uncracked; 2: a/h = 0.1; 3, a/h = 0.2; 4: a/h = 0.4)

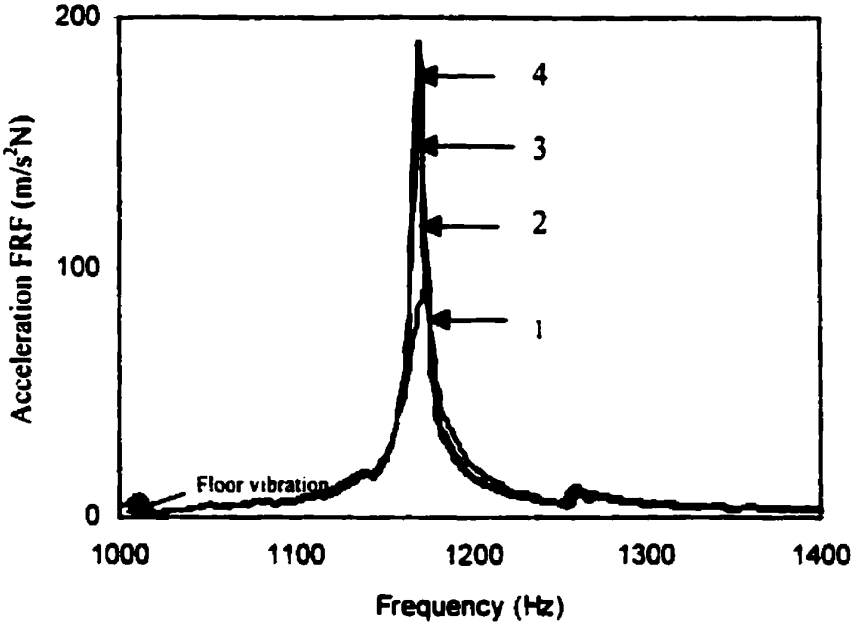

Fig. 5.26: Third Natural Frequency Shifts and FRF Amplitude Reduction for a Crack Located at a Crack Length Ratio c/l of 5/16 of a Simply Supported Beam for Various Crack Depth Ratios a/h (1:Uncracked; 2: a/h = 0.1; 3, a/h = 0.2; 4: a/h = 0.4)

The natural frequency ratios presented in the paper were for a crack located at the center of the beam for both the simply supported and the fixed beams. Tables 5.7 and 5.8 show the results obtained theoretically and experimentally. The results compare very well. The results (theoretical and experimental) were also presented graphically in Figures 5.27 and 5.28. The test results seemed to be slightly lower than the theoretical values (except for the second mode).

Appendix C shows some of the results obtained theoretically. Most of the curves in Appendix C show a similar pattern to the curves in Chapter five that have the same crack conditions.

5.8 Summary

The results obtained in this experimental study have been presented and analyzed in this chapter. It was noted (depending on crack location, crack depth, and mode number) that there could be significant changes in natural frequencies and mode shapes and also in the frequency response functions. Based on the observed changes in natural frequencies of the first three modes of vibration, a technique was developed to estimate a crack location and depth. It could also be seen that the theoretical and experimental results show a good agreement. Chapter Six gives the conclusions and recommendations based on the experimental investigations.

Table 5.7: Comparison of the Experimental and Theoretical Natural Frequencies of Fixed-Fixed Beams for a Centrally-located Crack (c/l = 0.5) having Different Crack Depths Ratios (a/h)

Crack Depth Ratio	First Mode			Second Mode			Third Mode		
	Exp♣.	TR♦.	(Rel. Diff.)♥ (%)	Exp♣.	TR♦.	(Rel. Diff.)♥ (%)	Exp♣.	TR♦.	(Rel. Diff.)♥ (%)
0.1	0.9985	0.9987	0.020	1.0000	1.0000	0.000	0.9932	0.9938	0.060
0.2	0.9923	0.9935	0.120	1.0000	1.0000	0.000	0.9864	0.9870	0.060
0.3	0.9746	0.9750	0.010	1.0000	1.0000	0.000	0.9728	0.9740	0.120
0.4	0.9608	0.9614	0.006	1.0000	0.9998	0.020	0.9524	0.9532	0.080
0.5	0.9159	0.9200	0.440	1.0000	0.9992	0.080	0.9388	0.9400	0.130

Table 5.8: Comparison of the Experimental and Theoretical Natural Frequencies of Simply Supported Beams for a Centrally-located Crack (c/l = 0.5) having Different Crack Depths Ratios (a/h)

Crack Depth Ratio	First Mode			Second Mode			Third Mode		
	Exp♣.	TR♦.	(Rel. Diff.)♥ (%)	Exp♣.	TR♦.	(Rel. Diff.)♥ (%)	Exp♣.	TR♦.	(Rel. Diff.)♥ (%)
0.1	0.9940	0.9946	0.060	0.9999	1.0000	0.010	1.0000	1.0000	0.000
0.2	0.9770	0.9780	0.100	0.9998	0.9997	0.010	0.9915	0.9920	0.050
0.3	0.9530	0.9536	0.060	0.9995	0.9993	0.020	0.9744	0.9750	0.060
0.4	0.9234	0.9240	0.060	0.9995	0.9990	0.050	0.9573	0.9580	0.070
0.5	0.8724	0.8730	0.070	0.9995	0.9988	0.070	09402	0.9410	0.080

where: ♣ = Experimental values; ♦ = Theoretical values; ♥ = Relative Difference (absolute relative difference expressed as a percentage)

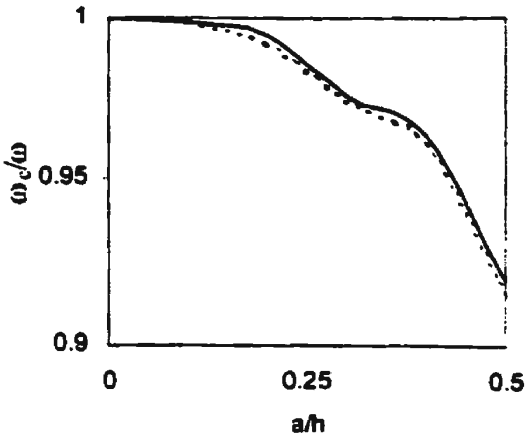

(a) First Frequency Ratio

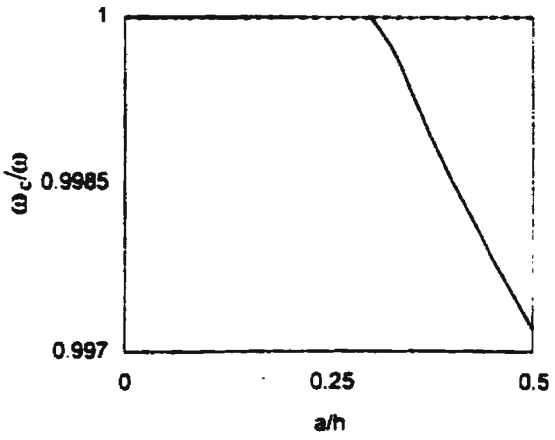

(b) Second Frequency Ratio

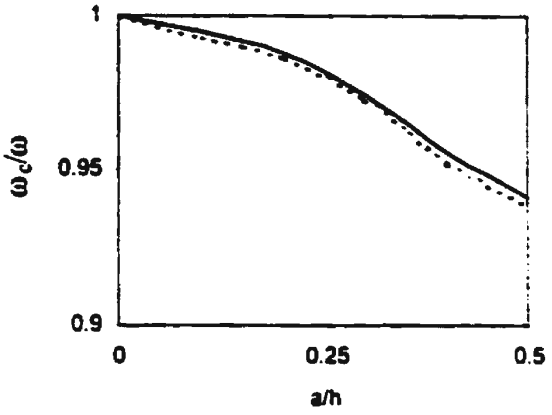

(c) Third Frequency Ratio

Figure 5.27: Comparison of Experimental and Theoretical Values of Natural Frequency ratios for a Fixed-Fixed Beam for a Crack Located at the Center (---Experimental; — Theoretical)

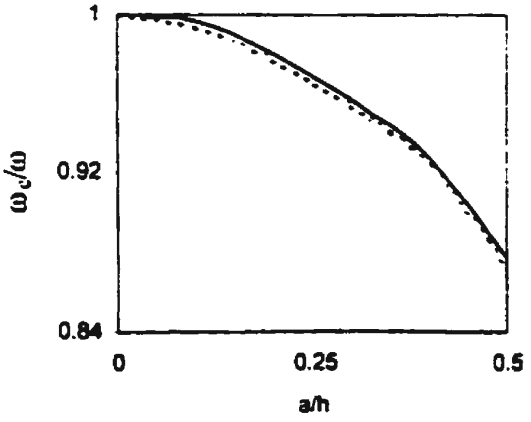

(a) First Frequency Ratio

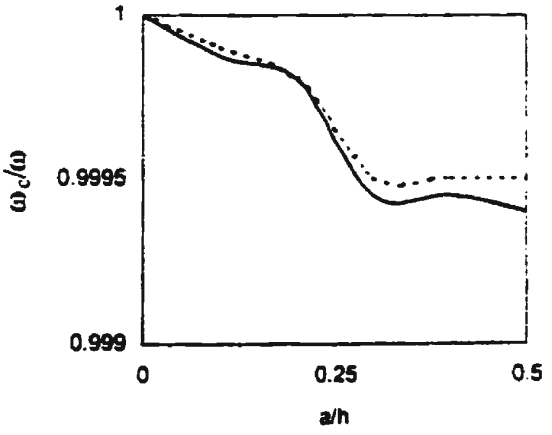

(b) Second Frequency Ratio

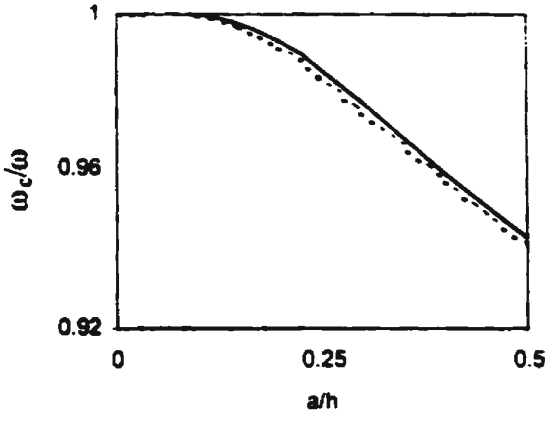

(c) Third Frequency Ratio

Figure 5.28: Comparison of Experimental and Theoretical Values of Natural Frequency ratios for a Simply Supported Beam for a Crack Located at the Center (---Experimental; —Theoretical)

CHAPTER 6: CONCLUSIONS AND RECOMMENDATIONS

6.1 Conclusions

Comprehensive experimental investigations of the effects of cracks on the first three modes of vibration of simply supported and fixed-fixed beams have been presented in this thesis. The influence of cracks on the vibration behavior of the beam is shown to be very sensitive to the crack location, and mode number. A simple method for predicting the location(s) and depth(s) of the crack(s) based on changes in the natural frequencies of the beam is also suggested, and discussed.

The following conclusions could be drawn based on the experimental investigations:

1) Small crack depth ratios have little effects on the sensitivities of the natural frequencies of simply supported and fixed beams. Based on this observation, it would be inadequate to use changes in natural frequencies alone to identify cracks in most real life situations. Consequently, it is appropriate to use both natural frequencies, and changes of mode shapes.
2) The extent of changes noticed in the natural frequencies of beams varies from one location to the other along the length of the beam. At certain positions, the changes are significant, and at some other positions, they are not observable, and are minimal. At a location where some of the frequencies are affected, it is observed

also that the changes become more significant as the crack grows bigger. It was further observed that all the modes measured at a point on the beam were not necessarily affected. Consequently, it could be concluded that changes in the natural frequencies in beams are not only functions of crack depth, and crack location, but, also of the mode number.

3) A comparison of the results obtained in the present experimental investigation with those obtained in an earlier theoretical study showed very good correlation. Hence, experimental modal analysis is a very powerful tool in verifying analytical results.
4) Discontinuities are likely to occur in mode shapes as the crack depth becomes bigger.
5) The shifts in the positions of the nodes of higher modes of vibration could also serve as a means of detecting crack in the structure.
6) Measurement of a sufficient number of natural frequencies is important for identifying the crack parameters (location and depth) in beams. The number of natural frequencies needed depends on the number of crack depths, and crack locations that are to be identified.

It is to be noted that the measurements obtained were based on some assumptions, and they were not assumed to be free of errors. The likely observable sources of errors have been enumerated in Chapter Four. Also, several structural and non-structural parameters (such as environmental disturbances, floor vibration, ambient temperature and humidity, density change etc) that vary with time could have affected the measured responses. These are not accounted for in these experimental investigations.

6.2 Recommendations

The experimental investigations conducted revealed a lot of information on the effects of cracks on the dynamic behavior of beams (simply supported and fixed-fixed beams) at different locations along the length of beams. The data obtained could serve as references for future investigations, and also for beams intended for use in real life situations.

The following recommendations are made based on the experimental investigations.

1) Several sources of errors were identified, and discussed, and certain precautions were stated (in Chapter Four). Efforts should be made to identify them quite early in future investigations to reduce or eliminate them.
2) Several research investigations have been carried out in the past with a view to detect cracks in structures. However, till date, no single method has been developed that is capable of detecting, locating, and quantifying the defects in most of the real life structures. It is suggested therefore that additional research in the field of experimental modal analysis should be conducted so as to develop a unified method capable of meeting the above-mentioned research objectives in most real life situations.
3) Different crack shapes, and crack widths may give different frequency responses. Consequently more complicated crack situations should be investigated, and more

sophisticated methodology and experimental techniques should be derived to detect cracks.

4) Conducting a sensitivity (to defects) analysis of all of the available damage indicators is very vital in experimental modal analysis. By so doing, a fixed order of priority could be set up for similar situations. Future investigations in the Faculty on modal analysis, could be carried out on investigating the sensitivities of the various damage indicators to cracks in beams.
5) In several cases, it is far better to use more than one method to identify cracking, as the success of any method depends on several factors.
6) The experimental investigations were based on certain assumptions. One of such assumption is the fact that the system was assumed to be linear. Efforts should be made in future analysis to investigate the effects of non-linearity.
7) The accuracy of the estimated modal parameters depends on several factors such as: sensors used, locations of the sensors, type of excitations, measurement duration, sampling technique etc. Consequently, these factors are to be chosen carefully before conducting experimental modal analysis.
8) For further study, a theoretical formulation should be obtained for the uniqueness of the intersection point that gives the crack depth and crack location. This could serve as a theoretical basis for the crack identification procedure suggested in this experimental investigation.

REFERENCES

Afolabi, D. (1990). "An Anti-Resonance Technique for Detecting Structural Damage." Proceedings of the 8th International Modal Analysis Conference, pp. 491- 495.

Allemang, R.J. (1990). "Vibrations: Experimental Modal Analysis," Structural Dynamics Laboratory, Department of Mechanical, Industrial, and Nuclear Engineering, University of Cincinnati, Ohio. 4522-0072, USA.

Budipriyanto, A. and Swamidas, A.S.J. (1994): "Experimental and Analytical Verification of Modal Behavior of Uncracked/Cracked Plates in Air and Water," Proceedings of the 12th International Modal Analysis Conference, pp. 745-752.

Brinckell, R., Kirkegard, P.H., Anderson, P., and Martinez, M.E. (1995). "Damage Detection in an Offshore Structure," Proceedings of the 13th International Modal Analysis Conference, pp. 661-667.

Bruel and Kjaer Instrumentation Manual, Vols. 1-3 (1987). B & K Dual Channel Signal Analyzer Type 2034, 138 pages (Vol. 1).

Cheng, S. (1998). " Non-Destructive Evaluation of Cracking in Tubular T-Joints Using Vibration Procedures," Ph.D. Thesis, Faculty of Engineering and Applied Science. Memorial University of Newfoundland, St John's, Canada. 292p.

Chen, Y (1996). " Crack Detection in Plated T- Joints Through Vibration Techniques." Ph.D. Thesis. Faculty of Engineering and Applied Science Memorial University of Newfoundland, St John's, Canada, 165p.

Chondros, T.G. and Dimarogonas A.D. (1980). " Identification of Cracks in Welded Joints of Complex Structures," Journal of Sound and Vibration, Vol. 69, No. 4, pp. 531-538.

De Silva, C.W. (1999). Vibration: Fundamentals, and Principles. CRC Press, London. ISBN 0-8493-1808-4.

Doebling, S.W., Farrar, C.R., Prime, M.B., and Shevitz, P.W. (1996). "Damage Identification and Health Monitoring of Structural, and Mechanical Systems from Changes in Their Vibration Characteristics," A Literature Review, Los Alamos National Laboratory, Los Alamos, New Mexico, 100p.

Ewins, D.J. (1995). Modal Testing: Theory and Practice. Research Service Publishers, New York, ISBN 0-86380-0173.

Fox, C.H.J. (1992). " The Identification of Defects in Structures." Proceedings of the 10th International Modal Analysis Conference, pp. 522-528.

Hewlett Packard System Operating Manual (1987). Function Generator 3314A. 10 pages

Hjelmstad, K.D. and Shin, S. (1996). "Crack Identification in a Cantilever Beam From Modal Response," Journal of Sound and Vibration, Vol. 198 (5), pp. 527-545.

Inagaki T., Kanki, H., and Shireki M. (1981). "Transverse Vibrations of a General Cracked-Rotor Bearing System," Journal of Mechanical Design, Vol. 104, pp. 1-11.

Ju, F. and Mimovich, M. (1986). " Modal Frequency Method in Diagnosis of Fracture Damage in Structures," Proceedings of the 4th International Modal Analysis Conference, pp. 1423-1429.

Kim, H.M. and Burtkowicz, T.J (1995). " An Experimental Study of Damage Detection Using a Hexagonal Truss structure." Proceeding of the 36th Structures, Structural Dynamics, and Materials Conference, pp. 3347-3556.

Krawczuk, M. and Ostachowicz, W.M. (1992). "Parametric Vibrations of a Beam with Cracks," Archive of Applied Mechanics, Vol. 62, pp. 463-473.

McConnell, K.G. (1995). " Vibration Testing: Theory and Practice," John Wiley and Sons Inc., New York.

McGonnagle, W. (1961). Non Destructive Testing. Gordon and Breach Science Publishers, New York, ISBN 60-9850.

Narkis, Y. (1994). "Identification of Crack Location in Vibrating Simply Supported Beam," Journal of Sound and Vibration, Vol. 172 (4), pp. 549-558.

Nwosu, D.I, Swamidas, A.S.J., Guigne T.Y., and Olowokere, D.O. (1995). " Studies on the Influence of Cracks on the Dynamic Response of Tubular T-Joints for Non Destructive Evaluation," Proceedings of the 13th International Modal Analysis Conference, pp. 1122-1128.

Perchard, P.R. and Swamidas A.S.J. (1994). " Crack Detection in Cantilever Plates Using Modal Analysis," Proceedings of the 11th International Modal Analysis Conference, pp. 1969-1777.

Qian, C.L., Gu, S.N. and Jiang J.S. (1990). "The Dynamic Behavior and Crack Detection of a Beam with a Crack." Journal of Sound and Vibration, 138 (2), pp. 233-243.

Richardson, M.H. (1980). "Detection of Damage in Structures from Changes in Their Dynamic (Modal) Properties," A Survey. NUREG/CR-1431. U.S. Nuclear Regulatory Commission, Washington, D.C.

Richardson, M.H. and Mannan, M.A. (1991). " Determination of Modal Sensitivity Functions for Location of Structural Faults," Proceedings of the 9th International Modal Analysis Conference, pp. 670-676.

Ruotolo, R. and Mares, C. (1987). "Theoretical and Experimental Study of the Dynamic Behavior of a Double-cracked Beam," Proceedings of the 6th International Modal Analysis Conference, pp. 1560-1561.

Rytter, A. (1993). " Vibration-based Inspection of Civil Engineering Structures," Ph.D. Thesis, Department of Building Technology, Aalborg University, Aalborg, Denmark.

Silva, J.M.M. and Gomes, A.J.M.A. (1990). "Experimental Dynamic Analysis of Cracked Free-Free Beams," Journal of Experimental Mechanics, 30 (1), pp. 20-25

Star Reference Manual (1990). Structural Measurement Systems, 58 pages.

Stubbs, N. (1990). "Global Nondestructive Evaluation of Solids," The International Journal of Analytical and Experimental Modal Analysis, Vol. 5(2), pp. 67-79.

Sundstrand Data Control Inc., Instruction Manual (1972). Model 912 (X) and Model 922 (X) Series Load Cells. 10p.

Tasi, T.C, and Wang, Y.G. (1996). "Vibration Analysis and Diagnosis of a Cracked Shaft." Journal of Sound and Vibration. Vol.192(2). pp. 607-620.

Yang, X.F, Swamidas, A.S.J, and Seshadri, R. " Crack Identification in Beams Using Energy Method," Accepted for Publication in Journal of Sound and Vibration (September 2000).

Yuen, M.M.F. (1985). "A Numerical Study of the Eigenparameters of a Damaged Cantilever," Journal of Sound and Vibration, Vol. 103(2), pp. 301-310.

Appendix A

The first three natural frequencies obtained for various combinations of crack depths. and crack locations considered are shown in appendix A. Note that "NA" implies "Non available data" due to experimental errors. It was observed that there were very slight changes in the natural frequencies of the uncracked beams. These may be due to the small discrepancies observed in the geometry of the models and the inability to apply exactly the same torque while dismantling, and fixing the various experimental models. Each column of the tables represents the natural frequencies obtained for each beam model. The first row of each Table represents the stated frequency when the beam is uncracked. All measurements of frequencies were given by the identifying software in Hertz (Hz) unit. Note that the third natural frequencies were rounded up to a whole number by the STAR Software package used in extracting it as it could not produce more than five digits number.

Table A1: Fundamental Natural Frequency (Hz) as a Function of Crack Location, and Crack Depth for a Fixed beam

a/h	c/l = 1/16	c/l = 3/16	c/l = 5/16	c/l = 7 /16	c/l = 8/16	c/l = 11/16	c/l = 14/16
0	263.91	264.77	263.57	264.05	264.68	264.16	264.37
0.1	NA	264.77	263.57	263.45	264.29	264.16	264.25
0.2	NA	264.77	262.91	261.45	262.65	263.87	263.87
0.3	NA	264.77	261.53	257.95	257.97	262.89	260.78
0.4	NA	264.77	258.96	255.23	254.32	260.86	257.36
0.5	NA	264.77	256.00	243.51	242.44	258.18	253.85
0.6	NA	264.77	252.40	230.88	230.96	255.87	247.16
0.7	NA	264.77	251.00	210.88	223.46	246.15	239.74

Table A2: Second Natural Frequency (Hz) as a Function of Crack Location, and Crack Depth for a Fixed beam.

a/h	c/l = 1/16	c/l = 3/16	c/l = 5/16	c/l = 7 /16	c/l = 8/16	c/l = 11/16	c/l = 14/16
0	723.96	722.76	726.34	725.58	726.27	726.42	724.37
0.1	723.56	721.48	725.35	724.85	726.27	725.43	723.48
0.2	720.85	718.26	719.22	723.56	726.27	722.39	717.84
0.3	719.01	713.72	711.83	722.31	726.27	712.25	713.46
0.4	716.60	712.91	701.73	719.15	726.27	703.60	711.00
0.5	715.02	693.53	676.37	713.36	726.27	690.93	708.35
0.6	713.72	686.45	656.76	709.17	726.27	666.67	704.01
0.7	712.32	670.98	627.14	705.69	726.27	656.67	701.42

Table A3: Third Natural Frequency (Hz) as a Function of Crack Location, and Crack Depth for a Fixed beam.

a/h	c/l = 1/16	c/l = 3/16	c/l = 5/16	c/l = 7/16	c/l = 8/16	c/l = 11/16	c/l = 14/16
0	1460	1460	1460	1470	1470	1470	1460
0.1	1460	1460	1460	1460	1460	1460	140
0.2	1460	1450	1450	1450	1450	1460	1460
0.3	1460	1440	1460	1440	1430	1450	1460
0.4	1460	1410	1450	1430	1400	1450	1460
0.5	1450	1390	1450	1400	1380	1450	1450
0.6	1450	1360	1450	1380	1320	1440	1450
0.7	1450	1320	1450	1320	1300	1440	1450

Table A4: Fundamental Natural Frequency (Hz) as a Function of Crack Location, and Crack Depth for a Simply Supported Beam.

a/h	c/l = 1/16	c/l = 3/16	c/l = 5/16	c/l = 7/16	c/l = 8/16	c/l = 11/16	c/l = 14/16
0	132.18	132.20	135.80	133.92	135.82	134.82	132.23
0.1	132.18	131.94	134.75	133.38	135.01	134.55	132.15
0.2	132.18	131.62	134.33	131.90	132.69	133.58	132.10
0.3	132.18	130.63	132.52	129.71	129.44	132.08	131.94
0.4	132.12	129.31	129.10	126.12	125.41	129.65	131.85
0.5	131.84	127.76	NA	120.00	118.49	124.37	131.50
0.6	131.26	123.88	117.87	111.39	110.27	115.22	130.82
0.7	130.17	115.76	107.23	94.62	96.23	103.99	129.97

Table A5: Second Natural Frequency (Hz) as a Function of Crack Location, and Crack Depth for a Simply Supported Beam.

a/h	c/l = 1/16	c/l = 3/16	c/l = 5/16	c/l = 7/16	c/l = 8/16	c/l = 11/16	c/l = 14/16
0	519.04	519.26	518.66	520.09	521.20	520.06	520.23
0.1	519.04	517.27	516.96	519.79	521.15	518.97	519.92
0.2	518.59	513.49	513.65	518.84	521.10	514.29	518.94
0.3	517.10	504.30	506.57	517.57	520.95	508.32	516.90
0.4	514.73	492.30	493.95	515.84	520.95	499.94	515.27
0.5	511.15	479.36	NA	512.88	520.95	485.57	511.09
0.6	504.19	457.87	461.09	510.28	520.73	467.45	504.39
0.7	495.39	424.48	436.90	504.68	520.47	452.08	498.29

Table A6: Third Natural Frequency (Hz) as a Function of Crack Location, and Crack Depth for a Simply Supported Beam.

a/h	c/l = 1/16	c/l = 3/16	c/l = 5/16	c/l = 7/16	c/l = 8/16	c/l = 11/16	c/l = 14/16
0	1170	1160	1170	1170	1170	1180	1160
0.1	1170	1160	1170	1170	1170	1180	1160
0.2	1160	1160	1170	1160	1160	1180	1160
0.3	1160	1140	1170	1150	1140	1170	1160
0.4	1150	1130	1170	1140	1120	1170	1150
0.5	1130	1110	NA	1100	1100	1170	1140
0.6	1120	1100	1170	1000	1070	1170	1100
0.7	1100	1080	1170	964	937	1170	1080

Appendix B

Normalized frequency plots for the first three vibration modes of simply supported and fixed-fixed beams.

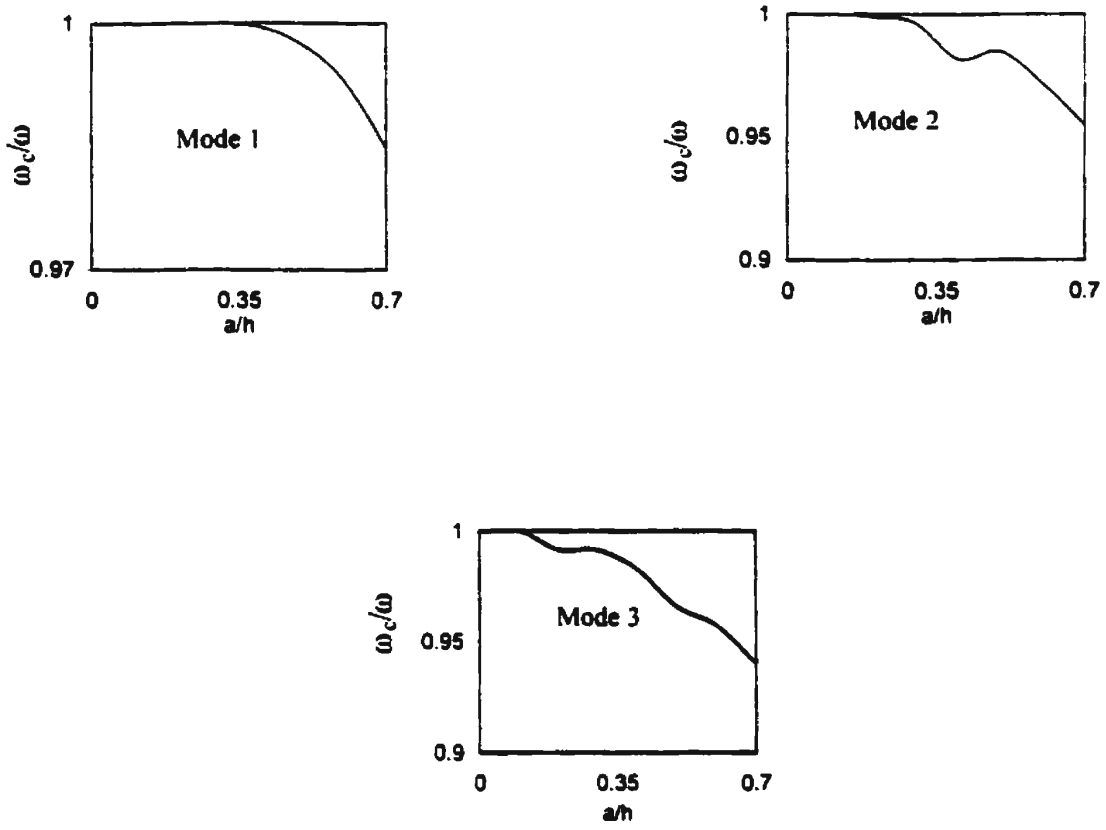

Fig. B1: Variations of the First Three Frequencies as a Function of Crack Depth for a Simply Supported Beam (Crack Location c/l = 1/16)

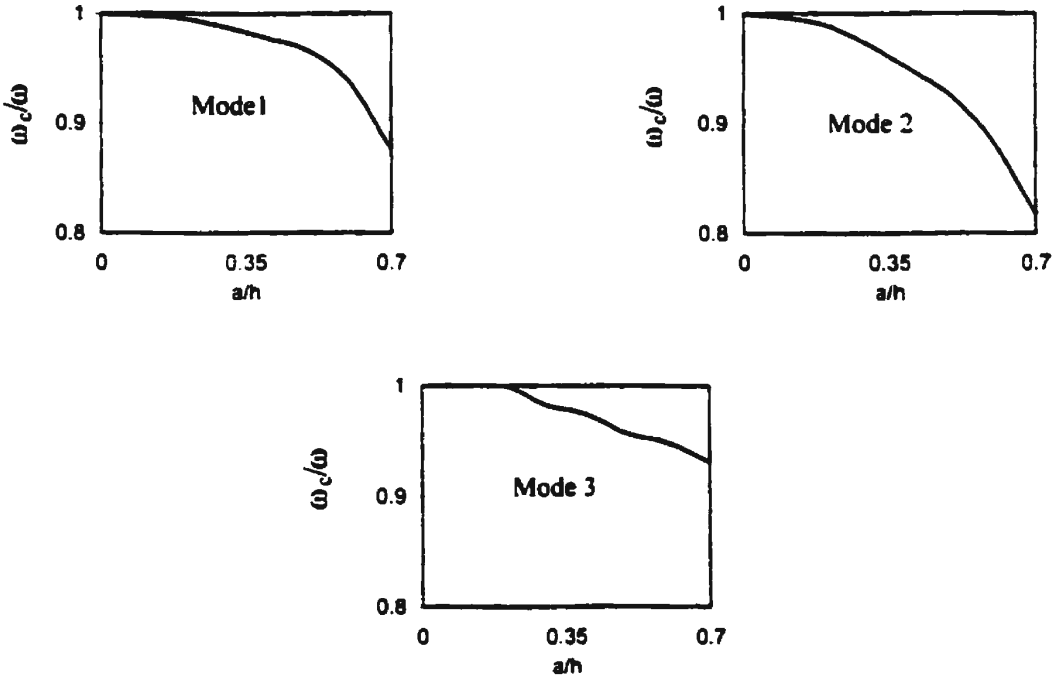

Fig. B2: Variations of the First Three Frequencies as a Function of Crack Depth for a Simply Supported Beam (Crack Location c/l = 3/16)

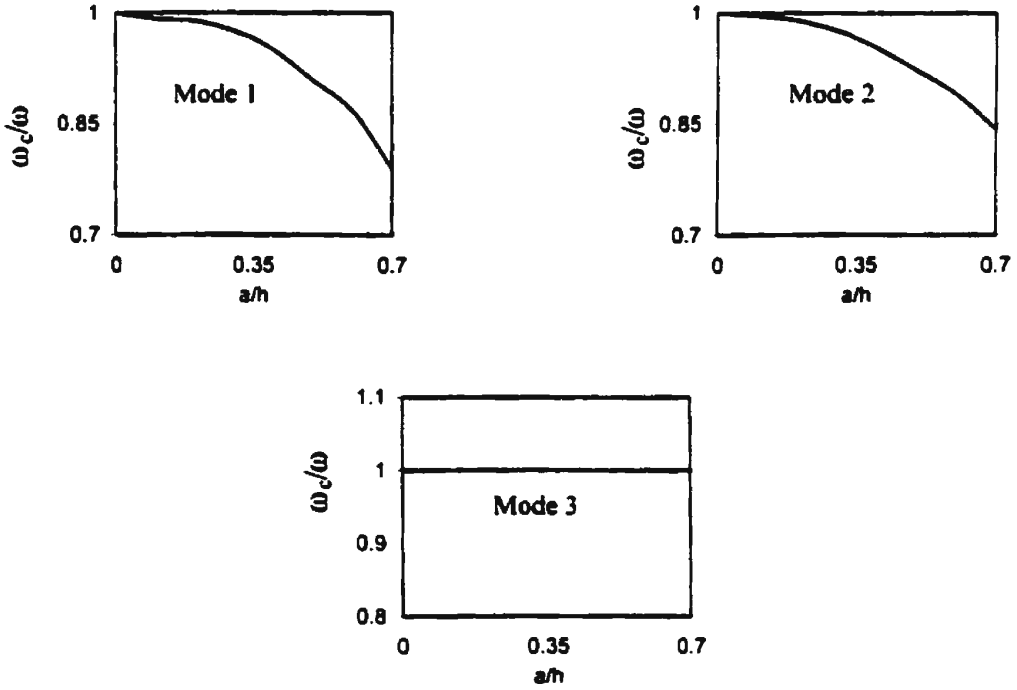

Fig. B3: Variations of the First Three Frequencies as a Function of Crack Depth for a Simply Supported Beam (Crack Location c/l = 5/16)

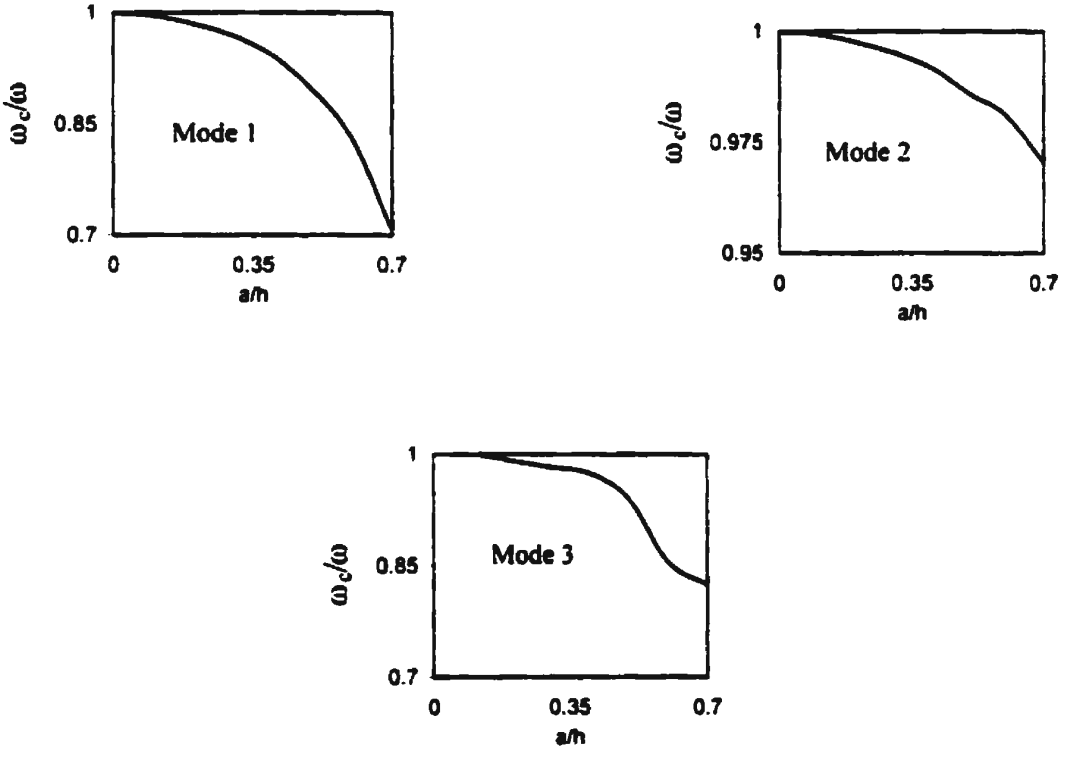

Fig. B4: Variations of the First Three Frequencies as a Function of Crack Depth for a Simply Supported Beam (Crack Location c/l = 7/16)

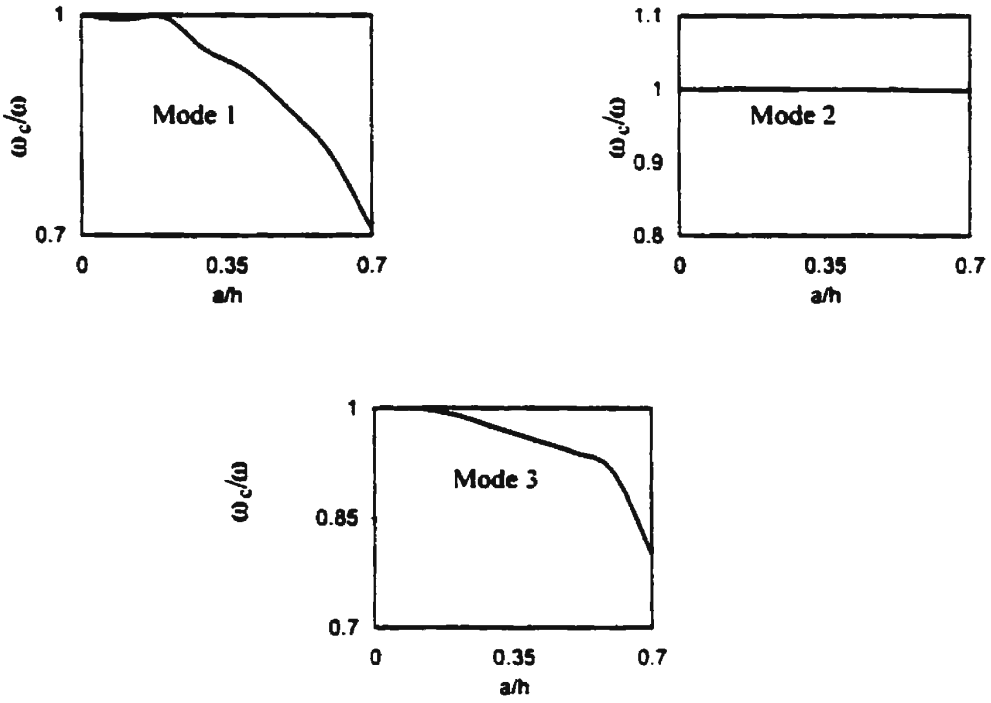

Fig. B5: Variations of the First Three Frequencies as a Function of Crack Depth for a Simply Supported Beam (Crack Location c/l = 8/16)

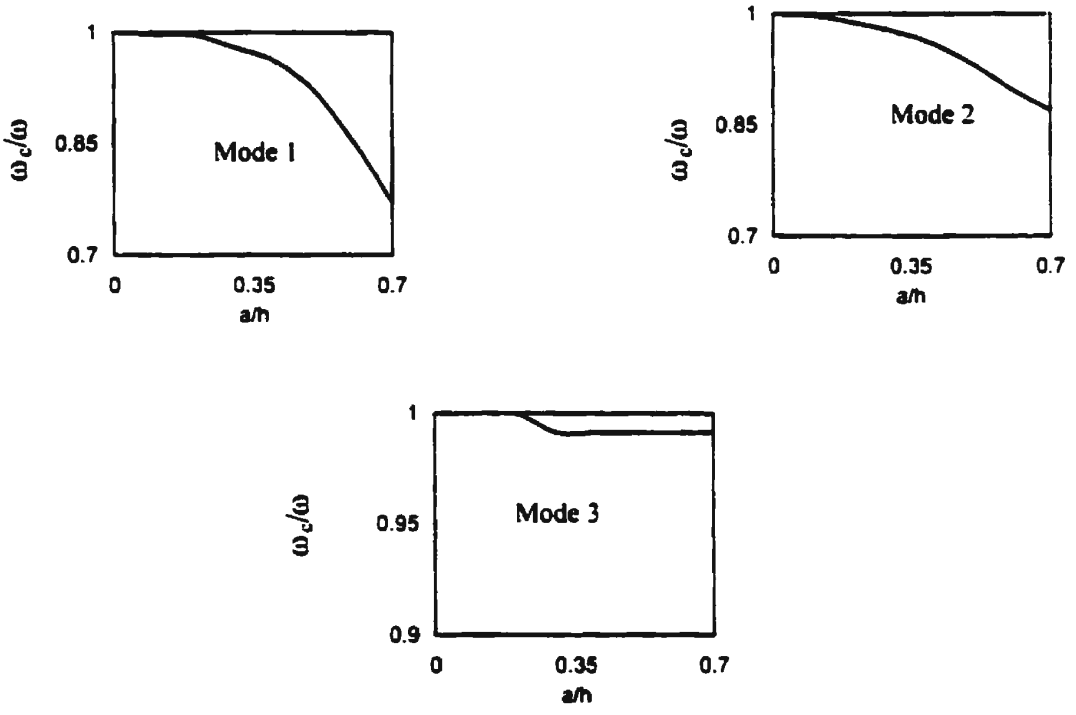

Fig. B6: Variations of the First Three Frequencies as a Function of Crack Depth for a Simply Supported Beam (Crack Location c/l = 11/16)

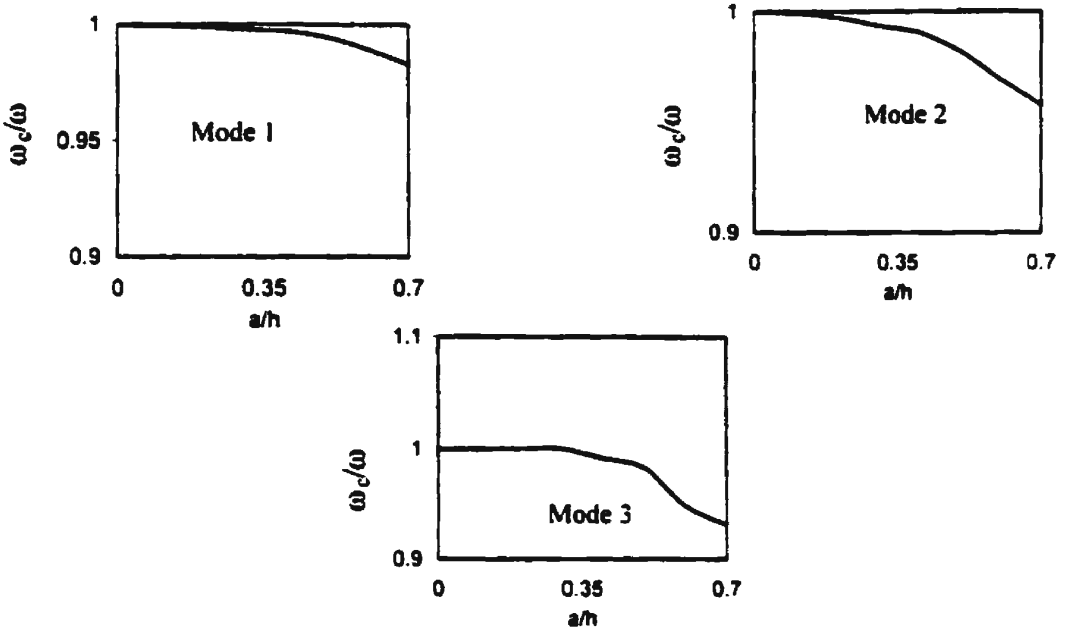

Fig. B7: Variations of the First Three Frequencies as a Function of Crack Depth for a Simply Supported Beam (Crack Location c/l = 14/16)

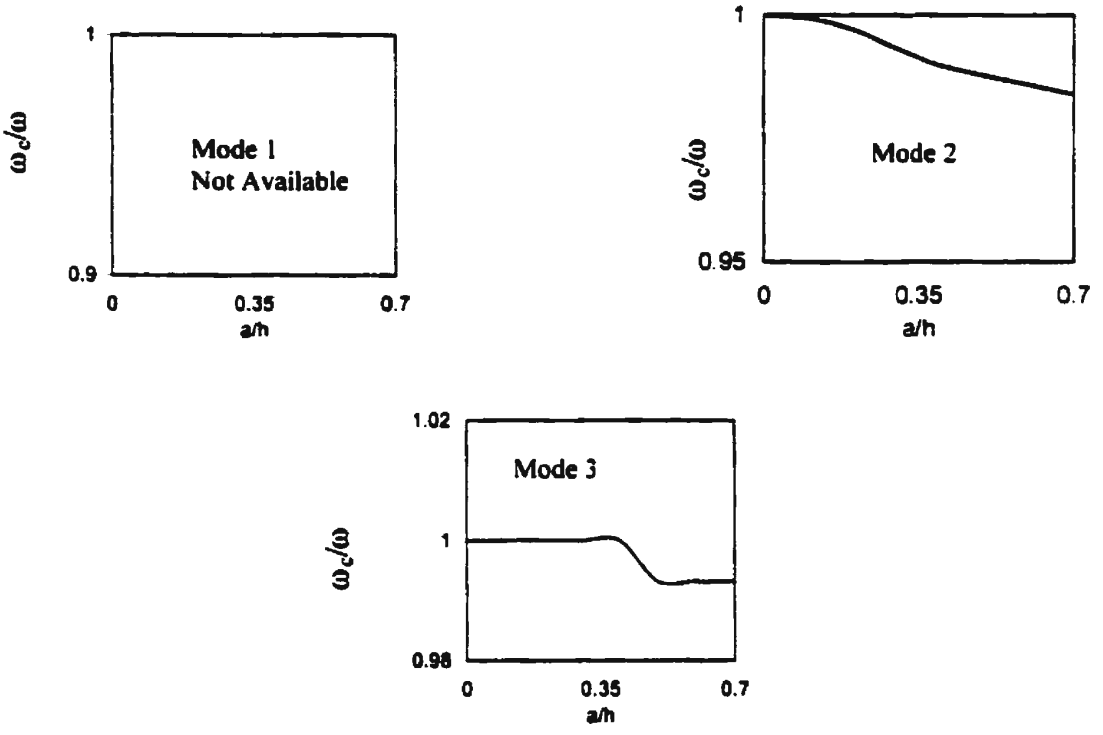

Fig. B8: Variations of the First Three Frequencies as a Function of Crack Depth for a Fixed-Fixed Beam (Crack Location c/l = 1/16)

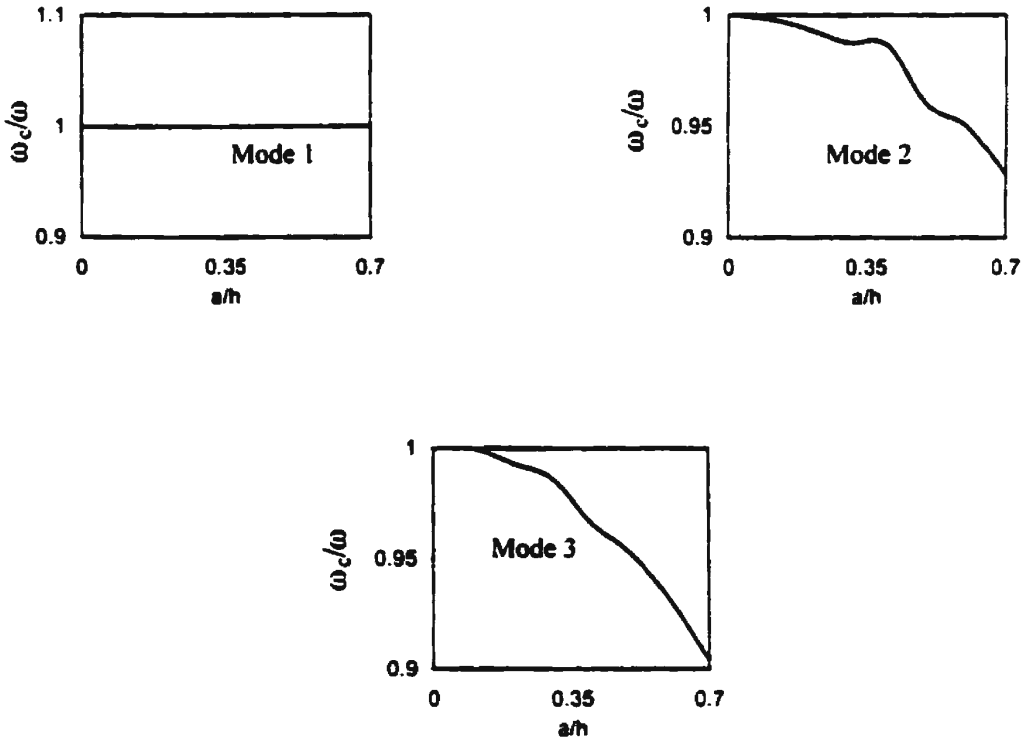

Fig. B9: Variations of the First Three Frequencies as a Function of Crack Depth for a Fixed-Fixed Beam (Crack Location c/l = 3/16)

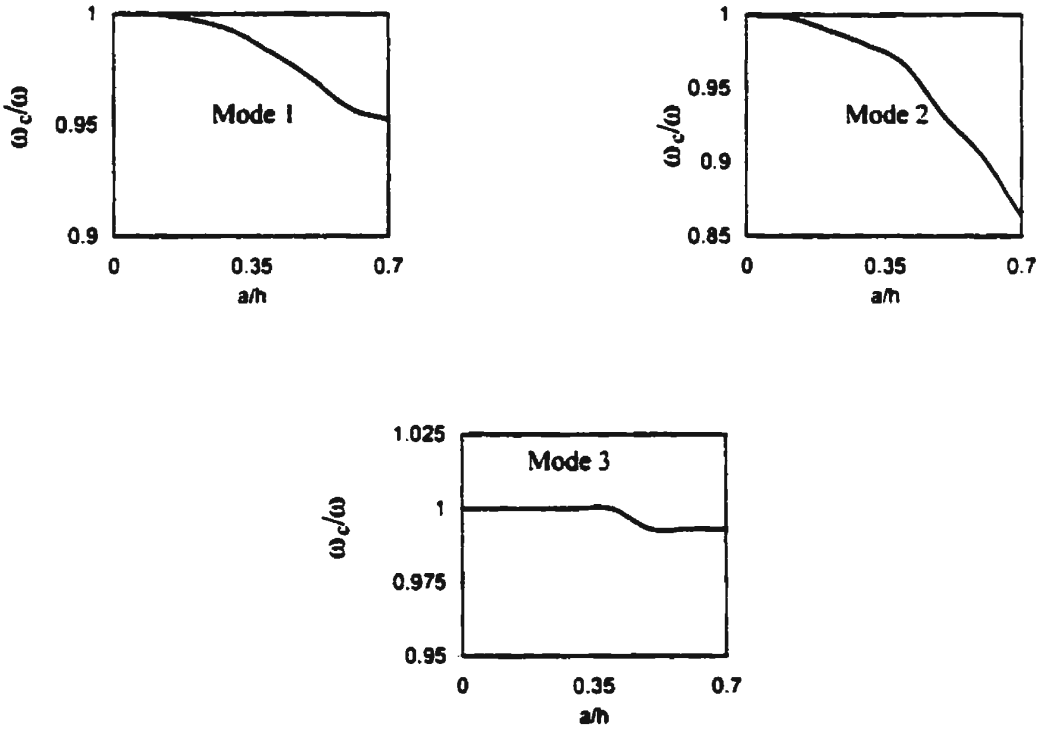

Fig. B10: Variations of the First Three Frequencies as a Function of Crack Depth for a Fixed-Fixed Beam (Crack Location c/l = 5/16)

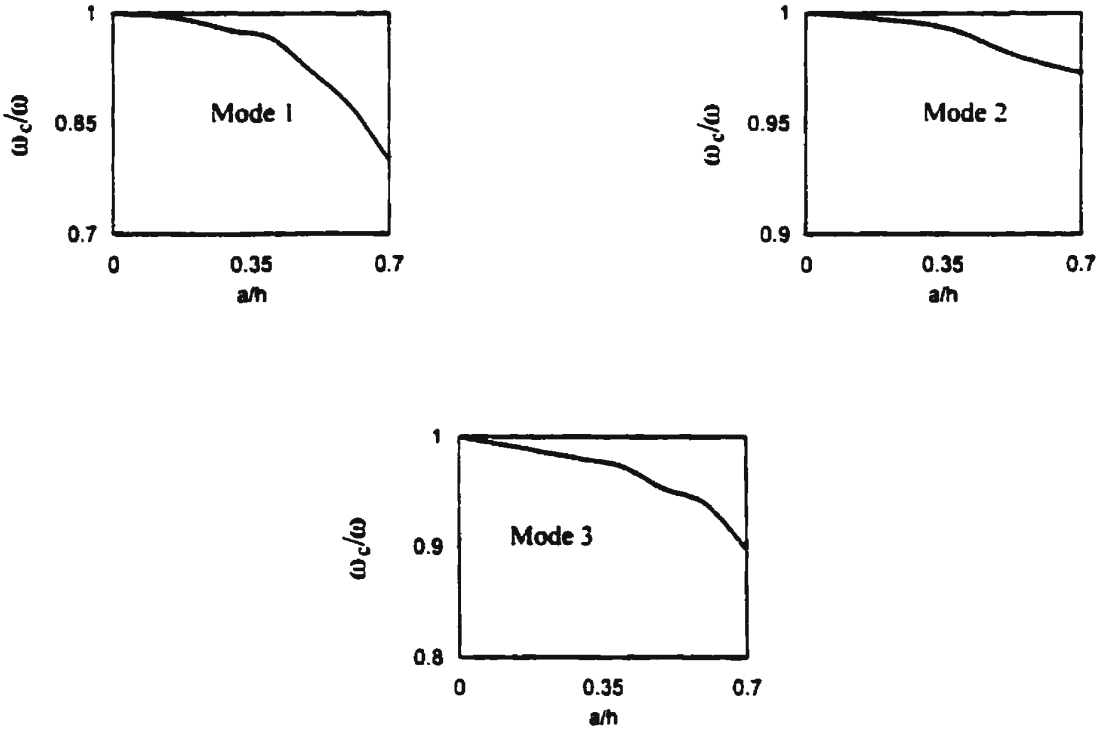

Fig. B11: Variations of the First Three Frequencies as a Function of Crack Depth for a Fixed-Fixed Beam (Crack Location c/l = 7/16)

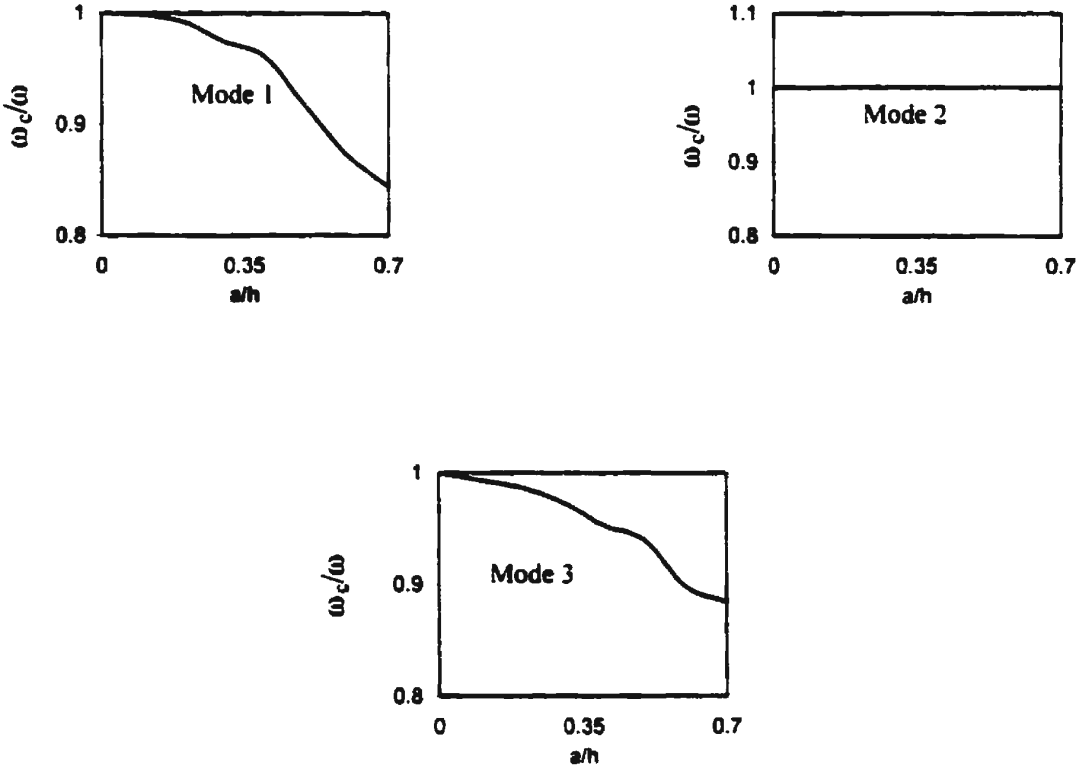

Fig. B12:Variations of the First Three Frequencies as a Function of Crack Depth for a Fixed-Fixed Beam (Crack Location c/l = 8/16)

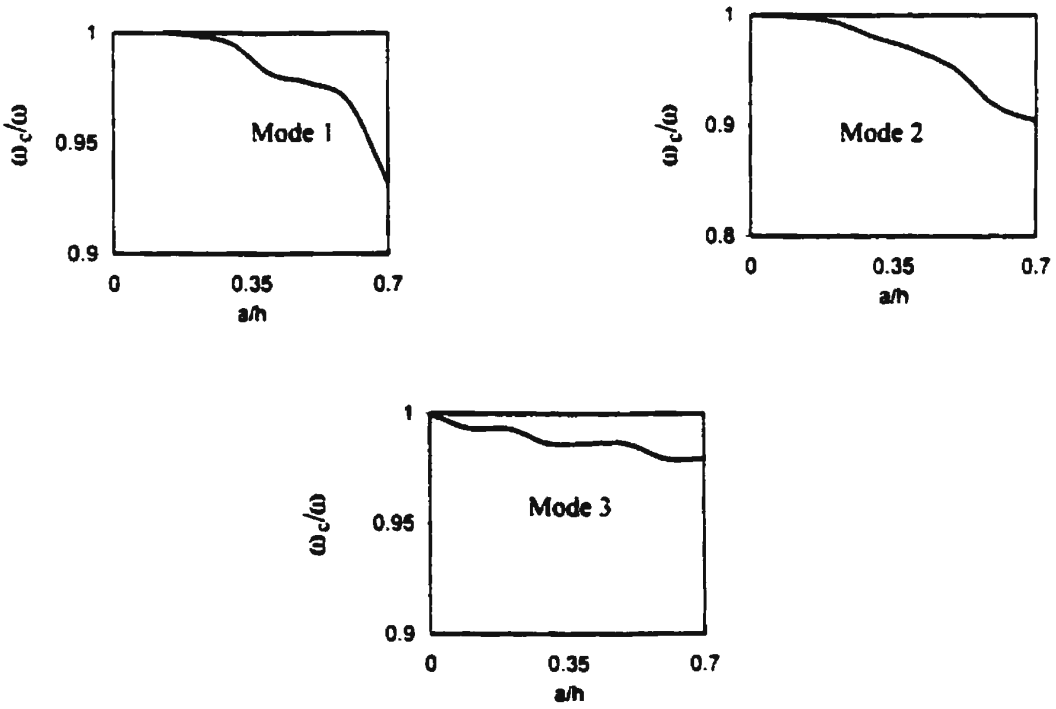

Fig. B13: Variations of the First Three Frequencies as a Function of Crack Depth for a Fixed-Fixed Beam (Crack Location c/l = 11/16)

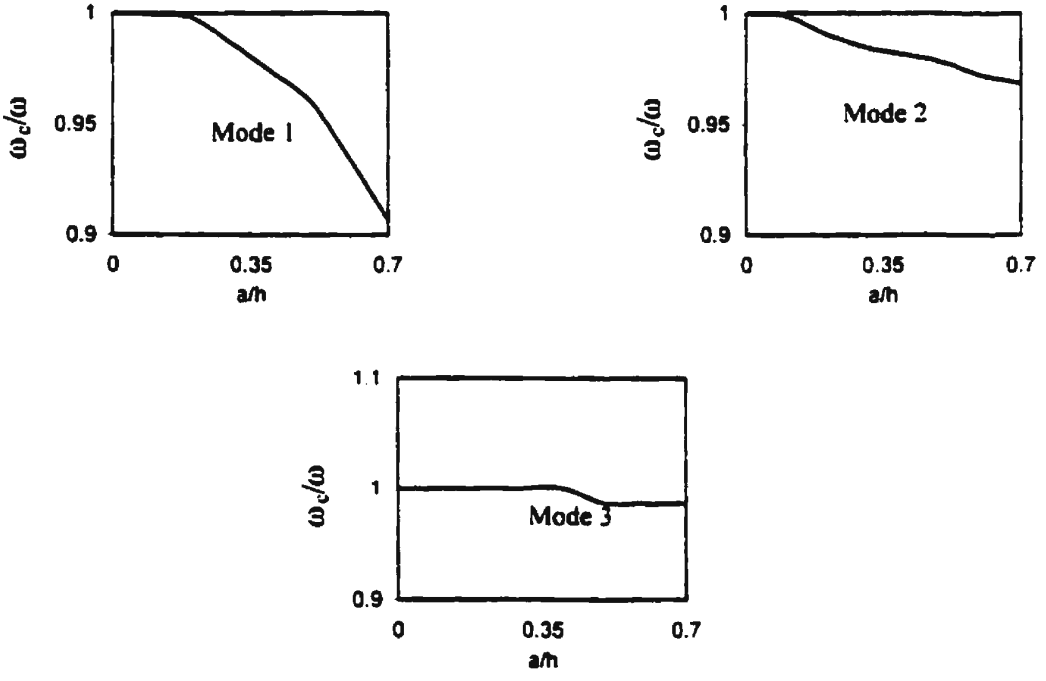

Fig. B14: Variations of the First Three Frequencies as a Function of Crack Depth for a Fixed-Fixed Beam (Crack Location c/l = 14/16)

APPENDIX C

Appendix C shows some of the curves obtained from the theoretical analyses carried out by Yang et al (2000). The results obtained were for the first four natural frequencies of fixed-fixed and simply supported beams (in this experimental investigation, the first three natural frequencies were taken). Most of the curves in Appendix C show a pattern similar to the curves in Chapter Five that have the same crack conditions.

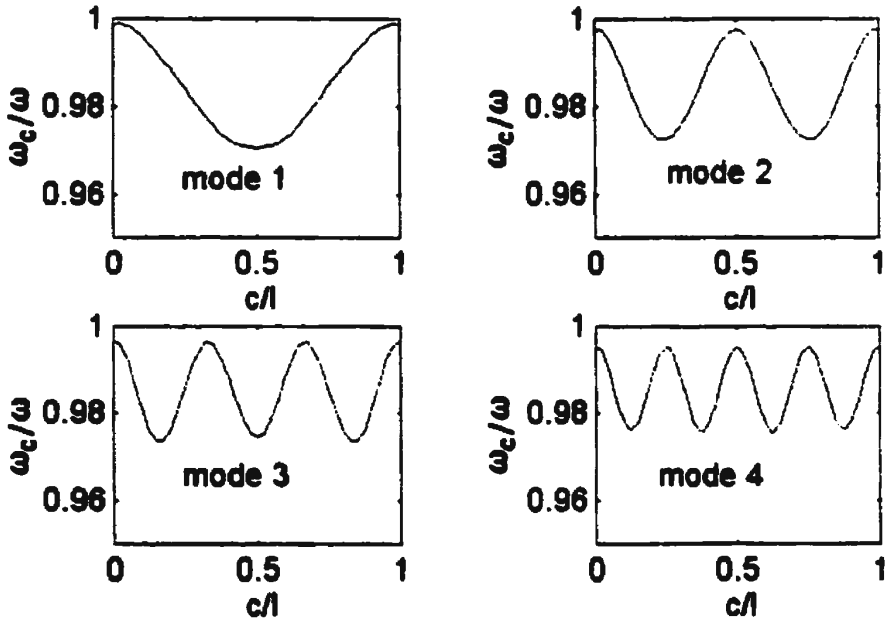

Figure C1: Variations of the First Four Frequencies as a Function of Crack Location for a Simply Supported Beam (Crack Depth Ratio $a/h = 0.25$)

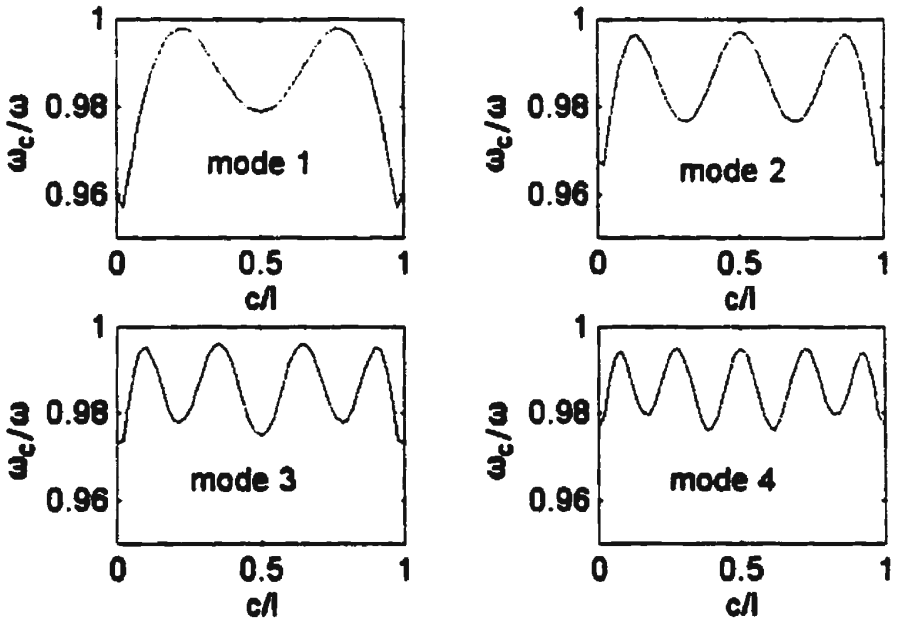

Figure C2: Variations of the First Four Frequencies as a Function of Crack Location for a Fixed-Fixed Beam (Crack Depth Ratio $a/h = 0.25$)

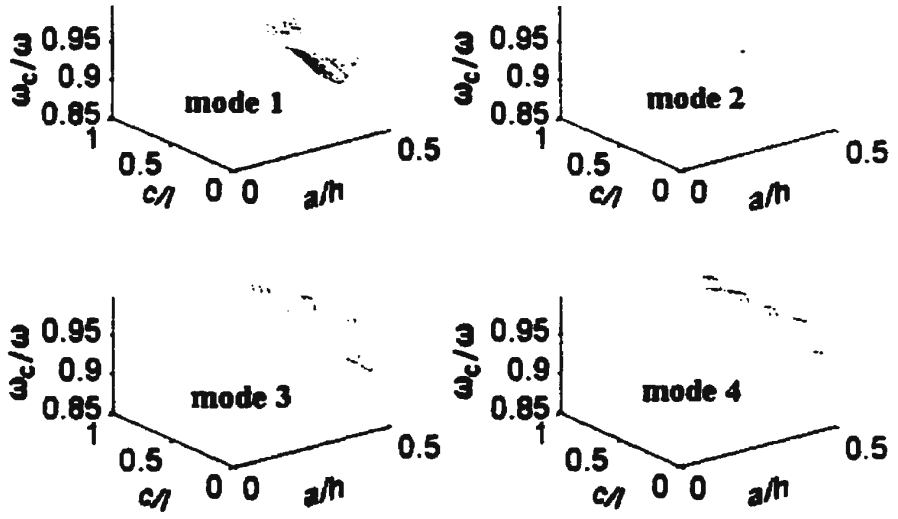

Figure C3: Three-dimensional Plots of Frequency Ratio versus Crack Location, and Crack Depth for a Simply Supported Beam

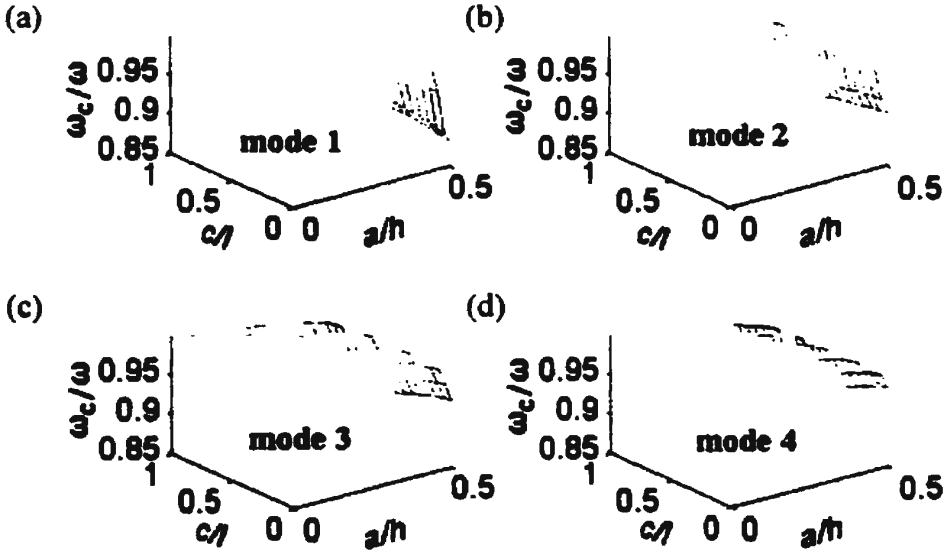

Figure C4: Three-dimensional Plots of Frequency Ratio versus Crack Location, and Crack Depth for a Fixed-end Beam

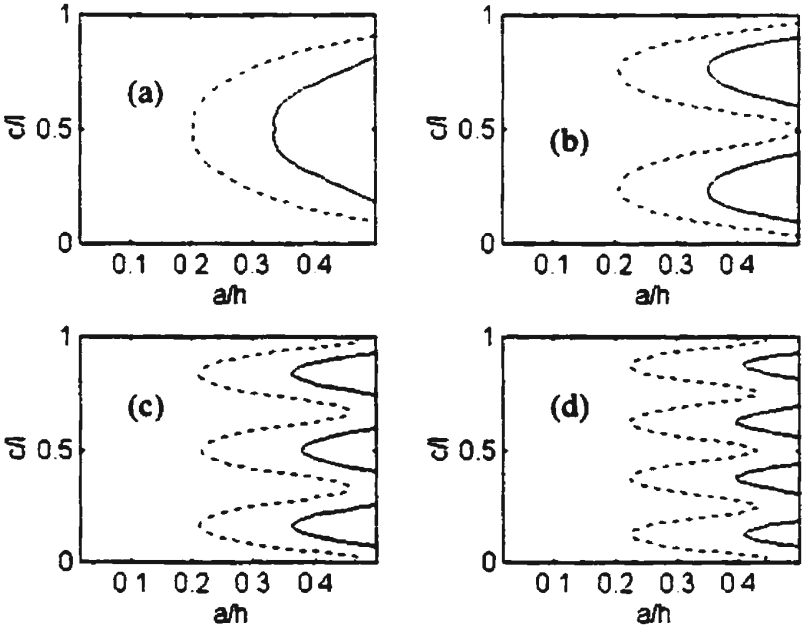

Figure C5: Frequency Contours for a Simply Supported Beam with a Single Crack ((a) mode one; (b) mode two; (c) mode three; (d) mode four; —$\omega_c / \omega = 0.95$; ----$\omega_c / \omega = 0.98$)

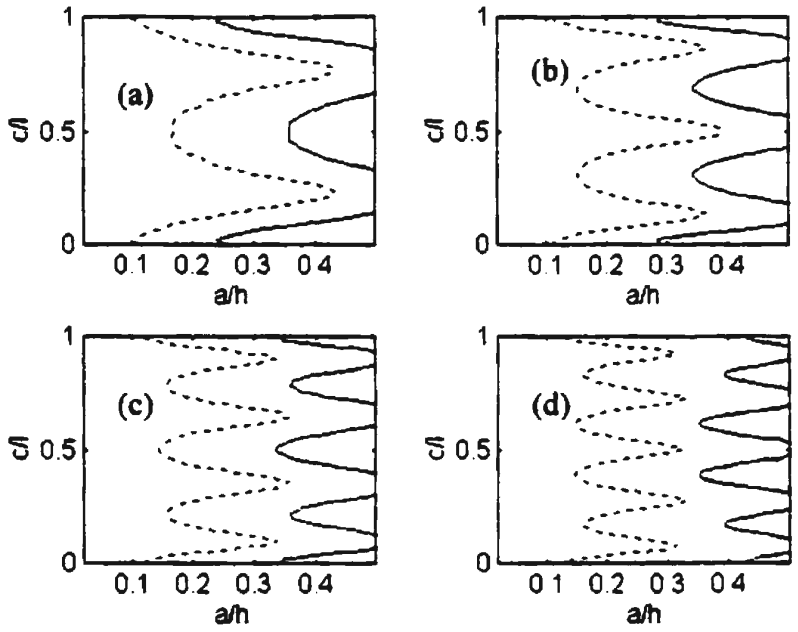

Figure C6: Frequency Contours for a Fixed-Fixed Beam with a Single Crack((a) mode one; (b) mode two; (c) mode three; (d) mode four; —$\omega_c / \omega = 0.96$; ----$\omega_c / \omega = 0.99$)